TRANSCRIPTOMIC AND REVERSE GENETIC ANALYSES OF *AEDES AEGYPTI* CULTURED CELLS AND MIDGUT EPITHELIAL CELLS UPON HEME EXPOSURE

A Dissertation

by

HEATHER L EGGLESTON

Submitted to the Office of Graduate and Professional Studies of
Texas A&M University
in partial fulfillment of the requirements for the degree of

DOCTOR OF PHILOSOPHY

Chair of Committee,	Zachary Adelman
Committee Members,	Kevin Myles
	David Threadgill
	Michel Slotman
Intercollegiate Faculty Chair,	David Threadgill

December 2019

Major Subject: Genetics

ABSTRACT

The female mosquito *Aedes aegypti* requires amino acids and other nutrients like heme and iron from a blood meal to initiate vitellogenesis. Heme is a pro-oxidant molecule that acts as a nutrient, signaling molecule and in large quantities, as a toxin. *Ae. aegypti* has developed a few strategies to handle heme toxicity, as during a typical meal ~10mM is released into the midgut lumen. These strategies include heme aggregation to the peritrophic matrix and the degradation of heme by heme oxygenase in the cytosol of the midgut epithelium. However, despite the importance of heme as a nutrient and toxin, the mechanism of entry into the midgut epithelial cells is not currently known. As no heme transport proteins in have been identified in any dipteran, heme fluorescent analog studies were performed to visualize changes in expression caused by heme followed by global expression analyses performed in both cultured cells and midgut tissues using NGS-based RNA sequencing with the end goal to identify the gene(s) that encode the membrane bound heme import proteins responsible for heme uptake during blood digestion. A list of candidate genes for RNAi knockdown was compiled based on differential expression, expression pattern across heme treatments and number of TM domains. These genes' function relating to heme transport was then identified through siRNA mediated knockdown and treatment with zinc mesoporphyrin to assess changes in heme uptake.

A number of candidate genes were identified in 2 or more cultured cell datasets out of 4 examined. In particular, 63 candidates were identified in heme exposed midguts, 23 of which were found in at least 1 cultured cell analysis as well. However, very few highly differentially expressed genes were found in any of the analyses indicating that heme

import may be controlled by a redundant system of multiple transport proteins instead of a single one. Alternatively, heme transport in *Ae. aegypti* could be regulated post-translationally. Knockdown of candidate genes AAEL004657 and AAEL008664 suggested a potential role in heme transport in Aag2 cultured cells, though more work is needed to localize and elucidate their specific functions.

ACKNOWLEDGEMENTS

I would like to thank my committee chair, Dr. Zachary Adelman, and my committee members, Dr. Kevin Myles, Dr. David Threadgill, and Dr. Michel Slotman, for their guidance and support throughout the course of this research.

Thanks also go to my friends and colleagues and the Entomology Department faculty and staff and the Genetics Program faculty and staff for making my time at Texas A&M University a great experience.

Finally, thanks to my mother, father, mother-in-law, and father-in-law, Jan & Jeff Lewenczuk and Lori & Richard Eggleston, for their encouragement and support. And a special thanks to my husband, Thomas Eggleston, for his continual support, inexhaustible patience, and unconditional love.

CONTRIBUTORS AND FUNDING SOURCES

Contributors

This work was supported by a dissertation committee consisting of Professor Zach Adelman [advisor], Professor Kevin Myles and Professor Michel Slotman of the Department of Entomology and Professor David Threadgill of the Department of Molecular and Cellular Medicine and of the Department of Biochemistry and Biophysics.

The initial heme overexposure experiment in Aag2 cells was performed by Michelle Anderson at Virginia Polytechnic and State University. RNAi screen of candidate midgut heme transporters was assisted by Loraine O. Springer at Texas A&M University.

The Genomics Sequencing Center at the Virginia Biocomplexity Institute was responsible for NGS-RNA sequencing all the cell culture samples and the midgut samples were NGS-RNA sequenced at Texas A&M's Institute for Genome Sciences and Society.

Portions of this research were conducted with the advanced computing resources provided by Texas A&M High Performance Research Computing.

All other work conducted for the dissertation was completed by the student independently.

Funding Sources

Graduate study was supported by a 2-year fellowship from Virginia Polytechnic and State University, a grant by the National Institute of Allergies and Infectious Diseases of the National Institutes of Health under award number AI115138 and the Texas A&M AgriLife Research Insect-Vectored Disease grant.

TABLE OF CONTENTS

Page

LIST OF FIGURES

Page

LIST OF TABLES

Page

CHAPTER I

INTRODUCTION: IRONING OUT THE DETAILS, EXPLORING THE ROLE OF IRON AND HEME IN BLOOD-SUCKING ARTHROPODS*

Overview

Heme and iron are essential molecules for many physiological processes and yet have the ability to cause oxidative damage such as lipid peroxidation, protein degradation, and ultimately cell death if not controlled. Blood-sucking arthropods have evolved diverse methods to protect themselves against iron/heme-related damage, as the act of bloodfeeding itself is high risk, high reward process. Protective mechanisms in medically important arthropods include the midgut peritrophic matrix in mosquitoes and hemosomes in ticks. Once heme and iron pass these protective mechanisms, they are presumed to enter the midgut epithelial cells via membrane-bound transporters, though relatively few iron or heme transporters have been identified in bloodsucking arthropods. Upon iron entry into midgut epithelial cells, ferritin serves as the universal storage protein and transport for dietary iron in many organisms including arthropods. In addition to its role as a nutrient, heme is also an important signaling molecule in the midgut epithelial cells for many physiological processes including vitellogenesis. This review article will summarize recent advancements in heme/iron uptake, detoxification and exportation in bloodfeeding arthropods. While initial strides have been made at ironing out the role of dietary iron and heme in arthropods, much still remains to be discovered as these molecules may serve as novel targets for the control of many arthropod pests.

*All text and figures in Chapter 1 were reprinted with permission from "Ironing out the Details: Exploring the Role of Iron and Heme in Blood-Sucking Arthropods" by Heather Eggleston, Shavonn Whiten and Zach Adelman, 2018. Frontiers in Physiology © 2018 by the authors previously mentioned

Introduction: Evolution of Arthropod Hematophagy

Estimates suggest there are more than 1 million insect and arachnid species inhabiting planet Earth, approximately 14,000 of which have adapted the ability to feed on vertebrate blood (Graça-Souza et al., 2006). Commonly known as hematophagy, this adaptation has arisen independently many times over the course of evolution (Graça-Souza et al., 2006). However, certain features are shared among the ancestors of bloodfeeding arthropods. Traditionally accepted ancestral pre-conditions to bloodfeeding include: 1) living in close proximity to vertebrates, 2) specialized feeding on skin remains, dung or fluids from animal carcasses and 3) specialized mouthparts for piercing and cutting (Graça-Souza et al., 2006). It is quite interesting that hematophagous arthropods can consume anywhere from 2 to 100x their normal body weight during a single blood meal. Subsequently, this blood meal, comprised largely of proteins, is digested by enzymes secreted from midgut epithelial cells (Barillas-Mury and Wells, 1993; Brackney et al., 2010; Edwards et al., 2000; Jiang et al., 1997). The amino acids that result from blood meal protein digestion are used for lipid, carbohydrate, and egg protein synthesis (Marquardt and Kondratieff, 2005). While the blood feeding process has obvious nutritional advantages for hematophagous arthropods, the digestive process releases the pro-oxidant molecules heme and iron in potentially toxic quantities. In response to this challenge, bloodfeeding arthropods have evolved a number of strategies to limit oxidative damage during blood digestion. This review seeks to compile and compare existing vertebrate and invertebrate literature as it pertains to iron and heme processing, with particular interest in applying knowledge gained in other systems to hematophagous arthropods.

Protective Adaptations Against Oxidative Stress After a Blood Meal: Specialized Midgut Defense Mechanisms

Hematophagous arthropods have evolved specialized defense mechanisms to avoid heme toxicity during blood meal digestion such as the hemosomes in the cattle tick (Braz et al., 1999; Lara et al., 2003), and Type I peritrophic matrix formation in larval and nymphal *Ixodes scapularis* ticks and adult Dipteran mosquitoes (except Tsetse adults which form Type II PM) (Narasimhan et al., 2014; Peters, 1992; Rose et al., 2014). Interestingly, all of the above-mentioned structures function in heme detoxification through various specialized forms of aggregation (Graça-Souza et al., 2006). Below we have highlighted recent advancements in knowledge regarding each of these structures, but refer the reader to Graça-Souza et al. (2006) for a more detailed review of earlier literature (Graça-Souza et al., 2006).

R. microplus are unable to endogenously synthesize heme (Braz et al., 1999). For the first seven days after a blood meal, hemoglobin-derived heme is directly absorbed for vitellogenesis (Lara et al., 2003). During this time, the largest amount of heme is concentrated at the basal lamina side of midgut digestive cells (closest to hemocoel) (Lara et al., 2003). This contrasts with other hematophagous arthropods where digestion occurs in the midgut lumen. After the first seven days PBM, the amount of heme absorption decreases and heme concentrates in midgut digestive cell organelles that specialize in heme sequestration, termed hemosomes (Lara et al., 2003). By the end of blood meal digestion, the mass of an individual hemosome was reported to be 90% heme (Lara et al., 2003). More recently, Lara et al. (2015) proposed a detailed model for heme movement in digestive cells of *R. microplus*. However, there remain unanswered questions regarding

movement of heme from digestive vesicles to the intracellular hemosomes (Lara et al., 2015).

While digestive cell hemosomes (*R. microplus*) have been documented as protective mechanisms against oxidative stress, *I. scapularis* ticks (vector of *Borrelia burgdorferi*) (Narasimhan et al., 2014) and most adult Dipterans (biting flies and mosquitoes) produce a peritrophic matrix in response to bloodfeeding (Devenport et al., 2006; Devenport et al., 2005; Dimopoulos et al., 1998; Dinglasan et al., 2009; Hao and Aksoy, 2002; Jochim et al., 2008; Morlais and Severson, 2001; Narasimhan et al., 2014; Ramalho-Ortigão et al., 2007; Rose et al., 2014; Shao et al., 2005; Shao et al., 2001; Shen and Jacobs-Lorena, 1998).

The peritrophic matrix (PM) is a semipermeable extracellular layer, which lines the midgut of most invertebrates (Peters, 1992; Tellam et al., 1999). The peritrophic matrix is classified as Type I or Type II based on location of synthesis within the insect midgut (Peters, 1992). The Type I peritrophic matrix is completely synthesized by midgut epithelial cells (Tellam et al., 1999). In contrast, the Type II peritrophic matrix is constitutively secreted by the cardia, a specialized organ found between the foregut and midgut (Moskalyk et al., 1996; Stohler, 1961; Tellam et al., 1999). Type I PM formation is induced by midgut distension (Freyvogel and Jaquet, 1965; Richards and Richards, 1977) and it is comprised of proteins, proteoglycans, and chitin fibrils (Pascoa et al., 2002; Shao et al., 2001). Peritrophic matrix proteins are integral components of the PM, and are commonly referred to as peritrophins (Tellam et al., 1999). Peritrophins are characterized by the presence of a secretory signal peptide, multiple chitin-binding domains containing cysteine-proline dipeptides, and intervening mucin-like domains rich in proline, serine, and

threonine (Tellam et al., 1999). The multiple chitin-binding domains of peritrophic matrix peritrophins function as cross-linkers for chitin fibrils, thereby providing structure and support for the peritrophic matrix (Schorderet et al., 1998; Shen and Jacobs-Lorena, 1998). In addition, PM peritrophins contain aromatic amino acid residues that facilitate binding with N-acetyl-glucosamine of the chitin fibrils (Toprak et al., 2010).

In addition to binding chitin, one peritrophin has been reported to bind heme. *Ae. aegypti* intestinal mucin 1 (AeIMUCI) is a 275-amino acid glycoprotein that contains three chitin-binding domains and a mucin domain between CBD 1 and CBD 2(Devenport et al., 2006; Rayms-Keller et al., 2000). Rayms-Keller et al. (2000) first identified *Ae*IMUC1 RNA in metal exposed *Ae. aegypti* mosquito larvae, metal fed adult females and blood-fed adult females (Rayms-Keller et al., 2000). Devenport et al. (2006), confirmed chitin and heme binding for AeIMUC1. Through deletion analysis using recombinant proteins, they also determined that chitin-binding and heme-binding functions are associated with the 3 CBDs of AeIMUC1 (Devenport et al., 2006). Most importantly, they confirmed AeIMUC1 as an integral PM peritrophin associated with the PM 12 to 24 hours post bloodfeeding (Devenport et al., 2006). Taken together, results from previous AeIMUC1 studies suggest this protein is important for PM structural integrity (Devenport et al., 2006) and blood meal heme detoxification (Devenport et al., 2006; Rayms-Keller et al., 2000). However, studies suggest there are potentially more *Ae. aegypti* midgut peritrophic matrix peritrophins (Moskalyk et al., 1996; Pascoa et al., 2002).

Despite the highly successful strategies deployed by bloodfeeding arthropods to sequester heme during the process of blood digestion, heme and molecular iron are also critical nutrients that must be absorbed during digestion and transported throughout the

body. In the following sections, we discuss recent progress on understanding heme and iron transport across cell membranes, as well as trafficking, packaging, signaling and ultimate deposition into the ovaries for oogenesis, in order to systematically track the fate of blood meal heme and iron in medically important hematophagous arthropods.

Heme Uptake Across Cell Membranes

Despite its importance as a nutrient and signaling molecule (Bottino-Rojas et al., 2015; Hooda et al., 2014), surprisingly little is known about heme transport/uptake in arthropods. New developments in this area would seem to be promising targets, particularly since this subject has been explored in many other organisms including mammals, fish, yeast and worms, as moving heme from either its point of synthesis (mitochondria) or from the diet (extracellular space) to the cell cytoplasm involves crossing membranes.

The feline leukemia virus subgroup C receptor (FLVCR1) heme transporter has been characterized in both humans and mice (Byon et al., 2013; Philip et al., 2015; Quigley et al., 2004; Vinchi et al., 2014). Flvcr1a is a 12 transmembrane (TM) domain protein while Flcvr1b is a 6 TM domain protein which is thought to homo/heterodimerize to form a functional transporter. Recently, Mercurio et al. (2015) found that Flvcr1a and Flvcr1b were both required for development of committed erythroid progenitors with Flvr1a exporting heme through the plasma membrane into the extracellular space while Flvr1b exports heme into the mitochondria (Mercurio et al., 2015). In erythroid cells, heme regulation is particularly important because it ensures the balanced production of the globin chain components (Tahara et al., 2004a; Tahara et al., 2004b). Experiments using

knockout mice showed that Flvcr1a and Flvcr1b both play a role in the expansion of committed erythroid progenitors as production of hemoglobin was reduced but only Flvcr1b is indispensable during terminal erythroid differentiation due to a block at the pro-erythroblast stage (Mercurio et al., 2015). RNAi in human lymphoblast K562 cells showed that the coordinated expression of both isoforms controls the cytosolic free heme pool; Flvcr1a deficiency resulted in cytosolic heme accumulation detrimentally effecting cell proliferation but promoted differentiation, while mitochondrial heme accumulation due to Flvcr1b loss was deleterious to both processes. While Flvcr1 has been characterized in vertebrates, a potential role in arthropod heme transport has not been explored.

In 2008, a new family of heme transporters was identified in the nematode *Caenorhabditis elegans*. Rajagopal et al. (2008) performed a genome-wide microarray analysis to identify genes transcriptionally regulated by heme and found F36H1.5 (hrg-4) and its 3 paralogues, R02E12.6 (hrg-1), F36H1.9 (hrg-5) and F36H1.10 (hrg-6) with only two, hrg-1 and hrg-4, found to be highly responsive to heme deficiency and the only genes that were not nematode-specific. White et al. (2013) identified a human/mouse hrg-1 ortholog localized on the macrophage phagolysosomal membranes in mice by immunofluorescence microscopy (White et al., 2013). Immunohistochemistry showed high levels of hrg-1 in the macrophages present in the tissues responsible for high levels of recycling of heme iron obtained from degraded red blood cells, the spleen, liver and bone marrow of mice and humans. Knockdown of the gene by siRNA in mice bone marrow-derived macrophages resulted in a reduction of the heme regulatory pool while overexpression increased cellular heme availability. Toh et al (2015) identified and characterized an hrg-1 ortholog in the blood fluke *Schistosoma mansoni* (Smhrg-1), which

had a low sequence identity and homology to the *C. elegans* genes hrg-1 and hrg-4 and was found localized via palladium mesoporphyrin IX fluorescence in the vitelline and ovary regions of the females of the species (Toh et al., 2015). However, heme transport by Smhrg-1 was only identified in these organs indicating that the heme transport mechanism after digestion to the vitelline and the ovary regions is not due to Smhrg-1 but some other unknown mechanism. A *Leishmania amazonensis* homolog of the *C. elegans* heme transporter hrg-4, LHR1, was identified by Huynh et al. (2012), and was found to localize to both the plasma membrane and the lysosomes as determined by measurement of GFP-LHR1 fusion proteins in cells via confocal laser fluorescence microscopy (Huynh et al., 2012; Rajagopal et al., 2008). Subsequent failure to generate a full knockout of LHR1 was interpreted to indicate the essential nature of this gene to organism survival. Partial knockout and overexpression resulted in reduced heme uptake and increased uptake respectively as measured by zinc mesoporphyrin (ZnMP). Taken together these three observations indicated that LHR1 accounts for the majority of the heme transport activity in *L. amazonensis*. Topology modeling identified four predicted transmembrane domains and cytoplasmic N- and C- termini in *C. elegans* hrg-1 and hrg-4 as well as LHR1 in *L. amazonensis* indicating similar protein structure between hrg family members in these distant eukaryotes (Huynh et al., 2012; Rajagopal et al., 2008).The fact that members of the hrg gene family are present in humans, worms and single-cell protozoan parasites suggests that this gene family is very ancient, however orthologues of this gene family in bloodfeeding arthropods have not been described.

Recently, Lara et al. (2015) identified ATP binding cassette subtype B10 (ABCB10) as a heme transporter in the midgut cells of R. *microplus*. Incubation of midgut

cells with Rhodamine 123 (a PgP protein transporter substrate), separately or combined with CsA (an ABC inhibitor) confirmed an ABC transporter was responsible for heme transport after a bloodmeal, while an anti-PgP-1 antibody identified the membrane of digestive vacuoles to be its location in the cells. RNAi of the RmABCB10 transporter in female blood fed ticks and Zinc protoporphyrin IX (ZnPp) fluorescence showed reduced ZnPp in the hemosomes, but more in the digestive vacuoles, which confirmed RmABCB10 as the transporter characterized above. Lara et al. (2015) confirmed previous reports that identified ABC transporters as key components of detoxification of acaricides by showing that Tin protoporphyrin IX and amitraz transport to the hemosome are increased in the amitraz-resistant Ibirapuã strain when compared to wild type (Koh-Tan et al., 2016; Lara et al., 2015; Pohl et al., 2014; Pohl et al., 2011; Pohl et al., 2012). Mangia et al. (2016) expanded this to *Ixodes ricinus* by examining expression of ABCB1, ABCB6, ABCB8 and ABCB10 after ivermectin treatment in cultured cells (Mangia et al., 2016). The authors found that only ABCB8 showed changes in expression showing a low-dose stimulation, but a high-dose return to control levels after exposure the increasing concentration of ivermectin. These results taken together indicate that ABC transporters transport acaricides in the detoxification pathway of multiple tick species with some family members also transporting heme out of the digestive vacuoles. Like FLVCR and HRG genes, orthologues of ABCB10 have not been described to date in other bloodfeeding arthropods.

Pereira et al., (2007) found evidence of heme transport into the midgut epithelium cells in *Ae. aegypti* and export of its degradation product biglutaminyl-biliverdin back into the lumen for excretion (Pereira et al., 2007). The authors observed a change in color from red to green during bloodmeal digestion and upon analysis identified it as a bilin pigment.

Heme degradation occurs via the cytosolic heme oxygenase reaction, thus heme must enter the midgut epithelium to be degraded and then the biliverdin biproduct must be secreted, although the mechanisms behind the transport of these 2 molecules are unknown. RNA sequencing following heme exposure in *Ae. aegypti* cultured cells identified several potential transport-related proteins that could be involved in this transport mechanism (Bottino-Rojas et al., 2015), however their activity has not been characterized to date. Although, strong evidence of the capacity of heme transport is available for bloodfeeding arthropods, only 1 transporter, RmABCB10 had been characterized to date.

Heme Catabolism

After heme is imported into the cell, a conserved heme degradation pathway is present in many organisms, during which heme is broken down into biliverdin IX α (BV α), iron and CO by heme oxygenase (HO) [for recent reviews, see (Wegiel et al., 2014; Wilks and Heinzl, 2014)]. However, at least two bloodfeeding arthropods, *Aedes aegypti* and *Rhodnius prolixus*, deviate from this pathway as discussed below. In addition, many species of ticks have completely lost the ability to breakdown heme due to absence of key enzymes in the heme degradation pathway in their genomes (Braz et al., 1999; Paiva-Silva et al., 2006; Pereira et al., 2007; Perner et al., 2016). In *Ae. aegypti*, after BV IX, iron and CO are produced, two glutamine residues are added, as determined by electrospray ionization mass spectrometry (ESI-MS)(Pereira et al., 2007). A BV IX product with one glutamine residue was isolated with the final product in reverse phase HPLC indicating that the glutamines were sequentially added instead of simultaneously. This addition to BV IX yields a more soluble product, and was thought to reduce toxicity caused by the

accumulation of the heme byproducts in the midgut by allowing for easier excretion (Pereira et al., 2007). The formation of a green pigment identified as biglutaminyl BV IX in the lumen indicates that this byproduct must exit the midgut epithelium cells to be eventually excreted, although the mechanisms behind the transport are unknown. This mechanism is so far unique to *Ae. aegypti*, the pathways utilized by other bloodfeeding dipterans are currently unknown.

In all cases previously reported, heme is broken down by HO prior to any modifications to the porphyrin ring, however the kissing bug contains a unique pathway in which two cysteinylglycine residues are added before oxidative cleavage of the porphyrin ring yielding the end product of dicysteinyl-BV IX ɣ (RpBV) as determined by ESI-MS (Paiva-Silva et al., 2006). While the biological advantage to these added residues is not clear, Paiva-Silva et al. (2006) hypothesized this change in structure is also enacted to increase solubility of the byproducts, easing excretion as confirmed by its elution with a more hydrophilic retention time during reverse-phase HPLC than BV IX α. In addition, while RpBV has been identified as the end product, the method of residue addition and the order added are unknown. In mammals, all the degradation products produced by heme play key regulatory roles, for example CO has both anti-inflammatory and anti-apoptotic effects and BV may function as antioxidants, however these roles have not been explored in insects to date (Al-Owais et al., 2015; Brouard et al., 2002; Dore and Snyder, 1999; Otterbein et al., 2000; Sedlak and Snyder, 2004; Stocker, 2004; Stocker et al., 1987). Given at least two variations on heme degradation pathways in arthropods have been described so far, it is likely that there are more not yet discovered. Figure 1 details the proposed mechanisms of the *Ae. aegypti* and *R. prolixus* heme degradation pathways.

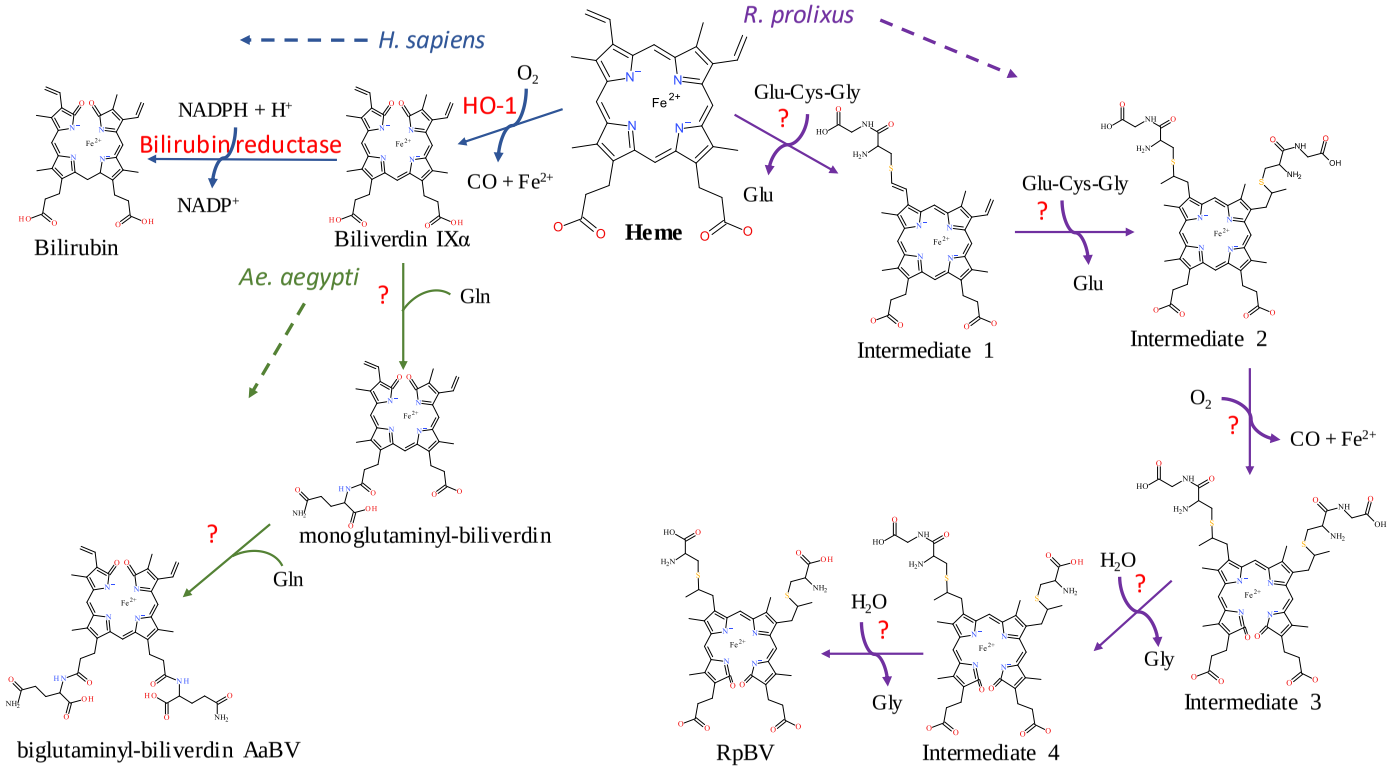

Figure 1: **Known heme degradation mechanisms**
The arthropods *Ae. aegypti* and *R. prolixus* have alternate heme degradation mechanisms from the shared mechanism of humans, mice and many other organisms. All three mechanisms are detailed above. Enzymes utilized for each reaction are given in red, with unknown enzymes indicated (?). The order in which the modifications are sequentially added to the intermediates in both the *Ae. aegypti* and *R. prolixus* mechanisms is not known, however only one method is detailed here for simplicity. The structural drawings shown here were made using BIOVIA 2017 R2 (Dassault Systemes, San Diego)

In *D. melanogaster*, heme oxygenase expression is necessary for the normal development of tissues. Whole body knockdown of HO in larval and pupal flies results in lethality, evidence of the necessity of heme-iron recycling in tissue development (Cui et al., 2008). Cui et al. (2008) observed the effects of tissue specific HO-knockdown utilizing the GMR-GAL4 driver system to target the eye imaginal discs which resulted in abnormal development of the adult eye tissue. Immunostaining the eye tissue of HO knockdown larvae revealed high concentrations of activated caspase 3, an apoptotic marker, as well as larger than normal iron deposits, both of which were thought to contribute to the rough eye phenotype observed. This observed phenotype was later linked to G1/S arrest of the cell cycle leading to cell death due to increased generation of reactive oxygen species (Ida et al., 2013). Ida et al. (2013) also observed a significant drop in proliferating cells and an increase of DNA damage detected in the eye imaginal discs of the larva after treatment with HO dsRNA. Ida et al. (2013) performed a genomic screen leading to the identification of eight genomic regions that suppressed the observed rough eye phenotype during HO knockdown. This indicates that specific genes on these isolated regions may interact with HO and help counteract its loss during a knockdown event, however further work is needed to isolate specific genes. Damulewicz et al. (2017) found that *ho* is a clock-controlled gene as it oscillates in expression during the day peaking at the beginning of the light phase and in the middle of the night (Damulewicz et al., 2017b). One of the reasons behind this pattern of oscillation was due to HO's protection of the retina photoreceptors against ROS-induced degradation brought on during the transition of the night to day phase at the start of UV and white light exposure. DNA damage was reduced when HO was activated by hemin and increased when HO activity was inhibited by Sn PP (Damulewicz

et al., 2017a, b). The decline in HO regulated two different canonical clock genes *period* and *clock*, increasing and decreasing respectively. This regulation is potentially mediated through CO as an increase in CO shows the same effect as the increase of HO expression (Damulewicz et al., 2017b). In conclusion, the results of the loss of HO in *Drosophila* tissues and whole body indicate that HO is very important for the successful development of these tissues. However, HO expression and its regulation of DNA damage response and canonical clock genes has not been examined in other insects. This would be particularly important to study in bloodfeeding arthropods as their ingestion of blood yields a much more iron rich diet than flies.

Iron Transport Across Cell Membranes

Iron-responsive genes including those implicated in membrane bound iron transport have been identified in multiple organisms, including arthropods [for recent reviews see, (Galay et al., 2015; Mandilaras et al., 2013). A recent study in *G. morsitans* for example, identified 150 iron-responsive genes, only two of which were previously identified, ferritin heavy chain and mRCK-alpha (Dashti et al., 2016; Tang and Zhou, 2013b). These genes were predicted by computational analysis of UTR regions searching for the characteristic stem loop structures present in iron regulatory element (IRE) regulated genes. Of these genes, 29 had functions potentially related to iron trafficking, including cell envelope, transport and binding proteins that localized in the extracellular environment or the plasma membrane. Genes involved in iron trafficking are particularly important for bloodfeeding arthropods as the blood meal contains a huge influx of iron in the form of transferrin and hemoglobin, 1884.8ng iron per female on average (Zhou et al., 2007).

Three genes in *Drosophila melanogaster* have been identified as playing a role in membrane bound iron transport, *malvolio (mvl)*, *zip13* and *mco1*. Mvl is a homolog of the human natural resistance-associated macrophage proteins (*Nramp*). Both loss and gain-of-function *mvl* mutants in adult flies resulted in altered taste perception, particularly sugar and salt perception (Rodrigues et al., 1995). Folwell et al. (2006) found high expression of *mvl* in adult and larval midgut tissue as well as in the Malpighian tubules, while elucidating its role in iron acquisition at multiple developmental stages and its role in divalent cation reabsorption (Folwell et al., 2006; Rodrigues et al., 1995). Subsequently, an ortholog of *Nramp/mvl* was also characterized in the mosquito *Anopheles albimanus* (Martínez-Barnetche et al., 2007). Martinez-Barnetche et al. (2007) determined that *anaNramp* localized to the head, midgut, Malpighian tubules and ovaries, the highest expression of which was in the Malpighian tubules (Martínez-Barnetche et al., 2007). These authors confirmed the role of *anaNramp* in Fe^{2+} transport by inducing full length cDNA expression in Xenopus embryos and measuring $^{59}Fe^{2+}$ isotope incorporation. An examination of the *anaNramp* 5' and 3' UTR sequences indicated that unlike *mvl*, no iron responsive elements (IRE) were present suggesting *anaNramp* may not be regulated by cytoplasmic Fe concentration. Few arthropods have been characterized that contain *h-Nramp* homologs, those that do contain the gene require further study as the regulation method behind their iron transport is unidentified.

Xiao et al. (2014) recently characterized the *Drosophila* ortholog of the human zinc iron permease 13 (*zip13*), an iron efflux pump that moves iron from the cytosol to the ER/Golgi (Xiao et al., 2014). RNAi knockdown of *dzip13* resulted in iron deficiency in the entire body of the fly with a reduction of about 50% of wild type iron levels except for iron in the cytosol of the gut cells which showed higher than wild type iron levels. On the other hand, *zip13* overexpression in the midgut resulted in increased iron content throughout the body. The authors then examined *ferritin* and *malvolio* as examples of genes involved in iron metabolism that could act as additional indicators of cytosolic iron levels. They found that when *zip13* expression was knocked down, ferritin expression increased and an Mvl expression decreased, with the opposite expression patterns observed when *dZip13* was overexpressed. The overexpression results matched ferritin and Mvl levels observed when larvae were fed an iron-supplemented diet indicating ferritin and Mvl expression levels seem to be a good indicator of cellular iron levels in *Drosophila*. With the exception of d*zip13* and *malvolio* no other iron transporters have been identified in *Drosophila*. While orthologs of *dzip13* and *malvolio* are present in many bloodfeeding arthropods, involvement in iron transport hasn't been confirmed in any to date, with the exception of *anaNramp* described above.

The multicopper oxidase enzyme family includes oxidases that target different types of substrates including iron, copper, ascorbic acid and bilirubin (Sakurai and Kataoka, 2007). dMCO1, while not an iron transporter, facilitates transport by acting as a ferroxidase at the membrane which oxidizes reactive aqueous ferrous iron (Fe^{2+}) to ferric iron (Fe^{3+}) in the hemolymph allowing its binding to transferrin and similar iron binding proteins for transport in *D. melanogaster*. Lang et al. (2012) found dMCO1 localized to

both the digestive system and Malpighian tubules, specifically the basal surfaces of each using RT-PCR on organ extracts to calculate expression of the transcript, followed by immunostaining tissues to visualize its location (Lang et al., 2012). dMCO1's role in iron homeostasis was confirmed by RNAi knockdown experiments yielding increased longevity when flies fed on high iron food and a decreased iron accumulation in the body. The MCO gene family is conserved in coleopterans, lepidopterans and dipterans (Lang et al., 2012; Liu et al., 2015; Peng et al., 2015; Ye et al., 2015). *An. gambiae* contains 5 putative multicopper oxidases, with AgMCO1 considered the functional ortholog to dMCO1, though experimental confirmation of this is lacking (Gorman et al., 2008). Very few putative MCO enzymes have been characterized to date in bloodfeeding arthropods and those that do contain these enzymes, require further work to identify which substrate they target and whether or not they are involved in iron metabolism.

Iron Chaperones

Metallochaperones facilitate metal ion storage in target proteins via specific protein-protein interactions at their docking surface tuned to recognize these partner proteins (Rosenzweig, 2002). Iron metallochaperones could be particularly important to iron homeostasis as they bind and safely transport ferrous iron around the cell, preventing oxidative damage from occurring (Philpott et al., 2017). Four cytosolic iron metallochaperones were discovered in humans that are thought to aid in ferritin iron loading: human poly(rC)-binding protein 1 (PCBP1) and its paralogues PCBP2, PCBP3 and PCBP4. When either PCBP1 or PCBP2 and ferritin are expressed in yeast cells, the amount of iron loaded into ferritin drastically increased when compared to ferritin

expression by itself (Leidgens et al., 2013; Shi et al., 2008). This was confirmed by RNAi knockdown of PCBP1, PCBP2 or both proteins in human cultured cells and observation of the amount of ^{55}Fe incorporated into endogenous cytosolic ferritin, which led to similar reductions in iron uptake into ferritin compared to control cells indicating that both proteins are needed independently for efficient delivery of iron to ferritin (Leidgens et al., 2013; Shi et al., 2008). The other two family members, PCBP3 and PCBP4 also showed increased iron loading into ferritin (Leidgens et al., 2013). PCBP2 was also shown to interact with NRAMP2 via its cytoplasmic N-terminal region and with ferroportin, the main ferrous iron exporter, lending further credence to its function as an iron chaperone (Yanatori et al., 2014). Interestingly, HO1 was found to complex with PCBP2 but not any of its paralogues (PCBP1, 3 or 4) or the NADPH-cytochrome P450 reductase (CDR) complex competitively, with PCBP2 affinity to HO1 seeing a significant reduction when in heme loaded cells or when PCBP2 is bound to ferrous iron (Yanatori et al., 2017). While these proteins have been characterized in humans, orthologous proteins have not been characterized in any arthropod species to date. If orthologues of the PCBP family of proteins exist in bloodfeeding arthropods, these could indicate a possible missing link in known mechanisms related to iron homeostasis as they may be involved in ferrous iron transport through the midgut epithelium cells, thus preventing the oxidative damage associated with free ferrous iron in the cell.

Iron Packaging and Ferritin Shuttling

Free iron can enter the cytosol through direct transport from outside the cell or be released internally following heme catabolism. Fe^{2+} is the reactive soluble form of iron

while Fe^{3+} is both unreactive and insoluble. Ferritins chaperone and transport iron preventing large concentrations of cytosolic Fe^{2+} which can easily react with lipids, proteins and other cellular components causing oxidative damage. The Ferritin-like superfamily is present in many organisms including arthropods, with all individual members thought to be evolved from a rubrerythrin-like ancestor which played a role in the defense against reactive oxygen species (Andrews, 2010). Ferritin is typically composed of 24 subunits, which fold to create a large cavity that can store 1500+ Fe^{3+} molecules as well as smaller amounts of other metals like zinc and magnesium (Gutierrez et al., 2013). Insects have two ferritin subunits, very similar to vertebrate ferritin subunits, heavy-chain homolog (HCH) and light-chain homolog (LCH) (Pham and Winzerling, 2010). HCH, like dMCO1, also has ferroxidase activity and thus catalyzes the oxidization of Fe^{2+} to Fe^{3+} for storage in ferritin; LCH is involved in iron core formation. In most insects, ferritin contains a signal peptide directing it to the endoplasmic reticulum for translation where it stays until iron loaded ferritin is exported out of the cell via secretory vesicles (Dunkov and Georgieva, 2006; Nichol et al., 2002; Pham and Winzerling, 2010). As ferritin loading occurs in the ER and not the basal surface of the midgut epithelial membrane, dMCO1's ferroxidase activity is not utilized to facilitate loading of the iron into ferritin. Excellent reviews are available covering insect ferritins (Dunkov and Georgieva, 2006; Pham and Winzerling, 2010; Tang and Zhou, 2013b), so they are only mentioned briefly here.

Loss of ferritin following gene knockdown or knockout resulted in growth abnormalities ending in death in *D. melanogaster* (González-Morales et al., 2015). Lack of iron present in embryos either due to knockout of ferritin or lack of maternally derived iron also resulted in serious abnormalities often culminating in death during early development.

When midgut specific knockdown was performed in *D. melanogaster*, iron accumulated in the iron cell region while systematic iron deficiency was observed throughout the rest of the body, confirming the importance of ferritin in serving as a transport mechanism (Tang and Zhou, 2013a). However, the exact mechanism of ferritin iron transport to non-intestinal tissues after its export out of the midgut epithelium remains unknown, as while labeled ferritin or its substrate iron has been identified in multiple tissues across both *D. melanogaster* and *Ae. aegypti* their entry method into other cellular tissues remains uncharacterized (Li, 2010; Tang and Zhou, 2013a; Zhou et al., 2007).

In mosquitoes and other bloodfeeding arthropods ferritin is particularly important due to the large influx of iron they obtain during a blood meal. In *Ae. aegypti*, both ferritin subunits, HCH and LCH, increase in expression after an iron overload or a blood meal, indicating that ferritin may serve as a cytotoxic protector (Dunkov et al., 2002; Geiser et al., 2003). In mosquitoes, different cell types handle ferritin iron storage in different ways. Geiser et al. (2015) found that CCL-125 *Ae. aegypti* larval epithelial-like cells and 4a3b *An. gambiae* larval hemocyte-like cells experienced high levels of iron uptake using Calcein fluorescence assays upon exposure to high levels of iron (Geiser et al., 2009; González-Morales et al., 2015). However, the inductively coupled plasma mass spectrometry (ICP-MS) they performed showed low levels of cytoplasmic free iron present indicating that upon uptake, iron is immediately bound to proteins like ferritin and secreted (Geiser et al., 2009; González-Morales et al., 2015). When comparing the two cell types examined, Geiser et al. (2015) noted that after packaging of iron into ferritin occurred, the CCL-125 cells exported the ferritin out of the cell while 4a3b cells retained it. They speculated that since hemocyte cells are involved in the immune response, hoarding an

essential nutrient like iron is likely done to prevent foreign cells access to it providing a more hostile environment for their growth. This immune response is observed in both *Ae. aegypti* and *Bombyx mori* (silkworm), when ferritin is upregulated during bacterial infection lending evidence that host-bacteria regulatory mechanisms involving ferritin production do exist in these organisms (Geiser et al., 2013; Otho et al., 2016). However, the signaling mechanism which determines when secretion occurs, or which cell types secrete iron loaded ferritin or retain it has not been identified to date.

Ticks and insects have evolved different mechanisms to ensure free heme is dealt with during digestion, however they both utilize ferritin to package and transport the molecular iron absorbed from the blood meal (Donohue et al., 2009). Recently, Galay et al. (2013, 2014) characterized two distinct ferritins in the hard tick, *Haemaphysalis longicornis* (Galay et al., 2013; Galay et al., 2014). Hlfer1 and Hlfer2 both have unique functions: storage of iron in the midgut, and secretion from the midgut for transport to other organs with the subunit composition of each potentially controlling their different functions (Galay et al., 2013). Unlike *hlfer1*, the sequence of *hlfer2* lacks an IRE, indicating that it may not be regulated by cytoplasmic Fe concentration, and contains a signal peptide much like the secretory ferritin characterized by Hajdusek et al. (2009) in the hard tick *Ixodes ricinus* (Galay et al., 2013; Hajdusek et al., 2009). RNAi experiments showed the importance of both ferritins present to successful feeding and reproduction in both *H. longicornis* and *I. ricinus*. While intestinal cell types have been studied extensively, knowledge of the regulation of ferritin subunits in non-intestinal cell types and whether multiple subunits work together in different situations is lacking.

Transferrin is an iron binding glycoprotein that is also conserved between vertebrates and arthropods. Unlike ferritin, transferrin can only carry two molecules of Fe^{3+} at a time. In mammals, transferrin is primarily utilized in iron transport in the blood to bring iron to the erythrocytes to be utilized in heme production (Zhang and Enns, 2009). *D. melanogaster* transferrin and *Ae. aegypti* transferrin 1 were both found to be expressed in larval, pupal and adult stages but not in embryos, with expression in *Ae. aegypti* found mainly in the fat body where it is secreted into the hemolymph with high levels of juvenile hormone acting as a negative regulator of its expression (Harizanova et al., 2005; Yoshiga et al., 1999). A second transferrin gene was described in *Ae. aegypti* with weaker iron binding due to key amino acid mutations in the binding pocket as compared to other members of the transferrin family (Zhou et al., 2009). Expression of both genes differ in the adult female mosquitoes, with *AaTf1* expression highest at 24 hours post bloodmeal and *AaTf2* expression highest at 72 hours post bloodmeal compared to sugar fed females (Zhou et al., 2009). This difference in expression suggests distinct roles in iron metabolism, however the precise role these genes play remains to be determined. Bacterial infection of *Ae. aegypti* also increases transferrin expression, particularly of *AaTf1*, suggesting that *AaTf1* may play a role in sequestering iron during pathogen infection (Zhou et al., 2009). Other studies have also shown transferrin upregulation in mosquito host response to pathogen infection, particularly *Wuchereria bancrofti*, in *Ae. aegypti* and *C. quinquefasciatus* females (Magalhaes et al., 2008; Paily et al., 2007). An early genome survey by Dunkov et al (2006) identified members of the transferrin family in several insect species; including four in *A. gambiae* and *Ae. aegypti* (Dunkov and Georgieva, 2006). However, little is known about the biological role or specialization of these

transferrin genes. In summary, transferrin has been identified as an important regulator of iron homeostasis during blood digestion, larval and pupal development and bacterial infection in arthropods. However, most of the underlying data derives from inferred similarity with vertebrate transferrins. The exact signaling mechanism that activates transferrin expression upon pathogen infection has not been identified nor has the role of transferrin as an iron transporter been extensively studied in bloodfeeding insects.

Heme/Iron Signaling

In addition to its role as a nutrient, heme acts as a signaling molecule triggering many biological pathways. In *Ae. aegypti* cultured cells, heme was found to regulate the expression of several hundred transcripts, including those associated with redox stress, metabolism and transport related proteins, suggesting the existence of distinct signaling pathways regulated by heme (Bottino-Rojas et al., 2015). Analysis of these genes found that several immune genes were downregulated in response to heme exposure, indicating that the exposed cells may be more susceptible to immune challenge. This was confirmed both *in vitro* and *in vivo* by introduction of *E. cloacae* to heme incubated cultured cells and by orally challenging heme-fed females with *Serratia marcescens* resulting in diminished expression of immune genes both in cells and the midgut and a two-fold increase in microbial growth. However, the mechanism by which heme is affects the immune pathways and the molecular mechanisms behind certain induced genes are not currently well understood.

While the role of heme signaling in regulating the immune response of bloodfeeding arthropods is just being appreciated, the role of heme in regulating

reproduction in bloodfeeding mosquitoes is well established. In the arthropods *D. melanogaster* and *Ae. aegypti,* heme binding to the nuclear receptor E75 can result in the activation of the steroid hormone 20-hydroxyecdysone (20E), a key component in molting, metamorphosis and vitellogenesis (Kokoza et al., 2001; Martin et al., 2001; Segraves, 1994; Thummel, 1996). Cruz et al. (2012) found that heme was required for mediating 20E action via its stabilization of E75, implying its role as a signaling molecule to indicate the availability of a blood meal for vitellogenesis. E75's ligand binding pocket was characterized by Reinking et al. in *D. melanogaster*, where a single heme molecule was identified as a tightly bound prosthetic group (Reinking et al., 2005). The *Ae. aegypti* ortholog, like its *Drosophila* counterpart, has three isoforms, all three of which are vital to the regulation of multiple genes (Cruz et al., 2012; Pierceall et al., 1999; Segraves and Woldin, 1993). Aicart-Ramos (Aicart-Ramos et al., 2012) examined the heme binding of E75 hemoproteins in four different species of insect, *D. melanogaster, B. mori, O. fasciatus* and *B. germanica*. In the first two insects, heme is only tightly bound while in the latter two it is covalently attached (Aicart-Ramos et al., 2012; Reinking et al., 2005). In all four insects, heme is so tightly bound that E75 could not be purified without it. Reinking et al. (2005) also described E75 as a potential heme sensor, because upon treatment of cultured cells with an increased concentration of heme, the cells induced up to 8-fold increase of E75 expression indicating that the expression of E75 is directly proportional to the available heme level (Reinking et al., 2005). Aicart-Ramos et al (2012), however disagreed with this definition, stating that heme's tightly bound nature precludes it from acting as a heme sensor, since a heme sensor must be able to reversibly bind heme [for a detailed review of heme sensor proteins see (Girvan and Munro, 2013). However, this

appears to be a disagreement concerning the definition of a heme sensor, not experimental evidence disproving the evidence collected by Reinking et al (2005) (Aicart-Ramos et al., 2012; Reinking et al., 2005).

The regulation of E75 by·NO and CO, common in many organisms, occurs when either gas binds the heme-E75 complex, which blocks the heme active site and prevents binding to E75's other regulatory targets [for detailed reviews on NO and CO signaling see (Farrugia and Szurszewski, 2014; Gullotta et al., 2012; Jeffrey Man et al., 2014)]. Therefore, E75 is likely to act as a cellular oxidative state sensor since these gaseous molecules can only bind to ferrous iron not ferric, thus binding would only occur when the cellular state was reduced enough to allow the heme iron to be in its ferrous state (Figure 2). To determine E75's status as a redox sensor, further work must be completed to determine if the cellular environment can actually affect the binding capacity of the protein.

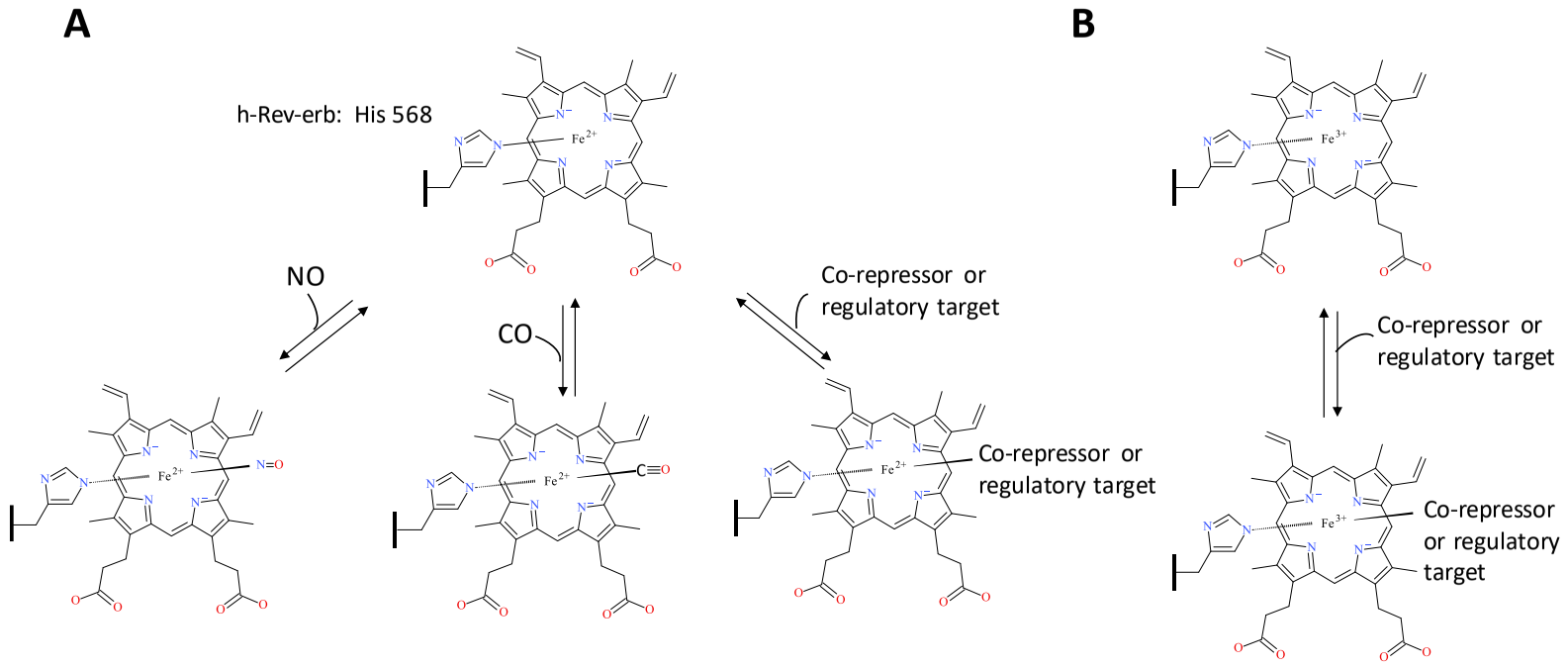

Figure 2. E75-Heme as a cellular oxidative state sensor
The human ortholog of insect E75, h-Rev-erb, acts as a carbon monoxide and nitric oxide sensor when the cell exists in a reducing environment, inhibiting binding of Rev-erb to its co-repressors and regulatory targets (A). Rev-erb's gas sensor ability is not present during a cellular oxidizing environment allowing uninhibited binding to its co-repressors and regulatory targets (B). The structural drawings shown here were made using BIOVIA 2017 R2 (Dassault Systemes, San Diego)

Conclusions

Although many arthropods have evolved the ability to feed on blood, relatively little insight into the internal processing of blood meal heme and iron is available. Much of the available information regarding iron processing in arthropods, more specifically insects, is gleaned from *Drosophila melanogaster*. While certain life history traits make *D. melanogaster* a powerful model organism, they do not blood feed, highlighting the need to perform direct experimentation on the bloodfeeding arthropods.

Through this review, we provide a framework for future studies aimed at obtaining a better understanding as it relates to the fate of heme and iron processing in hematophagous arthropods (Figure 3). With recent advancements in scientific tools such as high-throughput protein and RNA analysis, as well as CRISPR/Cas9, we are optimistic that many questions related to the detoxification, acquisition, transport and ultimate fate of iron/heme in bloodfeeding arthropods can be effectively addressed. Below we have highlighted some key take away points and scientific knowledge gaps that await tackling.

- Heme aggregation appears to be a common first line of defense in many hematophagous arthropods. Better understanding of this multifaceted protection playbook for each hematophagous arthropod can provide insight into key targets for breakdown of this system.

- To date, only one quantitative analysis tracking the fate of blood meal iron in a hematophagous arthropod (*Ae. aegypti*) has been conducted (Zhou et al., 2007). A detailed road map for blood meal iron trafficking in other hematophagous arthropods is needed.
- Heme digestion and utilization regardless of its source, biosynthesis pathway or intake through diet, requires heme to pass across cell membranes. Despite, the characterization of membrane bound heme transport in vertebrates and nematodes, only one transporter has been characterized in a bloodfeeding arthropod to date indicating further work is needed to identify the heme import mechanisms utilized in these organisms.
- Heme catabolism by heme oxygenase 1 to biliverdin IX α, iron and CO is a conserved process in many organisms, however *Ae. aegypti* and *R. prolixus* deviate from this standard and produce alternate bilin pigments, thus there may be more deviations from the known standard yet to be discovered in other bloodfeeding arthropods.
- Heme oxygenase was shown to be essential to *D. melanogaster* tissue development as it regulates the DNA damage response and specific canonical clock gene expression. However, heme oxygenase's role in these two pathways has not been explored in bloodfeeding arthropods despite their diet consisting of a much more iron rich diet than flies.

- In *D. melanogaster*, three genes have been identified as membrane bound iron transporters or facilitators of this process, *mvl*, *zip13* and *mco1*. While orthologs of both *mvl* and *zip13* do exist in bloodfeeding arthropods, their involvement in iron transport has yet be examined in any to date, with the exception of *anaNramp*.
- The human poly(rC)-binding proteins (PCBP1-4) facilitate iron loading of ferritin. Homologues of these proteins in bloodfeeding arthropods could represent a missing link in iron homeostasis in these organisms.
- While ferritin or its substrate, dietary iron, has been localized in multiple tissues in both *D. melanogaster* and *Ae. aegypti* the mode of entry and recovery of iron from ferritin into cells and tissues remains uncharacterized.
- Transferrin, another conserved iron binding transport protein between vertebrates and arthropods, is found in many bloodfeeding arthropods. While transferrins have been shown to be upregulated after a bloodmeal or during pathogen infection, little is known about the biological role or specialization of these transferrin genes.

Figure 3. Fate of blood meal heme and iron in selected hematophagous arthropods.
Hematophagous arthropods ingest a large amount of blood during a single meal (2-3x, 10x and 100x their normal body weight for *Ae. aegypti*, *R. prolixus* and *R. microplus*, respectively). Hematophagous arthropods deploy a multifactor mechanism to avoid oxidative stress after a blood meal. This multifactor mechanism includes: **1**) Aggregation/crystallization of heme for excretion; **2**) Transport of heme and iron across plasma membranes; **3**) Intracellular degradation of heme by Heme Oxygenase (HO); **4**) Enzymatic (shown in dark blue) and non-enzymatic low molecular weight (LMW) antioxidant molecules; and **5**) Heme and iron carrier proteins (shown in purple) which deposit these two molecules into ovaries, nerves, muscle or other recipient tissue. Abbreviations: *Anopheles albimanus* natural resistance-associated macrophage protein (anaNRAMP), ATP binding cassette subtype B10 (ABCB10), carrier protein (CP), endoplasmic reticulum (ER), ecdysone-induced protein 75 (E75), Ferritin (Fer), glutathione S-transferase (GST), heme lipoprotein (HeLp), *Ixodes ricinus* carrier protein 3 (IrCP3), multicopper oxidase 1 (MCO1), poly(rC)-binding protein (PCBP), *Rhodnius prolixus* heme binding protein (RHBP), superoxide dismutase (SOD), zinc iron permease 13 (Zip13), 20-hydroxyecdysone (20E).

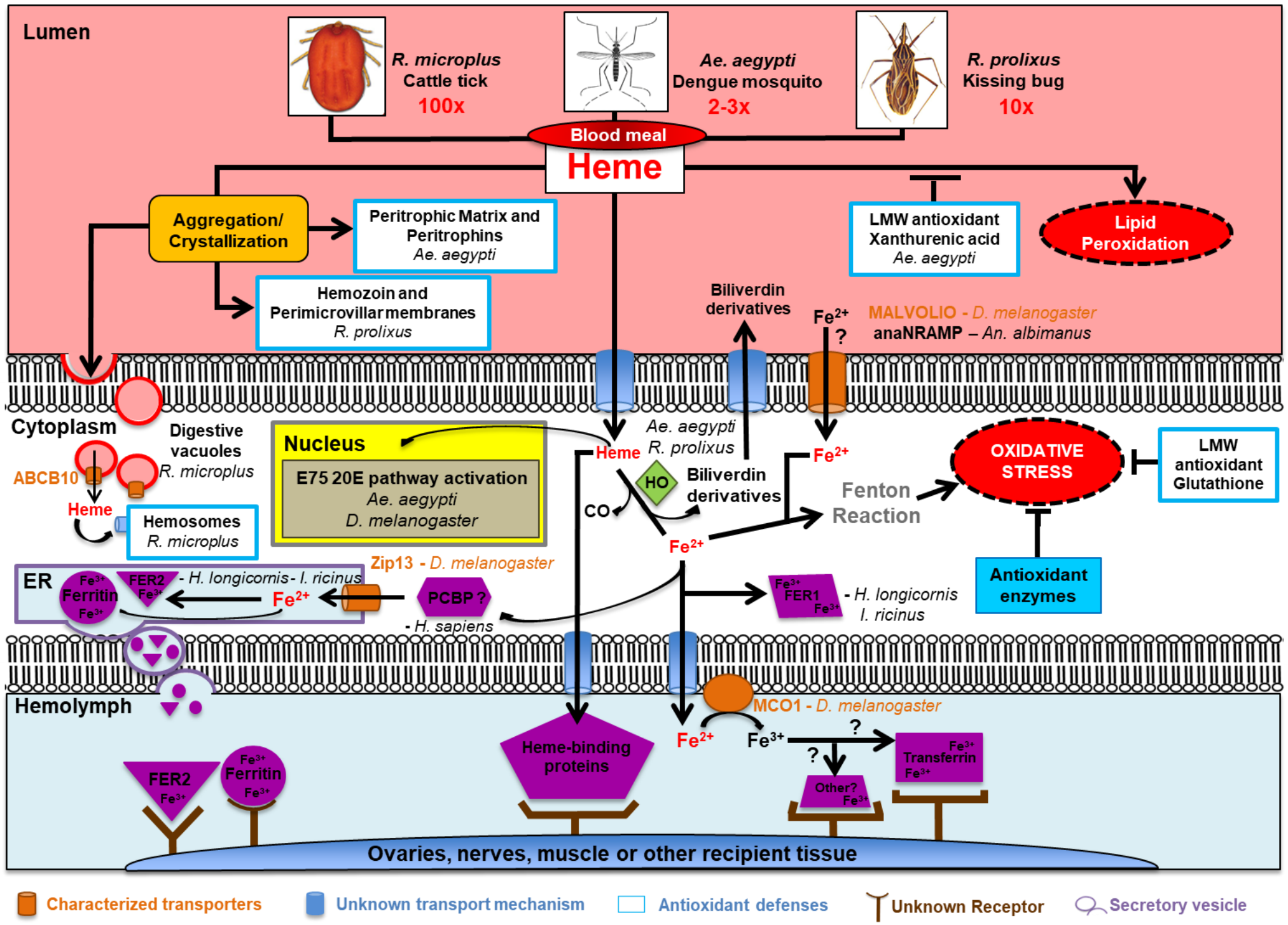

Figure 3. Continued

CHAPTER II

DIFFERENTIAL GENE EXPRESSION ANALYSIS OF CULTURED CELLS IN THE PRESENCE/ABSENCE OF HEME

Introduction

The culture of cells *in vitro* is a technique employed in many different organisms including insects, with the first successful insect immortalized lines created from the emperor gum moth in 1962 (Grace, 1962). Cell lines have many of the features of the organism they are derived from with the added benefit of allowing for sensitive and reproducible measurement of subtle changes in response to pathogens and other stimuli. The Aag2 cell line, derived from *Aedes aegypti* embryos (Peleg, 1968), has been characterized as an important model for pathogen immunity of the *Ae. aegypti* mosquito due to the similarity of immune responses observed between the two when infected with various types of pathogens including zymosan to induce experimental sterile inflammation, bacteria, and an active RNA interference pathway to target Sindbis virus and dengue virus as well as other viral vectors (Barletta et al., 2012; Sanchez-Vargas et al., 2009). In *Ae. aegypti* mosquitoes, the innate immune response to pathogen introduction includes multiple RNAi pathways with utilize small interfering RNAs, microRNAs or Piwi RNAs (Leger et al., 2013; Samuel et al., 2018).

In addition to the study of pathogen infection, cultured cells can be utilized to study the effects of exposure to chemicals and other potentially toxic stimuli. Heme, or iron protoporphyrin IX, is a pro-oxidant molecule that acts as an important nutrient across multiple species as it is a valuable source of iron for use in the synthesis of iron-containing

molecules and is often itself incorporated into hemoproteins with many diverse functions. Excess heme and iron can be toxic as their highly reactive nature can lead to the formation of reactive oxygen species. A study of heme and iron exposure in human intestinal Caco-2 cells found that while more iron entered the cell than heme iron upon exposure to the same concentration, heme-iron was more bioavailable (Arredondo et al., 2008). Arredondo et al. (2008) also determined that heme transport into the cell was both temperature dependent and saturated over time, thereby indicating that the mechanism behind this import involved both a receptor and the endocytic pathway. Heme fluorescent analogs like Zinc mesoporphyrin (ZnMP) can be used to characterize the type of heme transport into cultured cells. Worthington et al. (2001) examined ZnMP fluorescence in Caco-2 and the hepatic line HepG2 and showed that uptake was both dose and temperature dependent and that transport became saturated over time. In addition, co-exposure of ZnMP and heme resulted in ZnMP transport inhibition, and when cells were incubated with the heme synthesis inhibitor succinylacetone, ZnMP fluorescence increased indicating the possible ability of these cells to upregulate the heme import pathway (Worthington et al., 2001). These results taken together indicate the presence of a dedicated active heme transport mechanism in mammalian cells. While heme import has been extensively studied in mammalian cells, little is known about this topic in the *Aedes aegypti* mosquito, despite the vast quantity of heme released during blood digestion.

The RNA transcriptome, or the full range of mRNAs present in a cell or organism, changes in response to shifts in their external environmental conditions reflecting a shift in the number and type of genes expressed at any given time. These shifts in the transcriptome can be examined using next generation sequencing technology-based RNA

sequencing or the older method microarray gene expression analysis (Chu and Corey, 2012; Taub et al., 1983). A study of heme related transcriptome changes performed in Aag2 cells showed broad changes in gene expression upon exposure to 50µM heme in the areas of energy metabolism, cell cycling, immunity to pathogens and redox stress management (Bottino-Rojas et al., 2015). Most of the transcripts found regulated by heme in Aag2 cells were also found accumulated in adult female *Ae. aegypti* during blood digestion, indicating that the embryo derived cell line is a good model for examining the effects of heme exposure in the mosquito.

As the more well-known membrane bound heme transporters present in vertebrates are not conserved in *Ae. aegypti* [Chapter I and (Whiten et al., 2018a)], identification of previously unknown transporters is needed. A transcriptome analysis of *Ae. aegypti* cultured cells, embryo-derived Aag2 cells (Peleg, 1968) and larval-derived A20 (Mos20) cells (Varma and Pudney, 1969), incubated under heme overexposure and deficiency conditions was performed. The resulting transcriptomic changes indicated that many genes were differentially expressed in response to changes in heme concentration. A large number of genes containing transmembrane domains were isolated showing downregulation or upregulation in response to heme overexposure conditions indicating the possibility that heme membrane bound import and export genes were identified respectively, with the reverse trend observed in the presence of heme deficiency. However, few transporter candidate genes were identified that showed high differential expression (above 4-fold or below $1/4^{th}$ fold).

Methods

Cultured Cell Growth Conditions

Ae. aegypti A20 and Aag2 cells were maintained in Leibovitz's L-15 media (Gibco), supplemented with 10% FBS (Atlanta Biologicals) and 1% Pen-strep (Corning) at 28^{o}C. Aag2 cells were also maintained in Schneider's *Drosophila* Media (Thermo Fisher) with 10% FBS (Atlanta Biologicals) and 1% Pen-strep (Corning) at 28^{o}C.

Heme Dosage Experiment

Aag2 cells in Schneider's *Drosophila* media were treated with 0, 2.5 and 5µM Hemin Chloride (Sigma-Aldrich) or 0, 10 and 20µM Hemin Chloride. A20 cells in Leibovitz's L-15 media were treated with 0, 10 and 20µM Hemin Chloride. All cells were incubated in 12 well plates for 9 days in the heme treated media, cells were split every 3 days and reseeded onto a new plate with fresh media treatments, any remaining cells were pelleted and frozen at -80^{o}C at each timepoint.

RNA was isolated using the TRIzol reagent following the manufacturers protocol (Thermo Fisher) and the resulting RNA treated with DNase (DNase I: New England Biolabs). RNA was quantified using a Nanodrop (Thermo Fisher) and then 470ng RNA per sample was used to prepare cDNA using a random primer mix (SuperScript® IV Reverse Transcriptase: Thermo Fisher). Quantitative real-time PCR was performed using primers targeting AAEL008467 (Forward: CCGCACCAGAACCGACCACCAAT. Reverse: GACCCGGGCTTCAGCAGACCAC) a cysteine synthase as an indicator of heme stress using an Applied Biosystems^{TM} StepOne^{TM} Real-Time PCR System and Power SYBR® Green PCR Master Mix (Invitrogen). Actin primers (Forward: TTCGACGCTCAGTTGT.

Reverse: TTGGGGTACTTCAGGGTG) were used as a control across all samples with all plates and all samples were run in triplicate. The qPCR cycling conditions are given in Table 1. The amount of cDNA added per reaction was 2µL of a 1:10 dilution of the reverse transcriptase reaction products. The average cycle threshold (Ct) per sample was calculated and data was normalized by determining delta Ct using the Actin average Ct value for each sample. Finally, for each dataset, the DMSO control at day 0 was set to 0 and the log2 of values taken.

Table 1: qPCR cycling conditions

Temp (°C)	Time	
94	3 min	
94	30 sec	40 cycles
51	30 sec	
72	1 min	
72	10 min	

Zinc Mesoporphyrin Fluorescence Assay

Zinc Mesoporphyrin (ZnMP) (Frontier Scientific, Logan, UT) stock solution was made at 0.3mM concentration by dissolving the ZnMP into a 1% Ethanol-amine (Sigma Aldrich) and 10mg/mL Bovine Serum Albumin (Sigma Aldrich) solution (Vreman et al., 1989). This was filter sterilized using a 0.22µm filter (EMD Millipore), split into 500µL aliquots and stored at -20°C. Aag2 and A20 cells seeded onto 6-well plates were incubated for 72 hours in normal growth media, media containing 0µM heme or media + 10µM heme and were treated with 0, 2.5, 5, 10 & 20µM ZnMP for 30 minutes. The uptake buffer used during the incubation and wash procedures consisted of 50mM HEPES, pH 7.4, 130mM

NaCl, 10mM KCl, 1mM $CaCl_2$ and 1mM $MgSO_4$ (Worthington et al., 2001). All subsequent steps were performed in as dark of conditions as were practical. ZnMP stock solution was freshly diluted in uptake buffer prior to use and added to cells after medium was removed. Following the incubation, the cells were washed once with uptake buffer + 5% BSA, then 2x with uptake buffer. Cells were imaged in 1x PBS at 100x magnification using the DsRED filter or the propidium iodide (PI) filter of the EVOS FLoid Cell Imaging Station (Thermo Fisher) or the Zeiss Axio Observer Microscope (Carl Zeiss Microscopy, Thornwood NY).

Zinc Mesoporphyrin & Calcein AM Assay

Aag2 cells seeded onto 6-well plates were incubated for 48 hours in normal growth media, media containing 0µM heme and media + 10µM heme. The cells were then counted using a hemocytometer and a 96-well black clear bottomed BRANDplate® Cell grade Premium (Brand Wertheim, Germany) was seeded at 2 x 10^6 cells/mL per well and 32 wells per treatment type with a total volume in each well of 100µL. All subsequent steps were performed in as dark of conditions as were practical. Twenty-four hours later, the 96 well plate was incubated with 5µM ZnMP for 30 minutes at 28^{o}C, 100µL solution per well, after the media was removed from each well. Following the incubation, the cells were washed once with uptake buffer + 5% BSA, then 2x with uptake buffer, 100µL solution per well for each wash step. Next, 100µL of 2.5µM Calcein AM (Thermo Fisher) diluted in 1xPBS was added to each well and allowed to incubate at 28^{o}C for 30 minutes protected from light exposure. A total of 21 fluorescence measurements were measured across each well at Ex. 540/Em. 580 using a Spectramax i3x with the average fluorescence per well

determined from these values. The monochromator optical configuration, fluorescent read mode and well scan read type with pattern selected as 'fill' was selected for each Spectramax run. The number of cells present in each well was determined by Calcein fluorescence using a Minimax 300 (Molecular Devices, San Jose CA). The MiniMax optical configuration, Imaging read mode and Endpoint read type were selected for each Minimax run. Only the green channel was imaged, Ex. 456/Em. 541, with 4 photos taken per well focusing on the middle portion of each well. Pictures were taken at 5ms exposure and 120µm focus adjustment and cells were counted by training the software to identify cells based on their green fluorescence.

RNA-seq Treatments, Sample Preparation and Analysis

Aag2 cells were seeded in T25 flasks with 3 replicates treated with Schneider's *Drosophila* media +10% FBS +1% Pen-strep, while a separate set of 3 replicates were treated with the same media +20µM Hemin Chloride. All cells were incubated for 48 hours.

A20 cells were seeded into T25 flasks with 3 replicates treated with Leibovitz's L15 media + 10% FBS, 3 additional flasks treated with SF900II (Gibco) and a last 3 set of flasks treated with SF900II + 10µM Hemin Chloride. All cells were incubated for 72 hours prior to RNA extraction.

Aag2 cells were seeded into T25 flasks with 3 replicate flasks treated with Schneider's *Drosophila* media +10% FBS +1% Pen-strep (FBS), 3 additional flasks treated with Schneider's *Drosophila* media +1% Pen-strep (0µM Heme) and a last 3 set of flasks treated with Schneider's *Drosophila* media +1% Pen-strep (10µM Heme). All cells were incubated for 72 hours prior to RNA extraction.

Aag2 cells were seeded into T25 flasks with 3 replicate flasks treated with Leibovitz's L-15 media +10% FBS +1% Pen-strep (FBS), 3 additional flasks treated with Leibovitz's L15 media +1% Pen-strep (0µM Heme) and a last 3 set of flasks treated with Leibovitz's L15 media +1% Pen-strep (10µM Heme). All cells were incubated for 72 hours prior to RNA extraction.

All flasks had their media carefully removed to avoid disturbing the attached cells and were transferred to the chemical fume hood where the cells washed off with TRIzol (Thermo Fisher). The TRIzol solution was then transferred to a microcentrifuge tube and the RNA extracted following the standard manufacturer's protocol. The resulting RNA was DNase treated (DNase I: New England Biolabs) and then quantified using a Nanodrop (Thermo Fisher). One microgram of total RNA of each sample was prepared for sequencing using the TruSeq RNA v2 Illumina library preparation kit (Illumina San Diego, CA) or the NEBNext Ultra RNA library preparation kit (New England Biolabs Ipswich, MA). Both protocols utilized sequential first and second strand cDNA synthesis with random priming.

Sequencing & Computational Analysis

Paired-end mRNA sequencing with 150bp reads was performed on an Illumina HiSeq 2500 at the Genomics Sequencing Center at the Virginia Biocomplexity Institute for each set of cultured cell samples. Reads were aligned to the *Ae. aegypti* reference genome (AaegL5, obtained from www.vectorbase.org) using HISAT2 v2.1.0 with default parameters (Kim et al., 2015) through Texas A&M's High Performance Research Computing Ada server. Mapped reads were converted to BAM, sorted and the -q10 option

used to remove reads with low quality mapping scores with the SAMtools view and SAMtools sort v1.7. The number of reads per mRNA transcript was calculated with the CoverageBED command of the BEDtools suite v2.19.1. Differential expression was determined using EdgeR. Transcripts were only retained in the analysis if they had 5 or more read counts per million in 3 or more samples. Library normalization was performed by the weighted trimmed mean of M-values method. (Li, 2011; Li et al., 2009; McCarthy et al., 2012; Quinlan and Hall, 2010; Robinson et al., 2010). Transmembrane domain predictions of the genes found differentially expressed were determined by the TOPCONS webserver (Tsirigos et al., 2015). The mean number of genes with transmembrane domain predictions found in a subset of the *Ae. aegypti* gene pool was calculated for each of the differential expression analyses. The Linux command 'shuf' was used to randomly select a subset of genes from the gene list; the subset size was determined by the number of significant DE genes found in the comparison examined. The number of TM containing genes were counted using 'awk' and 'wc'. An example command is given here: "shuf -n 551 genes_TMdomain_predictions.txt |awk '$2 >= 1 {print $0}'|wc -l". This Linux command was repeated for a total of 30x and the average number of genes with predicted TM domains and the standard deviation were calculated. Lastly, a two-tailed z-test was performed for each comparison tested to determine whether the number of TM containing genes found in the analyses were significantly distinct from those found by random chance.

Soft cluster analysis was performed using the Mfuzz R package to identify genes with the expected expression pattern of heme importers and exporters (Futschik and Carlisle, 2005; Kumar and M, 2007). Default parameters were followed except for the

following: the optimal fuzzifier value, m, was determined using the mestimate function and the optimal number of clusters were determined using the cselection function. All four datasets were compared by using 4-way venn diagrams to identify candidate transporters found in more than 1 dataset.(Oliveros, 2007-2015)

qPCR Validation of Fold Change Values in Differential Expression Analysis

Aag2 cells treated with regular media growth media with or without the addition of 20µM hemin chloride were harvested and RNA extracted with the TRIzol reagent following the manufacturers protocol (Thermo Fisher) and then DNase treated (DNase I: New England Biolabs). RNA was quantified using a Nanodrop (Thermo Fisher) and then 380. One nanogram RNA per sample was used to prepare cDNA using a random primer mix (SuperScript® IV Reverse Transcriptase: Thermo Fisher). Quantitative real-time PCR was performed using primers targeting 6 genes highly differentially expressed in cell treated with heme for 48 hours; sequences and annealing temperatures for primers are given in Table 2. Primers were designed using SeqBuilder® software (SeqBuilder® v14 DNASTAR Madison, WI). RT-qPCR was run on an Applied Biosystems™ StepOne™ Real-Time PCR System and Power SYBR® Green PCR Master Mix (Invitrogen). Actin primers (Forward: TTCGACGCTCAGTTGT. Reverse: TTGGGGTACTTCAGGGTG) were used as a control across all samples with all plates and all samples were run in triplicate. The qPCR cycling conditions are given in Table 1. The amount of cDNA added per reaction was 2µL of a 1:10 dilution of the reverse transcriptase reaction products. The average cycle threshold (Ct) per sample was calculated and data was normalized by determining delta Ct using the Actin average Ct value for each sample.

Table 2: Primers used for qPCR

Name	Forward sequence	Reverse sequence	Temp
AAEL008467	CCGCACCAGAACCGACCACCAAT	GACCCGGGCTTCAGCAGACCAC	51
AAEL07383	TTCCCACGCCCACGACAAC	ACGCGCTCCCTACTCCACCTT	51
AAEL010105	TGCGGGCCCTGTCCATCAAC	GGCATAACCGCAGCTCCACTCCA	55
AAEL013407	TCCGGAGACTACCCATCAAATCA	CGGCACCAGCGAGTTCATC	51
AAEL014246	GCCGTGCTGGGTGGTTATGC	CTGCGGAGCTCCCTTGTGC	51

Results

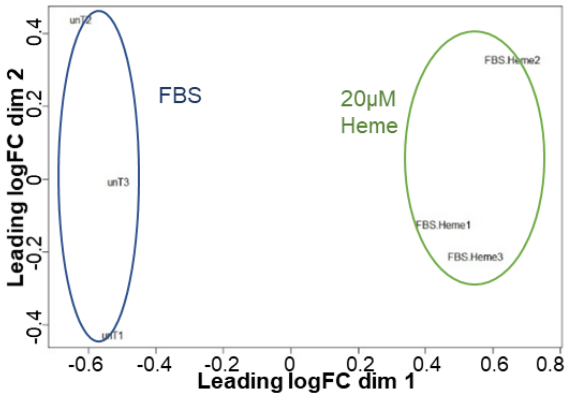

Figure 4: Multidimensional Scaling Plot of Aag2 cells treated with heme for 48 hours
Aag2 cells in Schneider's *Drosophila* medium +FBS & +FBS+ 20µM heme.

RNA Sequencing of Heme Overexposed Aag2 Cells in Schneider's Drosophila *Medium*

To examine the effects of heme exposure in *Aedes aegypti* cultured cells, RNA from heme treated Aag2 cells was harvested, cDNA libraries sequenced, and a differential expression analysis performed. Prior to differential expression analysis, an expression filter was applied to remove those genes with low expression across multiple samples; this

dropped the total genes in the analysis from 19712 to 8196. The multidimensional scaling plot for this analysis (Figure 4) shows that the replicate samples cluster together within the treatment groups, with the groups distinct from one another indicating that similar expression pattern was observed between replicates and differential expression was present between the 2 groups. We determined that 551 genes were significantly differentially expressed in the analysis with p-values adjusted for multiple testing of <0.0001, 269 which were upregulated and 282 downregulated during heme exposure as shown in Figure 5. Of these, we were particularly interested in multipass transmembrane proteins that might be responsible for the shuttling of heme between extracellular and intracellular space. To identify potential transmembrane transporters of heme we used the TOPCONS suite of prediction tools, which combines the predictions of multiple independent programs into a single best guess at the topology of each protein. Of the 551 genes found to be differentially expressed, 211 had at least 1 predicted transmembrane domain, with 106 upregulated and 105 downregulated in the presence of heme. If 551 genes were selected randomly from the entire *Ae. aegypti* gene pool, 175 of these would be TM domain containing genes on average. Therefore, a higher percentage of TM domain containing genes were found in this analysis than what was found by random chance (p-value=0.001248).

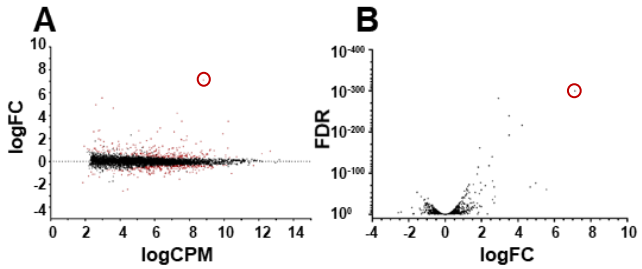

Figure 5: RNAseq-based differential expression after 48-hour heme treatment in Aag2 cells
Aag2 cells treated with Schneider's *Drosophila* medium + FBS vs medium+FBS+20µM heme. **(A)** Log2 fold change (logFC vs Log10 counts per million (logCPM) graph of genes found differentially expressed in analysis. Genes with an adjusted p-value corrected for multiple testing (False discovery rate: FDR) of <0.0001 are shown in red. **(B)** Volcano plot of genes found differentially expressed in analysis. The gene circled in red on both plots is the cysteine synthase AAEL008467

One of the genes most highly upregulated in the presence of heme, AAEL008467 (7.12 log2, ~140-fold change) was a cysteine synthase; the availability of cysteine being a limiting factor in the synthesis of glutathione, an antioxidant and free radical scavenger. High upregulation of this gene during heme overload could indicate substantial oxidative stress in these cells. One of the genes highly downregulated in the presence of heme, AAEL004870 (-1.83 log 2, ~3.56 fold change), was a cytochrome p450 a member of a large family of hemoproteins involved in the generation of reactive oxygen species (ROS) (see reviews: (Guengerich, 2007; Shoji and Watanabe, 2014; Zhu and Silverman, 2008)). As the high amount of heme present in the media would generate many ROS if not contained by chaperone proteins, the presence of a protein that generates ROS during these conditions would be unfavorable. Only 2 genes were identified as potential heme transporters as they have 2+ transmembrane domains and have over 4-fold expression change in the presence of heme, AAEL014246 (4.22 log2, ~18.7-fold change) a

glucosyl/glucuronosyl transferase and AAEL006113 (2.93, ~7.6 fold change) a cystinosin. Glucuronosyl transferases are involved in the removal of toxins and endogenous substances thus the high upregulation observed in the heme treated samples could indicate its involvement in heme detoxification. Cystinosin is a membrane bound cystine/H^+ symporter out of the secretory organelles. Cystine serves 2 main purposes, it serves as a site of redox reactions and as a mechanical linkage that allows proteins to retain their 3-dimensional structure. Thus, cystinosin seems to be involved in mitigation of the ROS generated by heme overload.

Multipass transmembrane domain containing genes with increased expression in the overload of heme when compared to cells grown in normal growth media may code for heme export proteins, while genes with decreased expression in the overload of heme may code for heme import proteins. A soft cluster analysis was performed to help identify those genes with these expression patterns from the list of genes present in the differential expression analysis (7707 genes). All genes that matched to a cluster in this analysis passed a membership score of 50% or greater, keeping 3247 genes split between the 6 clusters (Figure 6). Clusters 3 and 4 show the expected expression pattern of potential heme importer, of these, 455 (272 & 183 respectively) have at least 1 predicted TM domain. Clusters 5 and 6 show the expected expression pattern of heme exporter genes, of which 385 (71 & 314 respectively) have at least 1 predicted TM domain. The remaining clusters (clusters 1 & 2) shown in Figure 6 indicate those genes that do not appear to be regulated by heme exposure as some replicates of each treatment match expression pattern with some replicates of the other treatment.

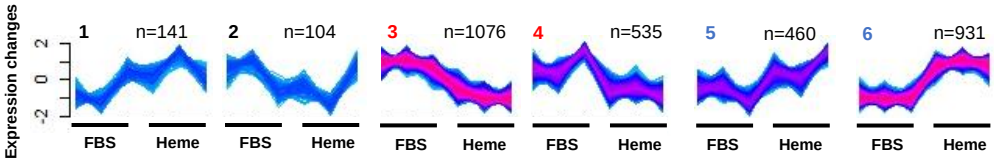

Figure 6: Cluster Analysis of Aag2 cells treated with heme in Schneider's *Drosophila* medium for 48 hours
Aag2 cells were treated in Schneider's *Drosophila* media with fetal bovine serum (FBS) or FBS and 20μM heme for 48 hours, 3 samples per treatment type. Six different clusters were identified during the analysis. Only genes containing a membership score of above 50% are shown in each cluster. Red lines indicate high membership values in the cluster, blue indicates low membership. Heme import clusters are highlighted in red and export clusters are highlighted in blue.

Ae. aegypti *Cultured Cells May Not Be Able to Limit Heme Uptake over Time*

Despite the successful identification of genes regulated by heme treatment, one of the assumptions of the previous experiment was that upon exposure to high heme concentrations, mosquito cultured cells can in fact modulate gene transcription to reduce heme uptake. To examine whether *Aedes aegypti* cultured cell lines Aag2 and A20 can in fact adapt to heme overexposure, both cell lines were exposed to high concentrations of heme over the course of 9 days. RNA was extracted at 0, 3, 6, & 9 days and the effects of heme exposure examined using AAEL008467, a cysteine synthase, as a marker of heme-induced cellular stress. AAEL008467 was selected for use in this analysis due to its high upregulation observed (7.12 log2, ~140-fold change), in the differential expression analysis in heme exposed cells. This high upregulation during heme overload may indicate this gene's importance in maintaining glutathione levels and thus redox balance during heme-induced cellular oxidative stress. Aag2 cells showed consistent upregulation of cysteine synthase after exposure to 10 & 20μM heme (Figure 7A, 7B). In contrast, A20 cells treated with heme showed no upregulation of AAEL008467 until day six, with

expression continuing to increase up to day nine, indicating that these cells were much more resistant to heme-induced oxidative stress (Figure 7C). Thus, both cell types were either not able to substantially prevent the import of heme or that heme oxidative damage to the exterior of the plasma membrane led to the oxidative stress observed.

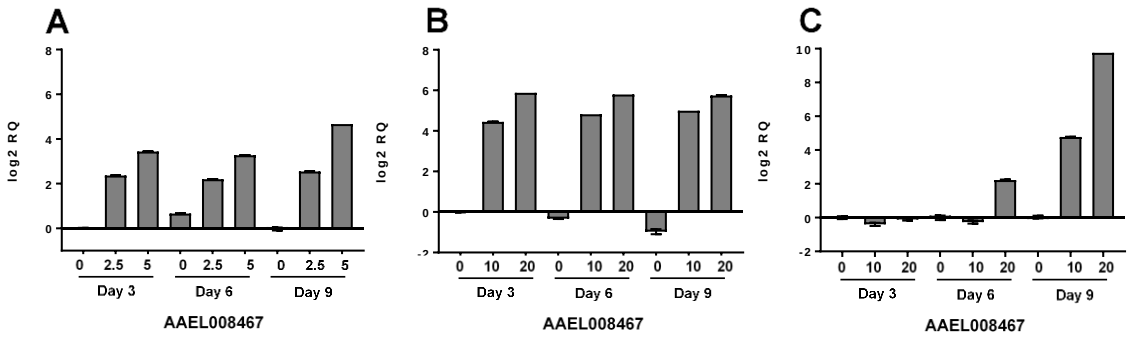

Figure 7: Heme treatment induces continuous activation of a cysteine synthase in cultured *Ae. aegypti* cell lines
(A) Aag2 cells in Schneider's *Drosophila* media with FBS and either 0, 2.5 or 5μM hemin chloride or **(B)** Aag2 cells in Schneider's *Drosophila* media with FBS and either 0, 10 or 20μM hemin chloride added. **(C)** A20 cells in Leibovitz's L15 media with FBS and either 0, 10 or 20μM hemin chloride added.

Heme Import Visualization Using Zinc Mesoporphyrin in Ae. aegypti *Cultured Cells*

As the ability of *Aedes aegypti* cultured cells to adapt to heme overexposure was called into question, we sought to determine whether these cells can adapt to heme deficiency conditions, prior to preparing further samples for transcriptional profiling. Zinc Mesoporphyrin (ZnMP), a heme fluorescent analog, was used to visualize heme uptake in cultured mosquito cells. Each cell line was incubated in heme-deficient media or media containing 10μM heme, with uptake of ZnMP compared to untreated cells. After 72 hours of incubation in treated media conditions, the cells were incubated with ZnMP and photos taken under fluorescent light. In all 3 experiments, uptake was observed at 10μM ZnMP in

all media conditions. However, only the heme-deficient treatments had detectable fluorescence at 5µM (Figures 8, 9 & 10A). This indicates that an upregulation of importers may have occurred when the cells were deprived of nutritional heme. To confirm this quantitatively, the total ZnMP fluorescence of cells treated with each media type was measured using a Spectramax i3x at Ex. 540/Em. 580. To account for the differing number of cells present in each well due to loss of cells during the wash steps prior to measurement, the number of cells in each well was calculated using Calcein fluorescence and the total ZnMP fluorescence normalized to obtain ZnMP fluorescence per cell. This analysis, shown in Figure 10B, confirms that cells grown in heme-deficient media do uptake more ZnMP than cells grown in either the normal media or heme treated cells. Interestingly, the heme-treated cells also had higher uptake of ZnMP than the FBS group, but lower than the heme deficiency group. This may be due to the unquantified amount of heme present in the normal growth media due to the FBS nutritional supplement present being higher than the 10µM added to the heme treated cells.

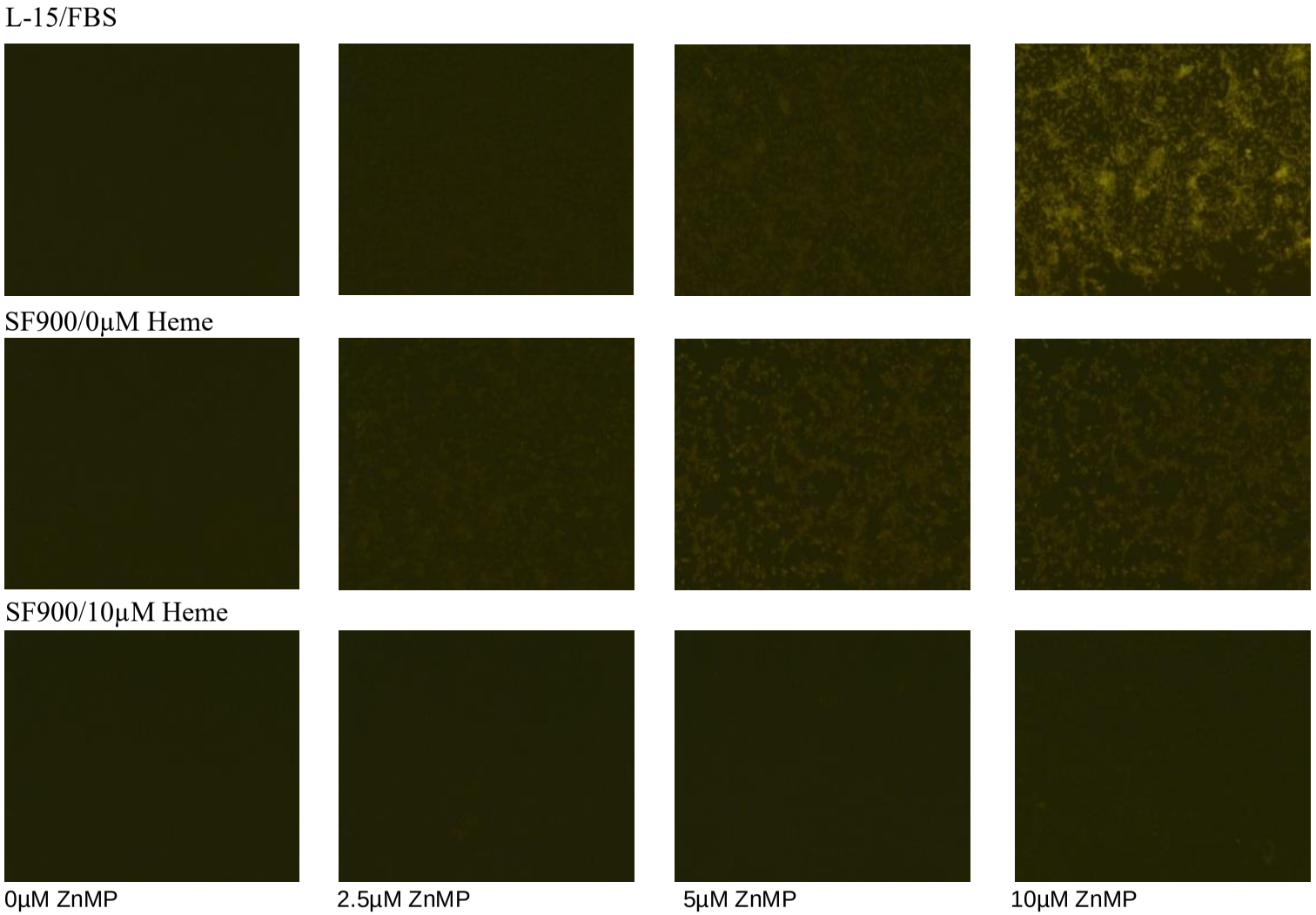

Figure 8: Heme deficiency treated A20 cells induces increased ZnMP fluorescence.
SF900 II is a serum free media. Leibovitz's L15 media with 10% fetal bovine serum (L-15/FBS). Photos were taken with a propidium iodide (PI) filter at 600ms exposure and 100x magnification.

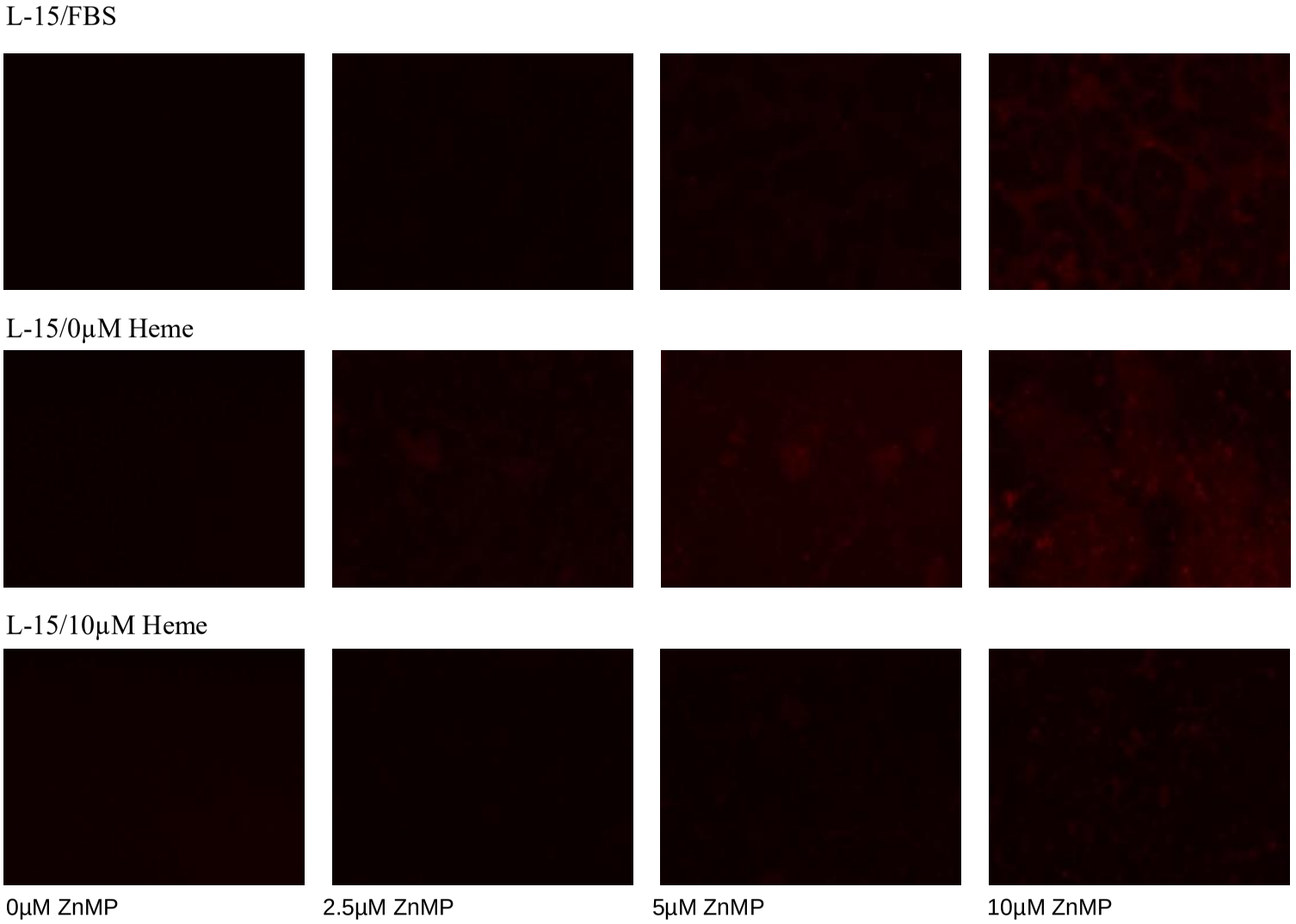

Figure 9: Heme deficiency treated Aag2 cells induces increased ZnMP fluorescence in L-15 media
Leibovitz's L15 media with 10% fetal bovine serum (L-15/FBS). Photos were taken with a DsRed filter at 80% light exposure and 100x magnification.

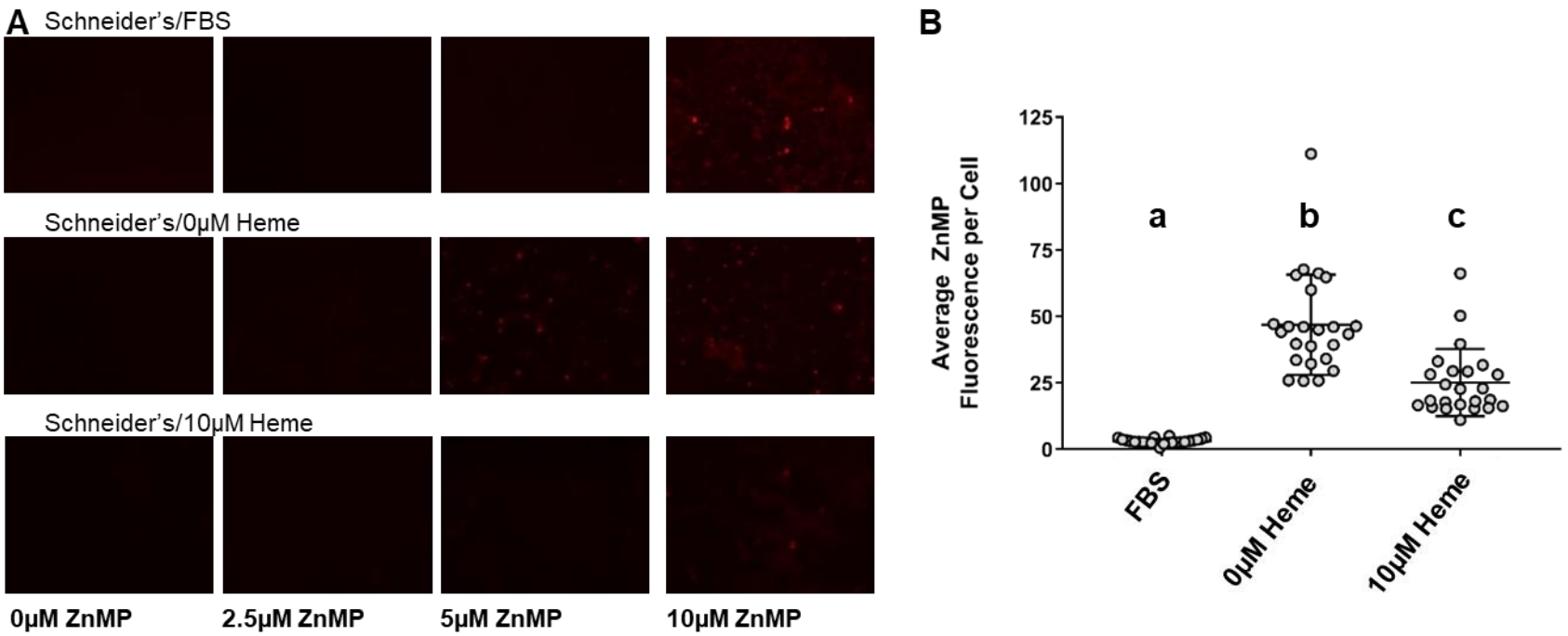

Figure 10: Heme deficiency treated Aag2 cells induces increased ZnMP fluorescence in Schneider's media
(A) Schneider's *Drosophila* media with 10% fetal bovine serum and 1% Pen-strep (Schneider's/FBS). Imaging was performed with a DsRED filter at 80% light and 100x magnification. **(B)** Cells exposed with each of the 3 treatments mentioned above were treated with 5μM ZnMP and fluorescence measured by the Spectramax i3x. ZnMP fluorescence was normalized by cell counts as determined by Calcein fluorescence.

Independent RNA Sequencing and Differential Expression Analysis of Multiple Cultured Cell Lines

In both cell types examined, the ZnMP assay showed increased fluorescence in cells when grown in heme-deficient media, indicating changes in cell physiology that might be due to modulation of gene expression when heme is absent from the growth media. Therefore, A20 cells and Aag2 cells incubated in these media treatments for 72 hours were harvested, the RNA extracted, and cDNA libraries prepared, sequenced and each dataset analyzed for differential expression. Prior to differential expression analysis, the number of reads that mapped to each of the 19712 genes were counted for each sample. To remove the lowly expressed genes across all samples, an expression filter was applied dropping the total genes in the analysis to 8220. The multidimensional scaling plots for these analyses (Figure 11A-C) show that the replicate samples cluster together within the treatment groups for each dataset, with the groups being distinct from one another indicating that similar expression patterns was observed between replicates and differential expression was found between each of the 3 groups.

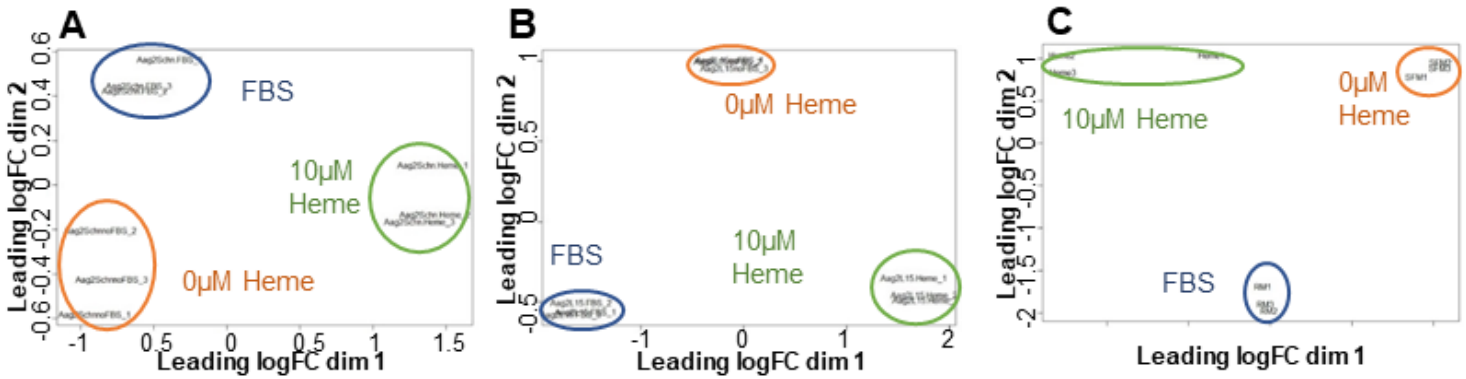

Figure 11: Multidimensional Scaling Plots cell culture RNAseq samples
(A) Aag2 cells in Schneider's *Drosophila* medium, with FBS, 0µM heme or 10µM heme. **(B)** Aag2 cells in L-15 medium, with FBS, 0µM heme or 10µM heme. **(C)** A20 cells in L-15 media +FBS, SF 900 II and SF 900II + 10µM heme

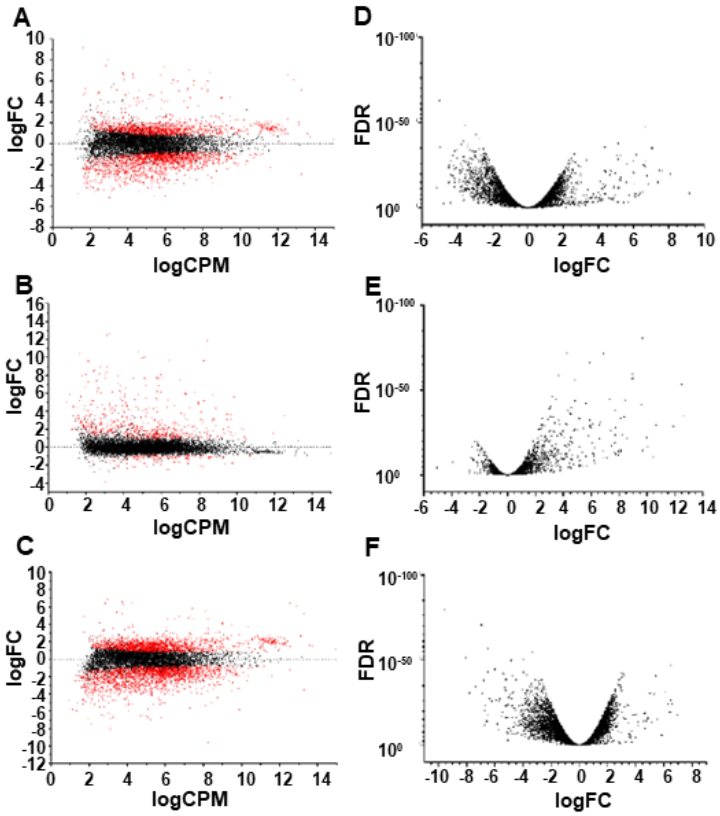

Figure 12: RNAseq-based differential expression after 72-hour heme treatment in A20 cells
A20 cells grown in L-15 media +FBS, SF 900 II (0µM heme) and SF 900II + 10µM heme cells (10µM heme) **(A-C)** Log2 fold change (LogFC) vs Log10 counts per million (LogCPM) graph of genes found differentially expressed in analysis for each comparison. Genes with an adjusted p-value corrected for multiple testing (False discovery rate: FDR) of <0.0001 are shown in red. **(D-F)** Volcano plot of genes found differentially expressed in analysis. **(A&D)** FBS vs 10µM heme **(B&E)** FBS vs 0µM heme **(C&F)** 0µM heme vs 10µM heme

In the A20 cells, 2815 genes in the normal media vs 10µM heme (Figure 12A,D) were significantly differentially expressed (FDR <0.0001), 745 significant DE genes were isolated when grown in normal media vs 0µM heme (Figure 12B,E), with 3692 genes with significant differential expession in the 0µM heme vs 10µM heme comparison (Figure 12C,F). As before, we performed transmembrane domain predictions for all DE genes, resulting in 658, 300, and 942 DE genes, respectively predicted to contain 1 or more transmembrane domains. If 2815 genes were selected randomly from the entire *Ae. aegypti* gene pool, on average 900 of these would be TM domain containing genes indicating that TM genes were underrepresented in the normal media vs 10µM heme comparison (p-value <0.00001). In the genes found differentially expressed in normal media vs 0µM heme and 0µM heme vs 10µM heme comparisons, 300 and 942 TM genes were identified which is an enrichment of genes with TM domains (240 genes, p-value=0.00006) and a depletion respectively (1186 genes, p-value <0.00001). As before, multipass transmembrane domain containing genes with increased expression in the absence of heme (0µM heme media treatment) may encode heme import proteins, while genes with decreased expression in the absence of heme may code for heme export proteins. In total, 39 genes containing 2+ TM domains and that were upregulated in the absence of heme (>2 log2) and downregulated in the presence of heme (<-2 log2) and were not significant in the normal media vs 10µM heme comparison were identified as potential heme importers in this analysis. The 3 with the highest fold change differences were AAEL011470 (7.71 log2, ~209.4; -6.74 log2, 0.0094), AAEL001794 (6.88 log2, ~117.8; -6.95 log2, ~0.0081) and AAEL010379 (5.47 log2, ~44.32; -4.76 log2, ~0.0369), which are annotated as a cis-muconate transport protein, macroglobulin and an ATP-binding cassette transporter respectively. No genes

were identified as potential heme exporters as the reverse trend was not observed in the dataset.

To identify genes with these expression patterns, a soft cluster analysis was performed on all genes analyzed in the differential expression analysis (7722 genes). All genes that matched to a cluster in this analysis passed a membership score of 50% or greater, keeping 6219 genes split between the clusters. Figure 13 shows the 15 expression patterns identified in this analysis. Clusters 8 and 11 show the expression pattern expected of potential heme importer genes, and of these 448 (219 & 229 respectively) genes have at least 1 predicted TM domain. Clusters 9 and 13 show the expression pattern expected of heme exporter genes, of which 143 (74 & 69 respectively) have at least 1 predicted TM domain. In addition to identifying heme related clusters of expression, change in nutrient levels across the treatment types have also appeared to change expression levels of some genes, as shown in clusters 1, 4 & 15 of which have the FBS samples and both of the heme deficiency and overload samples.

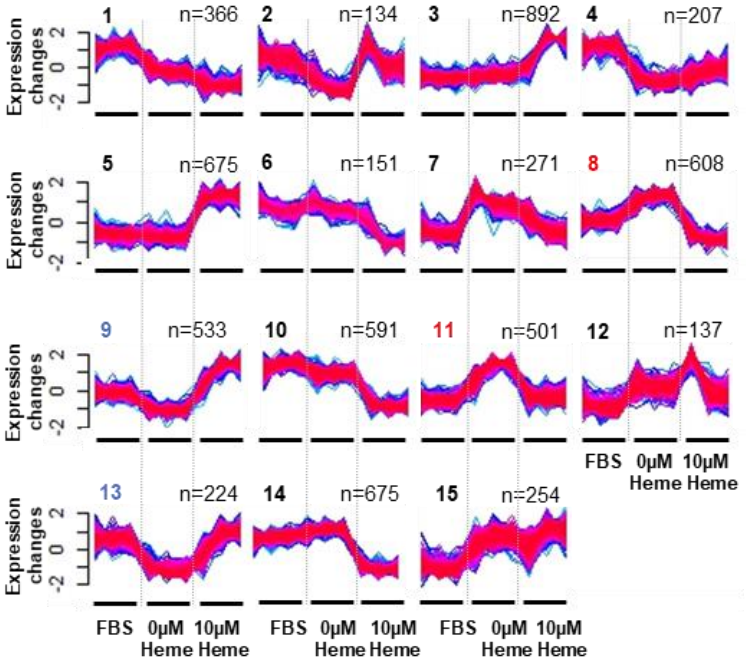

Figure 13: Cluster Analysis of A20 cells treated with heme for 72 hours A20 cells were treated with Leibovitz's L15 media with fetal bovine serum (FBS) for 72 hours or SF900 II media with 0μM or 10μM heme. Only genes containing a membership score of above 50% are shown in each cluster. Red lines indicate high membership values in the cluster, blue indicates low membership. Heme import clusters are highlighted in red and export clusters are highlighted in blue.

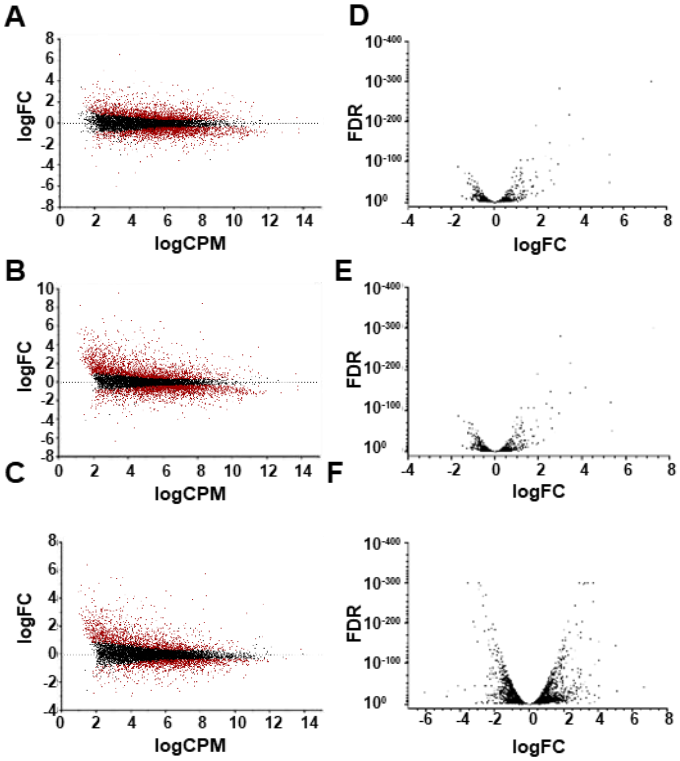

Figure 14: RNAseq-based differential expression after 72-hour heme treatment Aag2 cells in L15 medium differential expression analysis Aag2 cells grown in L15 medium, with FBS, without FBS (0µM heme) or without FBS+ 10µM heme **(A-C)** Log2 fold change (LogFC) vs Log10 counts per million (LogCPM) graph of genes found differentially expressed in analysis for each comparison. Genes with an adjusted p-value corrected for multiple testing of <0.0001 are shown in red. **(D-F)** Volcano plot of genes found differentially expressed in analysis. **(A&D)** FBS vs 0µM heme **(B&E)** FBS vs 10µM heme **(C&F)** 0µM heme vs 10µM heme

As A20 cells were found to respond differently to heme-induced stress than Aag2 cells, we also performed differential expression analysis in Aag2 cells using the same treatments. Additionally, Aag2 cells were grown in two different media types, Leibovitz's L-15 and Schneider's *Drosophila*, in an attempt to account for differential gene expression due to the varying nutrient composition present in each of the two medias. Prior to differential expression analysis, the number of reads that mapped to each of the 19712 genes were counted for each sample for both sets of growth conditions. Lowly expressed

genes were removed from the spreadsheets prior to differential expression analysis by applying an expression filter, dropping the total genes in the analysis to 9484 for the cells grown in L-15 and 8644 for the cells grown in Schneider's *Drosophila* medium. In the differential expression analysis of Aag2 cells grown in L-15, 4166 genes were found to be significantly differentially expressed (FDR <0.0001) when comparing normal media vs 0µM heme (Figure 14A,D). For the other comparisons, 4979 genes were differerntially expressed in the normal media vs 10µM heme comparison (Figure 14B,E) and 3200 genes in the 0µM heme vs 10µM heme comparison (Figure 14C,F). Transmembrane domain predictions were performed for all DE genes, and 1218, 1568 and 1121 DE genes in each comparison were predicted to contain at least 1 TM domain. When the total DE genes identified with TM predictions were compared to those derived by a random sampling of genes from the *Ae. aegypti* gene pool for each heme treatment comparison, the amount of TM genes differentially expressed in normal media vs 0µM heme were underrepresented (Average: 1339 genes, p-value=0.00002), the TM genes in normal media vs 10µM heme were not significantly different from those found by chance (Average: 1588, p-value=0.378) and in 0µM vs 10µM heme the amount of TM containing genes were overrepresented (Average: 1019 genes, p-value=0.00005). When examining the genes that contained 2+ TM domains and greater than 4 fold expression changes between heme treatment types no genes were identified as potential heme transporters.

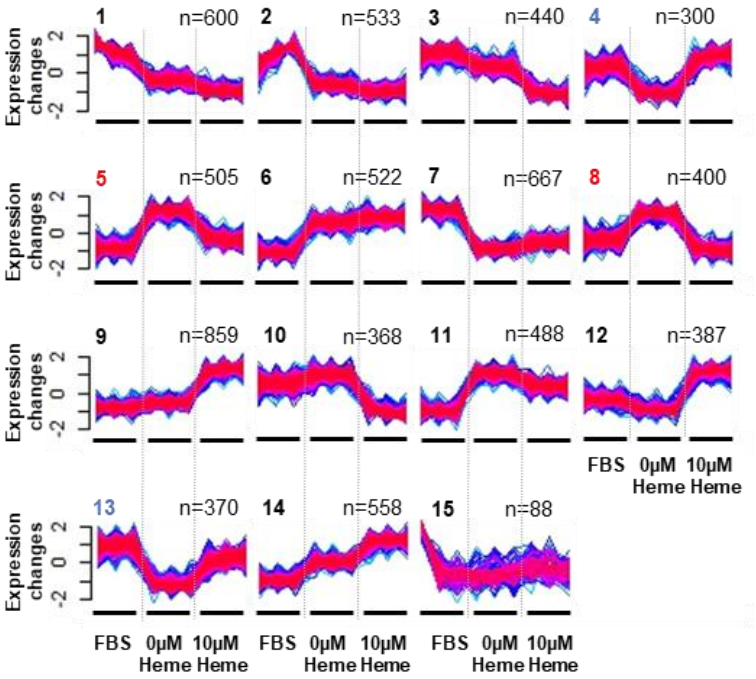

Figure 15: Cluster Analysis of Aag2 cells treated with heme in Leibovitz's L-15 medium for 72 hours
Aag2 cells were treated in Leibovitz's L15 media with fetal bovine serum (FBS), 0μM heme or 10μM heme for 72 hours. Only genes containing a membership score of above 50% are shown in each cluster. Red lines indicate high membership in a cluster, blue indicates low membership. Heme import clusters are highlighted in red and export clusters are highlighted in blue.

Once again, to identify potential heme importers and exporters by their observed expression patterns a soft cluster analysis was performed. All genes run in the differential expression analysis were run in the cluster analysis (8851 genes) as shown in Figure 15. Each cluster only contains genes that passed a membership score of 50% or better, keeping 7085 genes split between all the clusters. Clusters 5 and 8 show the expression pattern expected for heme importer genes, with 229 (123+106 respectively) genes having at least 1 TM domain predicted. Clusters 4 and 13 showed the expression pattern expected for heme exporter genes, with 197 (93+104 respectively) genes identified with one or more TM domain. In addition to examining expression due to heme changes in the media, changes in

nutrient content can also be examined as the fetal bovine serum was only present in the first set of samples as shown in Figure 15 clusters 1, 2, 6, 7 & 11.

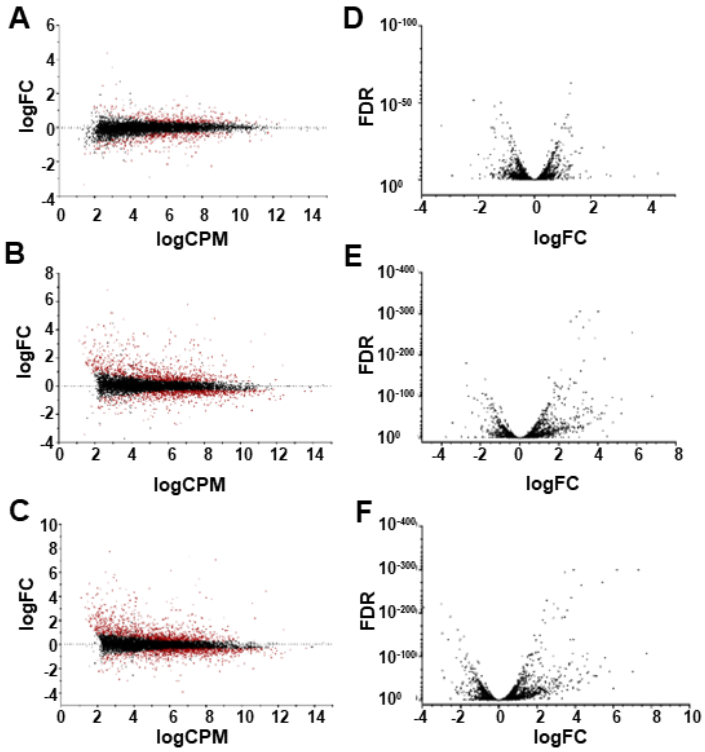

Figure 16: RNAseq-based differential expression after 72-hour heme treatment in Aag2 cells in Schneider's *Drosophila* medium
Aag2 cells grown in Schneider's *Drosophila* medium, with FBS, without FBS (0µM heme) or without FBS+ 10µM heme **(A-C)** Log2 fold change (LogFC) vs Log10 counts per million (LogCPM) graph of genes found differentially expressed in analysis for each comparison. Genes with an adjusted p-value corrected for multiple testing (False discovery rate: FDR) of <0.0001 are shown in red. **(D-F)** Volcano plot of genes found differentially expressed in analysis. **(A&D)** FBS vs 0µM heme **(B&E)** FBS vs 10µM Heme **(C&F)** 0µM heme vs 10µM heme

In the differential expression analysis of Aag2 cells grown in Schneider's *Drosophila* media, 587 genes were found differentially expressed significant to a p-value adjusted for multiple testing (FDR) of less than 0.0001 in the normal media vs 0µM heme comparison, 1990 genes found in the normal media vs 10µM heme comparison and 2274

when comparing the 0µM heme vs 10µM heme groups as shown in red in Figure 16A-C. After TOPCONS transmembrane domain predictions were performed on the DE genes 251, 737 and 856 were identified in each comparison respectively with 1 or more transmembrane domain. All of the comparisons performed showed enrichment in the number of TM domain containing genes compared to those found by random chance; 185, 638 and 729 respectively (All p-values <0.00001). When examining the genes that contained 2+ TM domains and greater than 4 fold expression changes between heme treatment types no genes were identified as potential heme transporters.

The soft cluster analysis of all genes run through the differential expression analysis, 8089 genes, was performed to identify heme transporters by their expression pattern across the treatment groups is shown in Figure 17. All clusters contain genes with above 50% membership score, keeping 4728 genes split between the 15 clusters. 240 were identified as potential exporters as shown in clusters 8 and 13. Clusters 3 and 9 show the expression pattern expected for heme importer genes, of the total genes present in both clusters 238 (85+153 respectively) had 1 or more TM domain predicted. While clusters 8 and 13 showed the expression pattern for heme exporter genes with 240 (99+142 respectively) of the total number of genes identified with at least 1 TM domain. Changes gene expression caused by the nutrient content across the samples with a high level of nutrients in the FBS samples and a low level of nutrients in the heme deficiency and heme overload samples are shown in clusters 1, 4, 10 and 12.

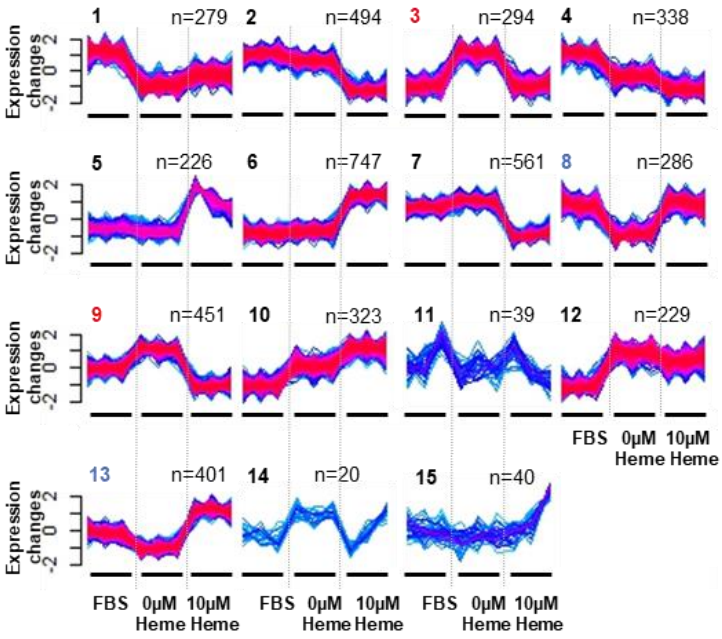

Figure 17: Cluster Analysis of Aag2 cells treated with heme in Schneider's *Drosophila* medium for 72 hours
Aag2 cells were treated in Schneider's *Drosophila* media with fetal bovine serum (FBS), 0µM heme or 10µM heme for 72 hours. Only genes containing a membership score of above 50% are shown in each cluster. Red lines indicate high membership values in a cluster, blue indicates low membership. Heme import clusters are highlighted in red and export clusters are highlighted in blue.

Validation of Differential Expression Results Through qPCR of Select Genes

To validate the differential expression analysis of the RNA sequencing on heme overexposed Aag2 cells, quantitative real-time PCR was performed. The computationally derived fold change values obtained from the sequencing of 48 hour heme exposed Aag2 cells were compared to the relative quantification (RQ) qPCR values. The expression of 6 genes out of the 551 total found highly differentially expressed in the presence of heme, see Figure 18, was examined; AAEL008467, AAEL014246, AAEL07383, AAEL014318, AAEL013407 and AAEL010105. When comparing the qPCR log2 RQ to the log2 fold change values determined computationally, the qPCR values were found to be very similar to those derived computationally.

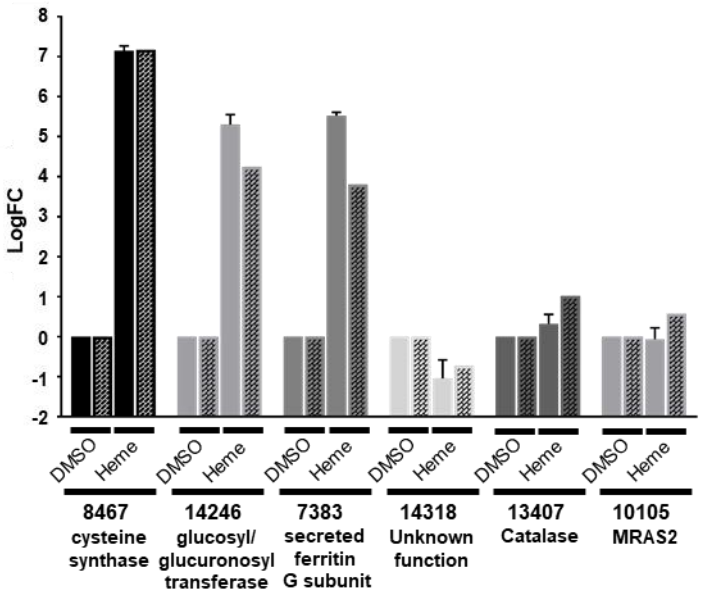

Figure 18: qPCR validation of Computational Results
6 genes highly expressed in Aag2 cells treated with heme when compared to a DMSO control were selected to validate computational results, AAEL008467, AAEL014246, AAEL007383, AAEL014318, AAEL013407 and AAEL010105. Solid bars indicate qPCR RQ values and patterned bars indicate computational FC values.

Synthesis of all Transcriptional Profiling Experiments for Common Differentially-Regulated Genes

As two different types of analyses were performed on each dataset, differential expression analysis (DE) and soft cluster analysis, we thought to answer the question of whether or not DE genes were identified in the import and export clusters. In the initial experiment examining Aag2 cells treated with 20μM heme for 48 hours the DE identified genes (n=106) with predicted transmembrane domains that were upregulated in the presence of heme, 97.1% of which (n=103) matched those found in the export clusters (n=401)(Figure 19B). Like the downregulated DE genes, the majority, 93.3% (n=98), were present between the TM genes found downregulated in the presence of heme and the 2 import clusters (n=468) (Figure 19A). Therefore the majority of the DE genes identified as potential importers and exporters were also identified as potential heme membrane bound transporters in both analyses. When examining the TM genes found in A20 cells exposed the heme deficiency and overexposure common genes were also found between the DE genes identified and those found using the cluster analysis. Of the 254 genes found upregulated in the absence of heme (FBS vs SFM comparison) and the 688 genes found downregulated in the presence of heme (SFM vs Heme) 161 were found in both comparisons as well as the import clusters, 13 between FBS vs SFM and import clusters and 178 between SFM vs heme and import clusters (Figure 20A). Therefore, 68.5% of genes found downregulated in the presence of heme and 49.3% of genes found upregulated in the absence of heme were also identified in the cluster analysis as importers leaving only 21.4% of the genes identified in the import clusters not previously identified in the differential expression analysis.

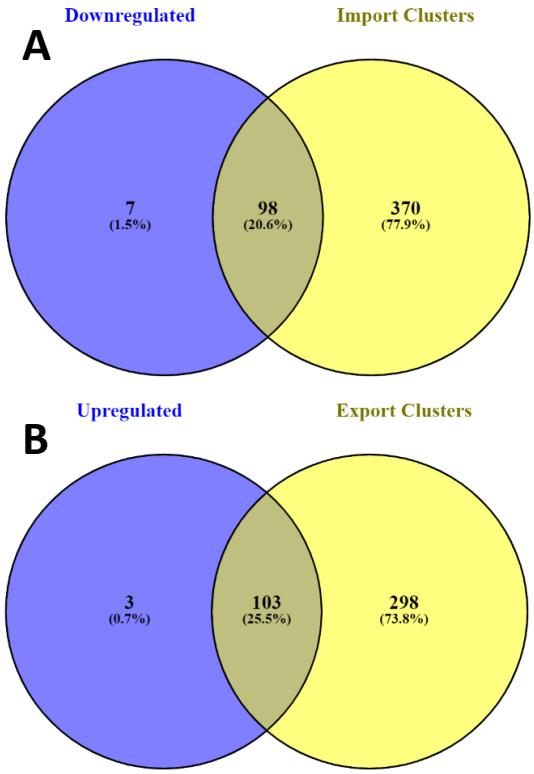

Figure 19: Common TM genes present between the differential expression analysis and the cluster analysis of Aag2 cells treated with heme for 48 hours
Aag2 cells in Schneider's *Drosophila* medium +FBS & +FBS+ 20µM heme were sequenced. Transmembrane domain containing genes found significantly expressed in DE analysis were compared to those identified in the cluster analysis A) Upregulated genes in the presence of heme vs those in import clusters. B) Downregulated genes in the presence of heme vs those found in export clusters

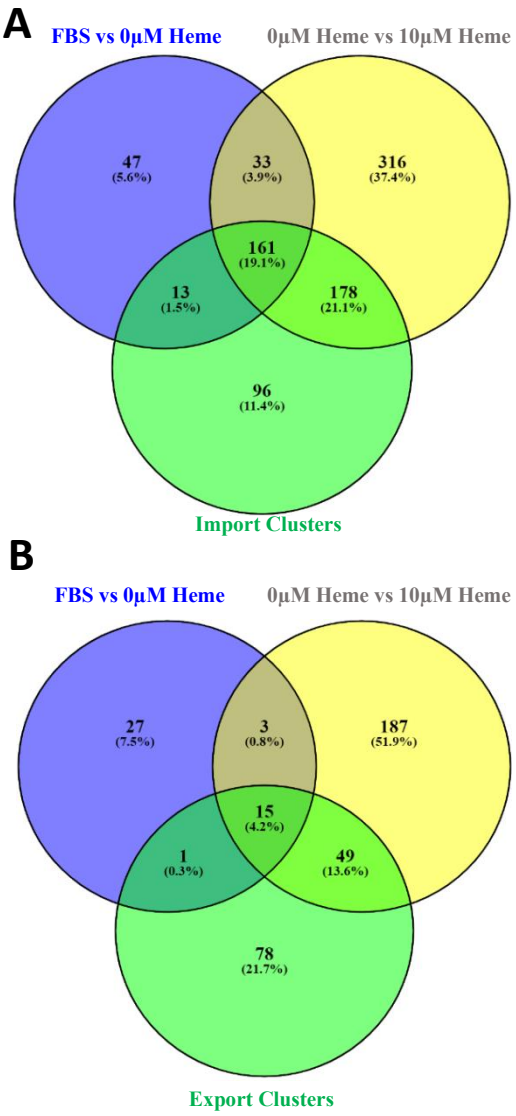

Figure 20: Common TM genes present between the DE analysis and the cluster analysis of A20 cells treated with heme for 72 hours
A20 cells in Leibovitz's L-15 medium +FBS, SF900II (0µM heme) & SF900II + 10µM heme were sequenced. Transmembrane domain containing genes found significantly expressed in DE analysis were compared to those identified in the cluster analysis A) Downregulated genes in the absence of heme vs Upregulated genes in the presence of heme vs those in import clusters. B) Downregulated genes in the absence of heme vs Upregulated genes in the presence of heme vs those found in export clusters

Similarily for the potential exporters found, of the 46 genes found downregulated in the absence of heme and the 254 genes found upregulated in the presence of heme, only 15 were common between the 2 comparisons and those found in the export clusters, 1 shared between the FBS vs SFM comparison and the export clusters and 49 between the SFM vs heme comparison and the export clusters (Figure 20B). Thus, 34.7% and 25.2% were shared with the export clusters with the FBS vs SFM and SFM vs heme comparisons respectively with 54.5% of the genes found in the export clusters unique to the cluster analysis.

The last 2 datasets examined, were Aag2 cells grown in either Leibovitz's L-15 or Schneider's *Drosophila*, then exposed to heme overexposure or deficiency. When examining the data from the cells grown in L-15 media, 25.2% (n=159) of the genes upregulated during heme deficiency conditions and 32.6% (n=144) of the DE genes downregulated during heme overexposure conditions were also found during the cluster analysis as potential importers (Figure 21A). Of the 159 and 144 genes, 126 were common between both heme conditions. Commonality was also observed between the export clusters and the differentially expressed genes downregulated during heme deficiency and upregulated during heme overexposure with 19.7% (n=116) and 14.8% (n=101) found in the predicted export clusters respectively with 78 genes found in both conditions (Figure 21B). However not all of the genes predicted as heme importers and exporters via cluster expression pattern were found also in the DE analysis, 29.4% of genes in the export clusters and 22.7 % of genes in the import clusters were not shared.

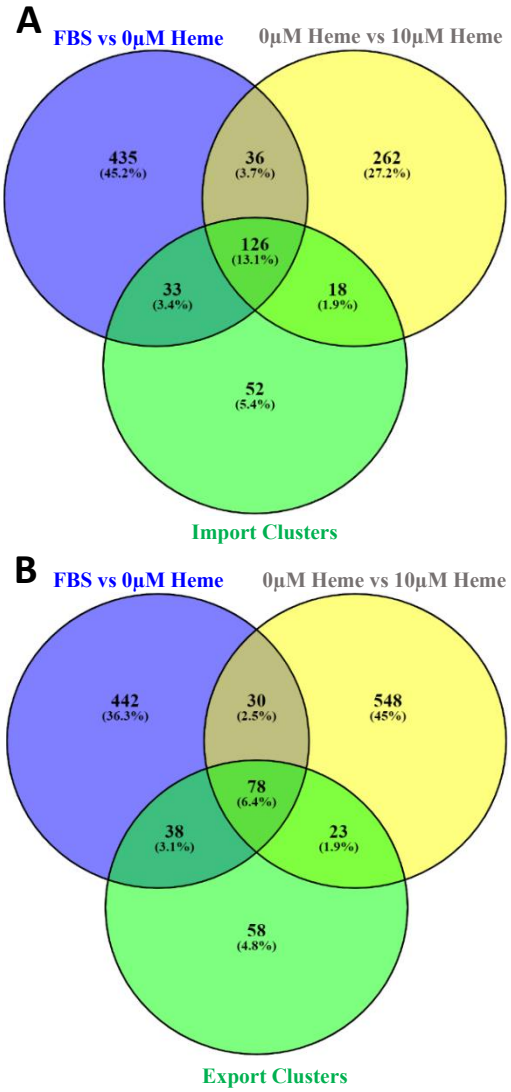

Figure 21: Common TM genes present between the DE analysis and the cluster analysis of Aag2 cells treated with heme for 72 hours in L-15 media
Aag2 cells in Leibovitz's L-15 medium +FBS, L-15 & L-15 + 10µM heme were sequenced. Transmembrane domain containing genes found significantly expressed in DE analysis were compared to those identified in the cluster analysis A) Downregulated genes in the absence of heme vs Upregulated genes in the presence of heme vs those in import clusters. B) Downregulated genes in the absence of heme vs Upregulated genes in the presence of heme vs those found in export clusters

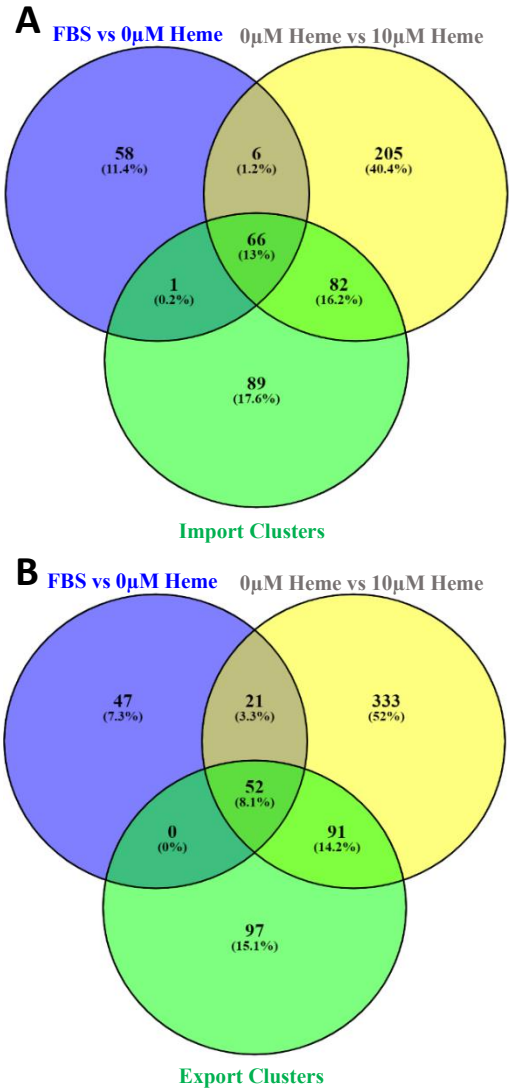

Figure 22: Common TM genes present between the DE analysis and the cluster analysis of Aag2 cells treated with heme for 72 hours in Schneider's *Drosophila* media
Aag2 cells in Schneider's *Drosophila* medium +FBS, Schneider's *Drosophila* & Schneider's *Drosophila* + 10µM heme were sequenced. Transmembrane domain containing genes found significantly expressed in DE analysis were compared to those identified in the cluster analysis A) Downregulated genes in the absence of heme vs Upregulated genes in the presence of heme vs those in import clusters. B) Downregulated genes in the absence of heme vs Upregulated genes in the presence of heme vs those found in export clusters

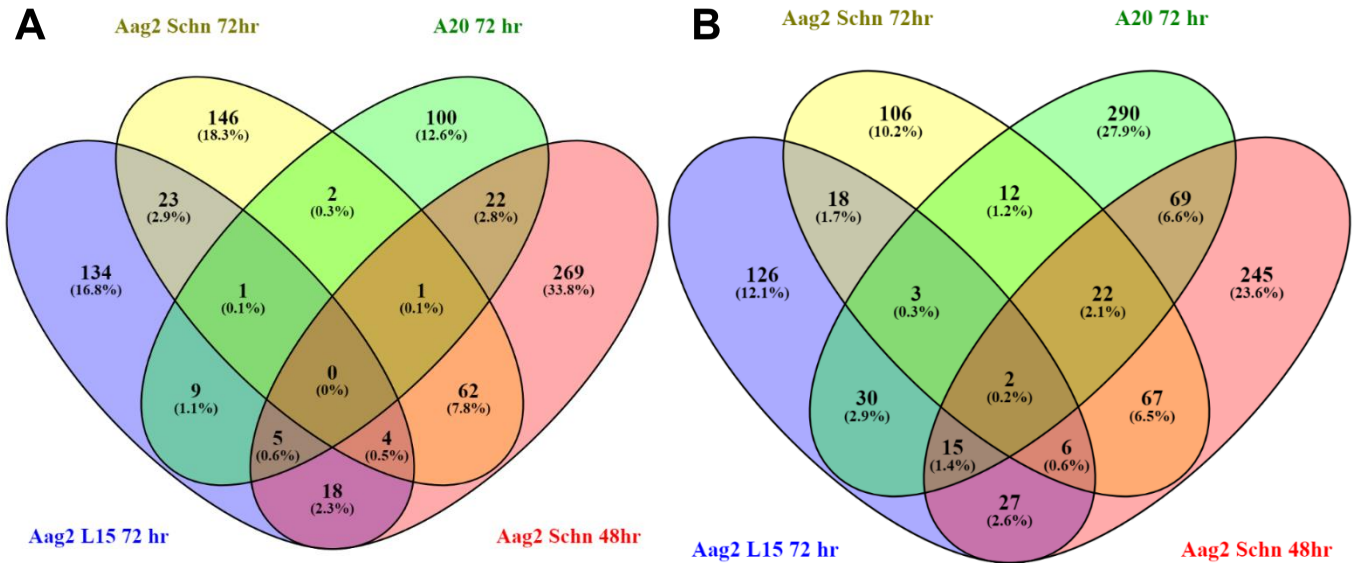

Figure 23: Potential Heme Importers and Exporters found in independent RNA-seq experiments after treatment with Heme

Candidates were chosen in each dataset based on expression pattern and having at least one transmembrane domain prediction A) Potential exporters B) Potential importers

When data from Aag2 cells grown in Schneider's *Drosophila* medium was examined, 51.1% (n=67) of the genes found upregulated during heme deficiency and 41.2% (n=148) of those found downregulated during heme overexposure were also identified in the clusters with the expression pattern of predicted importers with 66 of these genes shared between the heme experimental conditions (Figure 22A). Upon examining the DE genes identified as potential heme exporters, 43.3% (n=52) of those downregulated in conditions of heme deficiency all of which was also found during heme overexposure as well and 28.7% (n=143) of those upregulated during conditions of heme overexposure were located during the cluster analysis as potential heme exporters (Figure 22B). In the clusters with the predicted heme export and import patterns, not all the genes were shared with the DE genes, leaving 40.4% in the export clusters and 37.4% in the import clusters that were not shared between the 2 analyses.

Across each dataset examined, many heme-responsive genes were identified based on their expression pattern and number of transmembrane domains found. We reasoned that those most substantially involved in heme transport would differentially regulated across multiple experiments. For example, the majority of genes with at least 1 TM domain and found in clusters consistent with the expression patter of exporter (n= 649) or importer (n= 767) candidates were identified in only 1 dataset. Therefore, candidates were identified that were significantly differentially expressed in two or more datasets. Figure 23 shows a 4-way venn diagram comparing candidate genes identified as having an expression pattern consistent with our expectations for potential heme exporters (Figure 23A) and importers (Figure 23B) based on the soft cluster analysis. Only 136 of the potential exporter candidates were found in at least 2 datasets, with only 7 candidate genes found in 3. No

genes with the expression pattern expected for a heme exporter were recovered in all 4 experiments. For candidate heme importers 223 were identified in 2 datasets, with 46 candidate genes recovered in 3 experiments. Two genes (AAEL006432 & AAEL014003) were identified passed on their expression pattern in response to heme in all four cell culture exeperiments.

Discussion

Despite the vital role of heme and the iron it contains play in egg production in the *Ae. aegypti* mosquito, gaps of knowledge in the heme digestion pathway still exist. While heme digestion occurs via the cytosolic heme oxygenase in midgut epithelial cells, the method of entry into the cell and its biproducts' export out of the cell through the plasma membrane have yet to be discovered (Cruz et al., 2012; Pereira et al., 2007). A recent study of heme exposure in Aag2 cells determined that the majority of transcripts found regulated by heme in Aag2 cells were also identified in the midgut epithelium of adult females during blood digestion (Bottino-Rojas et al., 2015). Since Aag2 cells and adult female *Ae. aegypti* share many genes differentially regulated during heme overload, the embryo derived cell line may be a good model for examining the effects of heme exposure in this mosquito species. When these cells and a larval derived line, A20, were exposed to heme over the course of 9 days, A20 cells were found to be much more resistant to heme exposure than Aag2 cells, however neither cell type showed reduced transcription of a gene presumed to be important in managing oxidative stress. This could indicate the inability to prevent heme import in both cell types, or that they were unable to mitigate the continuous high levels of oxidative damage to the exterior of plasma membrane.

The use of zinc mesoporphyrin fluorescent assays in insect cultured cells allows for the identification of the presence/absence of active heme transport mechanisms. Changes in the expression of these transport mechanisms can also be easily observed due to the resulting changes in ZnMP fluorescence. As in the mammalian cell line experiment this protocol was based on (Worthington et al., 2001), ZnMP was utilized to observe heme import into cultured *Ae. aegypti* cells. An increase in ZnMP fluorescence was observed in both cell types incubated in heme-deficient media, indicating that an upregulation of heme import had occurred. During the ZnMP incubation procedure, a number of cells from both the Aag2 and A20 samples were lost due to loss of cell adhesion to the well surface and subsequent removal from the well during wash steps, which could account for the low fluorescence observed when photographing the cells. However, replication of this experiment and quantitative measurement of ZnMP fluorescence normalized by cell count using Calcein fluorescence reproduced the previously observed results indicating that the change observed was indeed due to heme deficiency conditions (Figure 10).

While examining the transcriptomic changes across all 4 cell culture experiments performed, many genes were found differentially expressed, indicating that these cell lines do react and alter expression of many genes in the presence and absence of heme in the growth media. Many of the DE genes identified were those with functional roles related to ROS stress response as well as genes with unknown functions. However only a few TM containing genes were identified with above 4-fold or below $1/4^{th}$ fold expression changes as potential highly expressed heme transport proteins. In fact, only two of the four datasets [Aag2 cells treated with heme for 48 hours and A20 for 72hr] contained genes that met this criteria (2 and 39 genes respectively), and no genes were common between them. In the

former experiment, AAEL006113 (4.23 log2, ~18.76), a cystinosin, and AAEL014246 (2.92 log2, ~7.62), a glucosyl/glucuronosyl transferase, which are involved in the ROS stress response and removal of endogenous substances, respectively. Of the 39 genes strongly differentially regulated in A20 cells, 2 were ABC transporters and 15 had no known function. Members of the ABC transporter family in other species have been characterized as heme transporters including in *Rhipicephalus (Boophilus) microplus* and *Caenorhabditis elegans* (Korolnek et al., 2014; Lara et al., 2015). Ultimately, as few strong candidates were identified by these studies, we consider the possibility that each cell line could have a redundant system of heme import, whereby multiple transport proteins each contribute to the total heme accumulation in the cell. Alternatively, it is possible that these cells lines do not regulate heme transport at the transcript level, but rather do so post-translationally. Stronger candidates for future characterization studies were found by comparing the candidate lists from each experiment to each other and only examining those found in at least 2 cultured cell experiments. Hopefully, eliminating the majority of the genes of the lists that had expression changes due to unknown experimental specific variables.

Heme transport in Aag2 cells and bloodfed *Ae. aegypti* females were briefly explored previously (Bonizzoni et al., 2011; Bottino-Rojas et al., 2015). Bottino-Rojas et al. (2015) found 8 genes with transport functions with fold changes greater than 4 fold. Of these, two were also found in our differential expression analysis in all 4 experiments: AAEL014762, a member of the ZIP family of zinc transporters, and AAEL006113, a cystinosin. AAEL014762 was recently identified as an iron transporter in *Ae. aegypti* which is most likely located in endocytic vesicles indicating its importance in sequestering

iron post heme degradation (Tsujimoto et al., 2018; Xiao et al., 2014). As previously mentioned cystinosin is involved in the transport of cystine which serves as a site of redox reactions thus cystinosin seems to be involved in mitigation of the ROS generated by heme overload. Therefore, these two genes are most likely not responsible for heme acquisition by the cell but are most likely involved in the heme stress response. As Bottino-Rojas et al. (2015) incubated Aag2 cells only for 24 hours, it is possible that some transport genes are missing from their analysis if the cells were slower than 1 day to increase or descrease their expression. Of the ~53 TM containing genes found highly differentially expressed (>2 log2 or <-2 log2; >100reads in at least 1 sample) in bloodfed females vs sugar fed, AAEL006113 was found in all 4 datasets, AAEL010650 a sodium/solute symporter and AAEL010691 a ribonucleoside-diphosphate reductase small chain were found in Aag2 cells treated for 48 hours and Aag2 in L15 media for 72 hours and 7 others including cytochrome p450 proteins, aquaporins, rh antigen, trypsin and 1 with unknown function were found in 1 experiment but not the others. AAEL009853, the trysin/serine protease found in A20 cells in the absence of the fetal bovine serum (0µM heme samples) and bloodfed females is involved in digestion of proteins. A20 cells appear to upregulate this gene in response to lower nutrient concentrations present in their growth media as they attempt to scavenge more nutrients. As 12 TM containing genes were found across the 4 analyses out of ~53 TM containing genes (23%) found differentially expressed in bloodfed females, some commonality exists between *Ae. aegypti* cultured cell response to heme exposure and female mosquitoes during blood digestion.

In the mosquito *Ae. aegypti*, very little is known about how heme enters the midgut epithelial cells to be degraded by heme oxygenase. This analysis examined the response of

two *Ae. aegypti* cultured cell lines to heme overload or deficiency, one of which, Aag2, had been shown to be a valid model for heme exposure previously (Bottino-Rojas et al., 2015). An examination of heme exposure in Aag2 and A20 cells over the course of 9 days indicated one of two possibilities that neither cell line could successfully shut down prevent heme import or that they were unable to mitigate heme's peroxidase activity which lead to the continuous high levels of oxidative damage to exterior of plasma membrane. A study of heme deficiency on the same cell lines showed that both cell types appear to upregulate heme import in those conditions as ZnMP fluorscence did increase. Therefore, 4 different cultured cell experiments were performed to examine changes to the transcriptome after heme exposure/deficiency. We found many different genes differentially expressed, indicating that these cells do react and initiate gene expression changes in response to changes in heme concentration. Despite this, only a few strong heme transport candidates were found as only a few TM containing genes were identified with above 4-fold or below $1/4^{th}$ fold expression changes. In the end, as only a small number of strong candidates were identified through the course of this analysis, it is possible that either these cell lines have a redundant system of heme import with the total heme accumulation in each cell due to multiple transport proteins or these cells do not regulate heme post-transcriptionally but instead do so post-translationally.

CHAPTER III

DIFFERENTIAL GENE EXPRESSION ANALYSIS OF *AEDES AEGYPTI* ADULT FEMALE MIDGUTS IN THE PRESENCE/ABSENCE OF HEME

Introduction

The *Aedes aegypti* mosquito is anautogenous, meaning a blood meal is required for the successful completion of vitellogenesis due to the influx of nutrients and signaling molecules released during blood digestion. Amino acids from digested blood proteins are transported into the midgut epithelium through amino acid transporters, like AaePAT1, with the eventual goal to be used in the production of proteins or converted into glucose or fatty acids to produce lipids and/or carbohydrates which are necessary for egg production (Evans et al., 2009; Marquardt, 2005). Heme is also released during blood digestion upon degradation of the blood protein hemoglobin and acts as both a nutrient and signaling molecule. Once heme enters the midgut epithelial cells it binds and stabilizes the nuclear receptor E75 allowing for the activation of the steroid hormone 20-hydroxyecdysone which plays a key role in molting, metamorphosis, and vitellogenesis in this mosquito species (Cruz et al., 2012; Kokoza et al., 2001; Martin et al., 2001). In addition, the iron once released from heme is either distributed across the mosquito in various tissues (13%), the majority of which is deposited into the developing eggs (7%), or exported back out of the cells into the lumen for excretion (87%)(Zhou et al., 2007). While free iron is also present in the meal, the majority of the iron utilized by the mosquito comes from heme digestion, as ~97% of the iron retained in the adult body was derived from hemoglobin as well as ~98% of the iron deposited into the eggs. While heme and iron do have nutrient

properties, these molecules also contain pro-oxidant properties with the ability to create reactive oxygen species when not bound to proteins. These ROS are handled through use of antioxidant proteins both intracellularly (Oliveira et al., 2017) and extracellularly (Lima et al., 2012) and heme is aggregated to prevent ROS formation through use of a Type I peritrophic matrix (Peters, 1992).

The formation of the peritrophic matrix and start of digestion is the result of the midgut distention caused by ingestion of a full meal not the contents of the meal itself. This was shown by inserting large enemas of saline introduced into *Ae. aegypti* females which resulted in termination of host-seeking behavior and by feeding females with either a blood or a protein and heme free meal both resulted in peritrophic matrix formation (Klowden and Lea, 1979; Whiten et al., 2018b).

The study of heme uptake and subsequent digestion has been performed in various organisms including *C. elegans* and *R. microplus*. Both of these organisms lack important enzymes utilized in the heme biosynthesis pathway, thus leaving them entirely dependent on dietary heme to survive (Braz et al., 1999; Rao et al., 2005). Radiolabeling heme-iron and free iron did determine that *C. elegans* does take in and incorporate dietary heme into its proteins. Incubation of the worms with the fluorescent heme analog zinc mesoporphyrin (ZnMP) confirmed this finding as confocal microscopy showed fluorescence accumulation across the worm including in the intestinal cells, eggs, and dividing embryos (Rao et al., 2005). Rajagopal et al. (2008) took this work a bit further to identify 2 heme transporter proteins, hrg-1 and hrg-4. Upon RNAi knockdown of hrg-4, no accumulation of ZnMP was observed in the worms, while hrg-1 knockdown resulted in higher fluorescence in the intestines compared to the control worms (Rajagopal et al., 2008). These results suggest

that HRG-4 is involved in heme uptake into the intestinal cells while HRG-1 maintains heme homeostasis by isolating excess heme in an intracellular compartment (Rajagopal et al., 2008). The ABC transporter subtype B10 (ABCB10) was characterized in the midgut cells of *R. microplus* using digest cells extracted from the gut wall and grown in culture (Lara et al., 2015). RmABCB10 was localized to the membrane of the digestive vacuoles were it exported heme from the vacuole as hemoglobin proteins were degraded allowing for heme transport into the hemosomes for storage (Lara et al., 2015). While *Ae. aegypti* contains a functional heme biosynthesis pathway (Perner et al., 2019), midgut epithelial cells do need to handle a large influx of heme, like that of *R. microplus*. Use of the peritrophic matrix to aggregate the heme allows the midgut epithelium to transport it into the cell for degradation while preventing it from displaying pro-oxidant activity. However, the method of entry into the cell for degradation is still currently unexplored.

Aedes aegypti cultured cells when exposed to heme overexposure or deficiency conditions showed potential changes in heme import expression due to the changes in zinc mesoporphyrin fluorescence observed between heme treated and heme deficiency conditions (Chapter 2). When the transcriptome of these samples was analyzed, many genes were identified as potential membrane bound transporters based on their number of predicted TM domains, their expression pattern changes after exposure to heme overload or deficiency conditions, and their presence in more than one cultured cell dataset. However, no single or small set of highly differentiated genes were found that were significantly differentially expressed in all heme treated conditions. In the absence of a clear candidate heme transporter from our cell culture experiments, we moved to a direct examination of *Ae. aegypti* midgut epithelial cells and their response to heme overload.

The midgut epithelium was selected as it is directly involved in heme uptake and digestion making it the ideal system to identify the membrane bound heme importers and exporters used during blood digestion. As a blood meal taken in by *Aedes aegypti* contains many different components including proteins, heme, iron, and potentially pathogens, we sought to disentangle the effects caused by the different components present during digestion by using an artificial bloodmeal (protein-free with 0mM or 10mM heme)(Whiten et al., 2018b). However, this method was ineffective, therefore an *in vitro* application was performed, incubating freshly dissected *Ae. aegypti* female midguts in 10µM heme added to cultured cell medium, followed by RNAseq analysis. A large quantity of genes containing transmembrane domains were isolated showing downregulation or upregulation in response to heme treatment indicating the possibility that heme membrane bound import and export genes were identified respectively. However, the majority of which only had expression changes smaller than 4-fold or higher than $1/4^{th}$ fold, indicating once again the absence of a strong transcriptional regulation in regard to heme import.

Methods

Mosquito Rearing

Aedes aegypti (Liverpool strain) was reared at 28^{o}C in growth chambers at 70% relative humidity and a day: night cycle of 14 hours:10 hours. All mosquitoes were starved for 12 hours prior to feeding protein-free meal. All mosquitoes were fed a 10% sucrose solution with 1% Penicillin-streptomycin 2 days prior to dissection.

Feeding of Protein-free Artificial Meal

3-5 day old adult female *Ae. aegypti* were fed a protein-free meal composed of 150mM NaCl, 20mM $NaHCO_3$, 20mM ATP and 0.2% low melt agarose to provide bulk and induce distension after feeding. Hemin Chloride was added to the prepared meal solution and incubated at 42^{o}C for 6 hours. Heme concentrations tested include: 0.625mM, 1.25mM, 2.5mM, 5mM and 10mM.

Midgut Dissection and Treatment with Heme

Midguts were dissected from 3-5 days old sugar fed female *A. aegypti*. Midguts (n=60) were dissected in 1x PBS, transferred to a biosafety cabinet to prevent further microbial contamination, and split evenly between 3 treatments in 6-well culture plates with 2mL of media per well. Midguts were subject to one of the following treatments: Schneider's *Drosophila* Media (Thermo Fisher) with 10% FBS (Atlanta Biologicals) and 1% Pen-strep (Corning) (FBS), Schneider's *Drosophila* Media + 1% Pen-strep (0µM Heme) and Schneider's *Drosophila* Media + 1% Pen-strep + 10µM Hemin Chloride (Sigma-Aldrich) (10µM Heme). Dissected midguts in six-well plates were incubated at 28^{o}C for 35 hours with media treatments. Every 8-12 hours, midguts were transferred to a new culture plate with fresh media.

Heme Dilution Series

Midguts (n=150) were dissected in 1x PBS and split between 6 different media treatments in wells of a 6 well culture plate: Schneider's *Drosophila* Media + 1% Pen-strep (0µM Heme), + 0.5µM Heme, + 1µM Heme, + 3µM Heme, + 5µM Heme and + 10µM Heme.

Midguts were incubated for 35 hours with media treatments changed every 8-12 hours by transfer into a new culture plate with fresh media.

ZnMP Fluorescent Assay

Zinc Mesoporphyrin (ZnMP) (Frontier Scientific, Logan, UT) stock solution was made at 0.3mM concentration by dissolving ZnMP into a 1% Ethanol-amine (Sigma Aldrich) and 10mg/mL Bovine Serum Albumin (Sigma Aldrich) solution (Vreman et al., 1989). The solution was filter sterilized using a 0.22µm filter (EMD Millipore), split into 500µL aliquots and stored at -20^{o}C. The uptake buffer used during the incubation and wash procedures consisted of 50mM HEPES, pH 7.4, 130mM NaCl, 10mM KCl, 1mM $CaCl_2$ and 1mM $MgSO_4$ (Worthington et al., 2001). All subsequent steps were performed in as dark of conditions as were practical. ZnMP stock solution was freshly diluted in uptake buffer prior to use and added to midguts after medium was removed from the 6-well plate. Midguts were incubated with 10µM ZnMP for 30 minutes. Following the incubation, the midguts were washed once with uptake buffer + 5% BSA, then 2x with uptake buffer. Photos were taken using the DsRED filter of the Leica M165 FC stereomicroscope equipped with a DFC3000C digital camera at 16x magnification. Photos of 0µM ZnMP-treated midguts were taken prior to ZnMP incubation from a subset of the midguts in each treatment group. The resulting images were analyzed by ImageJ (Schindelin et al., 2012) to determine mean pixel intensity per midgut. Means were background corrected to remove channel and tissue autofluorescence. Means were compared using a one-way ANOVA with individual means compared using Tukey's multiple comparisons test as performed by GraphPad Prism v7.02 (San Diego, CA). If the data failed the D'Agostino-Pearson

omnibus normality test, Kruskal-Wallis test and Dunn's multiple comparison's test were performed instead.

Total RNA Isolation of Samples for Sequencing

Midguts were dissected from 3-5 day old sugar fed female *A. aegypti*. A total of 3 replicates for each treatment type were performed, with 30 midguts/replicate. The 0µM Heme and 10µM heme treatments previously described in the midgut dissection and treatment with heme section were performed for 35hrs at 28^{o}C in 6 well plates, 10 midguts per well in 2mL of media. Every 8-12 hours the midguts were placed into fresh media. At the end of the incubation, the midguts were placed into 1.5mL Eppendorf tubes and snap frozen in liquid nitrogen.

Following the manufacturer's protocol, RNA was isolated using the TRIzol reagent (Thermo Fisher). The resulting RNA was DNase treated (DNase I: New England Biolabs) and quantified using a Nanodrop (Thermo Fisher). One microgram of total RNA was prepared for sequencing using the NEBNext Ultra RNA library preparation kit (New England Biolabs Ipswich, MA). The protocol utilized sequential first and second strand cDNA synthesis with random priming and PCR library enrichment of 10 cycles.

Sequencing and Computational Analysis

Single-end sequencing with 75bp read length was performed on an Illumina Nextseq 500 at the Texas A&M's Institute for Genome Sciences and Society. Reads were aligned to the *Ae. aegypti* reference genome (AaegL5, obtained from www.vectorbase.org) using HISAT2 v2.1.0 with default parameters (Kim et al., 2015) through Texas A&M's High

Performance Research Computing Ada server. Output files containing mapped reads were converted to BAM format, sorted and the -q10 option used to remove reads with low quality mapping scores with the SAMtools view and SAMtools sort commands v1.7. The number of reads per mRNA transcript was calculated with the CoverageBED command of the BEDtools suite 2.19.1. Differential expression between the 10µM Heme and 0µM Heme samples was determined using EdgeR. Transcripts were only retained in the analysis if they had 5 or more read counts per million in 3 or more samples. Library normalization was performed by the weighted trimmed mean of M-values method. (Li, 2011; Li et al., 2009; McCarthy et al., 2012; Quinlan and Hall, 2010; Robinson et al., 2010). TOPCONS was utilized to obtain transmembrane domain predictions of the genes found differentially expressed in the analysis (Tsirigos et al., 2015). The mean number of genes with transmembrane domain predictions found in a subset of the *Ae. aegypti* gene pool was calculated for the differential expression analyses. The Linux command 'shuf' was used to randomly select a subset of genes from the gene list; the subset was determined by the number of significant DE genes. The number of TM containing genes were counted using 'awk' and 'wc'. The command used is given here: "shuf -n 328 genes_TMdomain_predictions.txt |awk '$2 >= 1 {print $0}'|wc -l". These Linux commands were repeated for a total of 30x and the average number of genes with predicted TM domains and the standard deviation were calculated. Lastly, a two-tailed z-test was performed.

qPCR Validation of Results

Primers were designed for 5 genes that were used to confirm differential expression results of heme treated midguts (Table 3). Primer design was performed using Primer3 server (version 4.1.0) aiming for sequence length of 80-150bp with DNA hairpin folding accounted for using mfold with the folding temperature set to 60ºC and Mg^{++} concentration set to 1.5mM (Untergasser et al., 2012; Zuker, 2003). While 2-5 pairs of primers were designed for each gene, only 1 was selected to use in each qPCR analysis based on the results of the primer gradient PCR and primer efficiency calculations. Quantitative real-time PCR (qPCR) was performed on CFX69 Touch Real-Time PCR Detection System with SsoAdvanced Universal SYBR Green Supermix (Bio-Rad, CA). Each primer pair was tested at 8 annealing temperatures ranging from 55-65ºC to determine the optimal temperature to use for each primer. The program run on the thermocycler was 95ºC for 30 seconds, followed by 39 cycles of 15 seconds at 95ºC and 30 seconds 55-65ºC annealing temperature gradient, finishing with a melt curve of 65-95ºC measuring every 0.5ºC. Primers that had a single peak in the melt curves at the 59 or 61.4ºC annealing temperature reactions were run with a tenfold serial dilution of cDNA at the annealing temperature selected. Primer efficiencies for each primer were calculated using the slope of the average C_T values for each cDNA dilution: $E = -1 + 10^{(-1/Slope)}$. The final primer pairs that showed low C_T values at 59ºC annealing temperature and primer efficiency between 90-110% were selected for qPCR analysis are shown in Table 3. The gene rpS7, AAEL009496, was used as a reference for each qPCR plate; the primer sequences, annealing temperature and primer efficiency are shown in Table 3.

Table 3: Primers utilized in confirmation of heme treated midgut differential expression

Gene	Forward	Reverse	Temp	Efficiency (%)
AAEL000434	ATGCCTTGGAGAGTCTGACC	TGCTCGACTACCATCCCATC	59	105.71
AAEL002406	CTTCATCGGATTGGCGTGTT	GCACTTTCAGCGTCAATTGC	59	95.08
AAEL002557	ATGGAAACCTTCGGACCCTT	TGACACTCGGGGAAGAATGG	59	100.35
AAEL012440	GGTGAGTTCAACGTATCGGG	CGTGAACACCTTGTCGATGA	59	98.36
AAEL015458	ATGATGGAGCGATCCGATGT	TACGCGCATTTGGATTCAGG	59	98.73
rpS7	ACCGCCGTCTACGATGCCA	ATGGTGGTCTGCTGGTTCTT	59	104.9

Results

Examination of Aedes aegypti *Fed with Varying Concentrations of Heme Using a Protein Free Meal*

To examine the effect of heme exposure during meal digestion in *Aedes aegypti*, varying concentrations of heme (0.625, 1.25, 2.5, 5 & 10mM) were added to a protein-free meal and fed to 3-5 day old females. Death rates of over 50% were observed at all concentrations tested. In addition, after the midguts were dissected, varying colors ranging from light brown to dark were observed in the meal indicating varying heme concentrations present after feeding from the same aliquot of prepared food. Further examination of the heme added to the protein-free meal at numerous concentrations determined that the heme had precipitated out of the aqueous solution, which resulted in varying amounts of heme fed to each mosquito.

ZnMP Assay of **Aedes aegypti** *Midguts Incubated with 10µM Heme*

In the absence of an ability to feed controlled doses of heme solution to mosquitoes, and to determine whether *Aedes aegypti* midguts reduce their competence for heme import after prolonged exposure to heme, midguts were dissected from 3-5 day old mosquitoes and incubated with and without heme in cell culture medium. Midguts were incubated for 35 hours in regular growth media, heme-deficient (0µM heme) media or heme-overload media (10µM heme), followed by a 30-minute incubation with the heme fluorescent analog ZnMP (10µM). Pre-treatment of dissected midguts with heme substantially decreased the uptake of ZnMP as compared to both FBS and heme-deficient controls (Figure 24). No significant difference in ZnMP fluorescence was observed between the normal growth media (FBS) and heme-starved midguts (Figure 24C &D). This indicates that the mosquito midgut is in a state of heme starvation in anticipation of a bloodmeal and suggests that the amount of free heme in the FBS component is not enough to alter this physiological readiness. Decreased ZnMP uptake indicates that the 10µM heme treatment was sufficient to alter the physiological readiness of the midguts similar to what may happen during bloodmeal digestion.

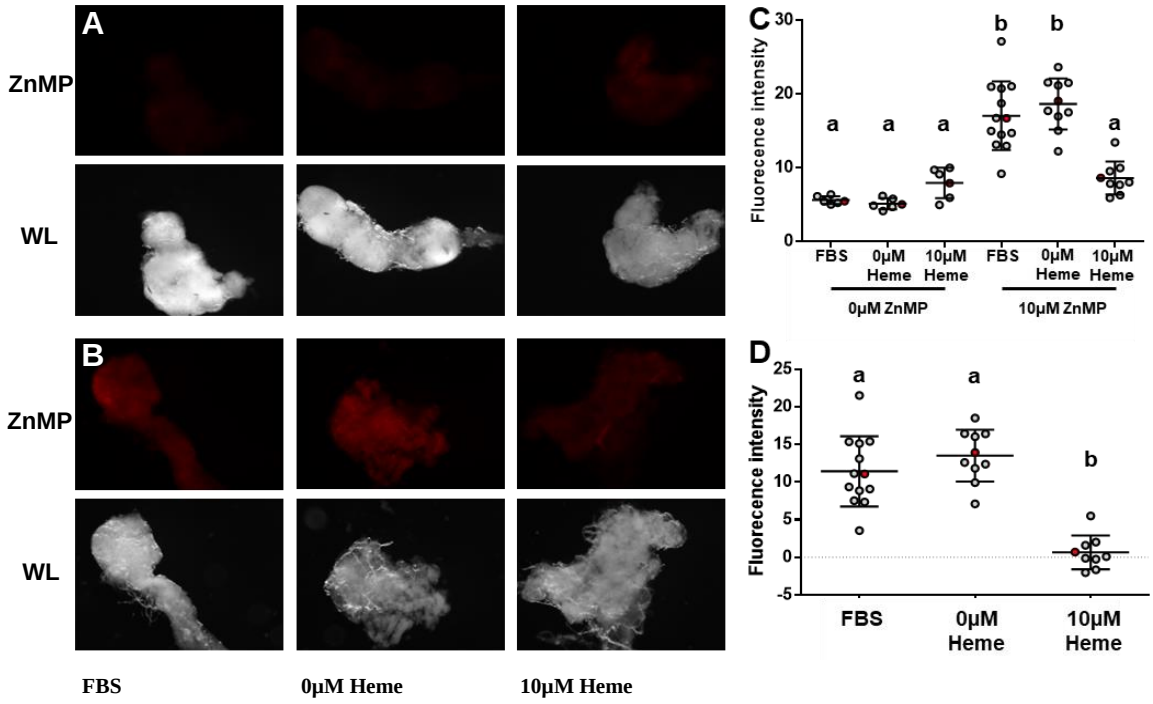

Figure 24: Heme treatment reduces ZnMP uptake in *Aedes aegypti* female midguts when treated for 35 hours
Photos for each treatment type taken before (**A**) or after (**B**) ZnMP incubation. Raw florescence intensity (**C**) or background corrected (**D**) measurements of each dissected midgut. Red-filled points correspond to the matching photo given in (**A**) or (**B**). WL=White Light

ZnMP Assay of Midguts Incubated with Varying Concentrations of Heme

As we have observed that ZnMP in too high a concentration can lead to cell death (similar to heme), we sought to identify the minimum concentration required to effectively change the competency of the midgut. *Ae. aegypti* midguts were dissected and placed in cultured cell medium containing various concentrations of heme for 35 hours. All media treatments were lacking fetal bovine serum as adding it in a previous experiment showed no significant difference from the 0µM heme sample. When the midguts were compared across the all treatments, only the 5µM and 10µM heme treated midguts were significantly different from the 0µM group with the largest difference found between the 0µM and 10µM groups (Figure 25).

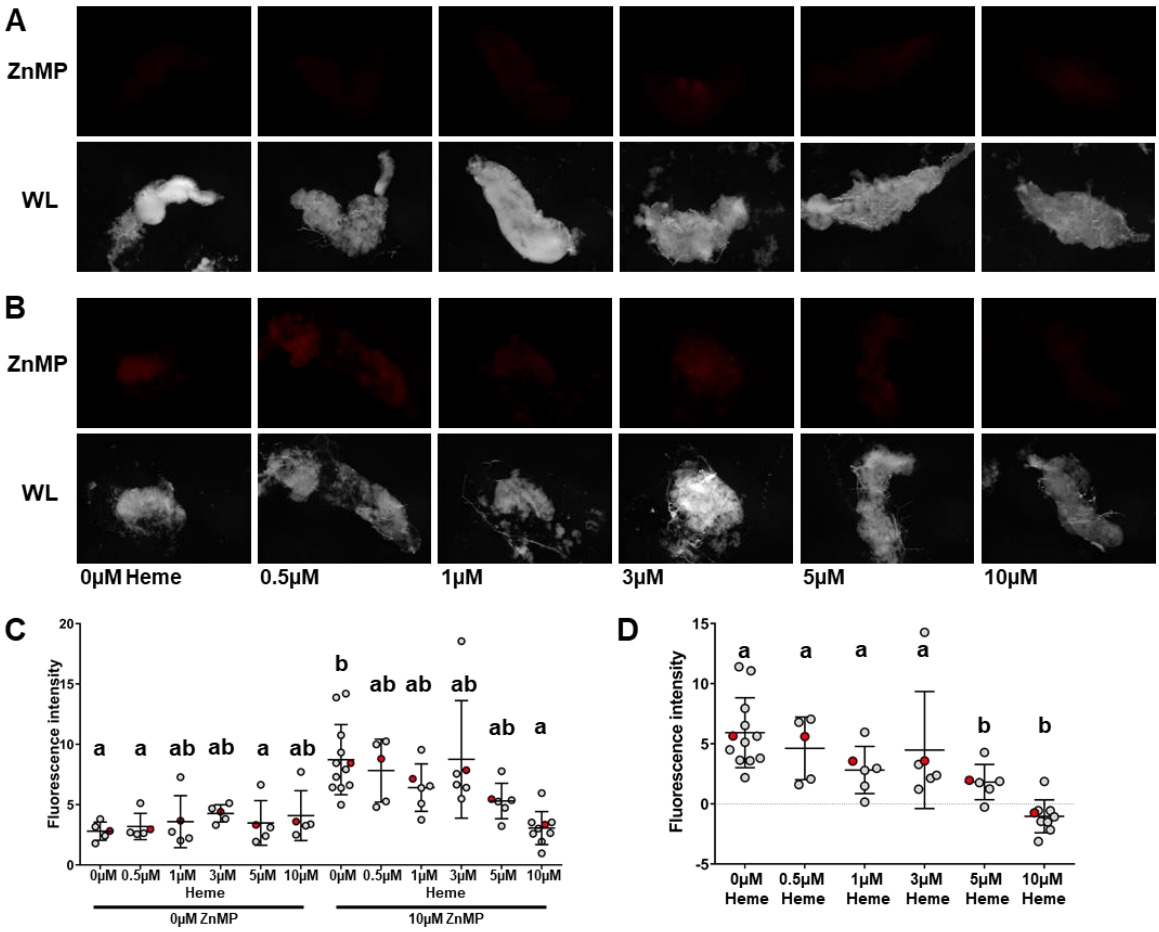

Figure 25: Heme treatment reduces ZnMP uptake in *Aedes aegypti* female midguts at multiple heme concentrations
Photos for each heme concentration taken before **(A)** or after **(B)** ZnMP incubation. Raw fluorescence intensity **(C)** or background corrected **(D)** measurements of each midgut. Red-filled points correspond to the matching photo given in **(A)** or **(B)**. WL=White Light

RNA Sequencing and Differential Expression Analysis

As treatment with heme was found to change the ability of the mosquito midgut to uptake ZnMP, we hypothesized that this physiological change was accompanied by changes to the transcriptional profile of the gut. To test whether these changes were due to changes in gene expression levels, midgut samples were prepared for sequencing with 4 replicate samples from each treatment type. After mapping the resulting data to the *Ae.*

aegypti genome and comparing it with the current annotation, we determined genes that were differentially expressed in the presence/absence of heme. A multidimensional scaling plot of the analysis shows that 3 of the 4 replicate samples for each treatment cluster within the treatment groups, with the two groups being distinct from one another (Figure 26). For each treatment, one of the biological replicates (0µM heme-1 and 10µM heme-2) cluster away from both groups and with the 0µM heme group respectively (circled in red in Figure 26A).

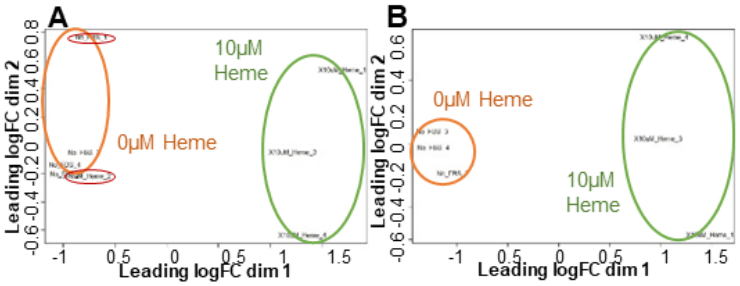

Figure 26: Multidimensional scaling plot of heme treated midguts midguts after dissection were incubated for 35 hours in Schneider's *Drosophila* medium containing either 0 or 10µM Hemin Chloride. **(A)** MDS plot of Midguts incubated in Schneider's *Drosophila* medium. 2 samples do not cluster with their other replicates, 0µM replicate 1 and 10µM replicate 2, circled in red. **(B)** MDS plot of the analysis with these 2 samples removed

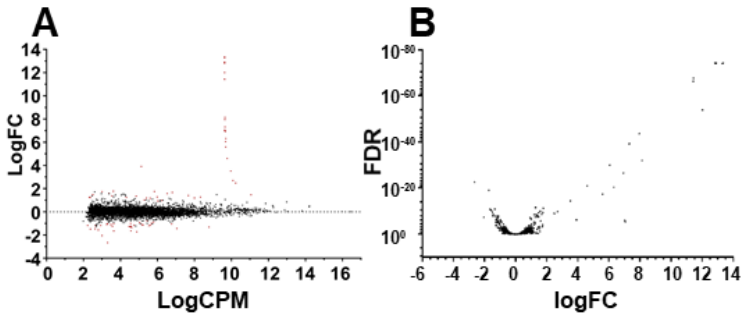

Figure 27: RNAseq-based differential expression after 35-hour heme treatment in midguts
Schneider's *Drosophila* medium 0µM vs 10µM hemin chloride. **(A)** Log2 fold change (LogFC) vs Log10 counts per million (LogCPM) graph of genes found differentially expressed in analysis. Genes with an adjusted p-value corrected for multiple testing of <0.00001 (false discovery rate: FDR) are shown in red. **(B)** Volcano plot of genes found differentially expressed in analysis.

The differential expression analysis found 65 genes with differing expression values between 0µM and 10µM treated midguts significant to a p-value corrected for multiple testing of 0.0001. Table 4 shows the number of genes found significant at the FDR cut off values of 0.0001, 0.001, 0.01 and 0.1. At the FDR cut off value of 0.1, 328 genes were found with differing expression patterns between the two heme concentrations (Figure 27). Of these, 173 genes were downregulated and 155 were upregulated in response to heme exposure. Of those with at least 1 predicted TM domain (152 total genes, or 46% of DEGs), 83 were downregulated and 69 upregulated. This number shows an enrichment of genes with TM predictions in response to heme, as on average 104 genes would have TM predictions if 328 genes were randomly selected from the entire known gene pool (p-value <0.00001). Unexpectedly, 11 of the 12 top upregulated genes were mitochondrial in origin, all of which contained logFC values of 2.7-12 and were highly expressed across the samples with logCPM values around 10 for each gene. These mitochondrial genes were removed from the analysis as we sought to focus on those genes

encoding membrane bound transporters relaying diet-derived heme, not synthesized heme. If we considered only those candidates not of mitochondrial origin with 2+ TM domains (n= 82), 45 were downregulated and 37 upregulated in the presence of heme. Of these, 40 were annotated as having unknown function, while 23 had functions relating to transport as described on Vectorbase (www.vectorbase.org). These 82 candidate genes can be reduced further by examining those with known function and eliminating those with functions not relating to transport like those with enzymatic activity or those related to ROS stress management, which reduces the list down to 63 genes, 40 were downregulated and 23 were upregulated in the presence of heme (Table 5)

Table 4: The number of significant genes found at different p-value cut offs

Adjusted p-value cut off	# of genes	# of TM genes
0.0001	65	38
0.001	84	47
0.01	154	76
0.1	328	152

Table 5: Membrane bound heme transporter candidate list

NAME	log2FC	FDR	# TM
AAEL000859 protein_coding	-1.3184	1.40E-08	2
AAEL019869 protein_coding	-1.2359	1.05E-05	2
AAEL002557 cationic amino acid transporter	-1.1718	9.42E-07	12
AAEL024460 protein_coding	-1.1243	0.0011500	4
AAEL020936 protein_coding	-1.0454	6.14E-05	2
AAEL021618 protein_coding	-1.0320	0.0278501	2
AAEL024267 protein_coding	-0.9820	0.0034265	2
AAEL003619 sodium/chloride dependent amino acid transporter	-0.9543	0.0004217	12
AAEL001938 ATP-binding cassette sub-family A member 3	-0.8521	0.0062384	17
AAEL007191 amino acid transporter	-0.8341	0.0023315	10
AAEL010905 protein_coding	-0.8260	0.0008207	6
AAEL005013 protein_coding	-0.7890	0.0014765	2
AAEL012440 sodium-bile acid cotransporter	-0.7835	4.60E-05	10
AAEL001495 protein_coding	-0.7597	0.0119851	6
AAEL004513 neurotransmitter gated ion channel	-0.7512	0.0058863	3
AAEL008664 protein_coding	-0.7068	0.0018782	2
AAEL006480 protein_coding	-0.7036	0.0057324	3
AAEL014355 symbol, putative	-0.6857	0.0402342	2
AAEL003618 sodium/chloride dependent amino acid transporter	-0.6854	0.0434105	12
AAEL002406 protein_coding	-0.6756	0.0698126	6
AAEL009531 niemann-pick C1	-0.6551	0.0005296	14
AAEL012226 protein_coding	-0.6385	0.0275240	4
AAEL009112 protein_coding	-0.6322	0.0315679	2
AAEL011918 protein_coding	-0.6194	0.0277839	2
AAEL027190 protein_coding	-0.5945	0.0026887	8
AAEL000461 protein_coding	-0.5927	0.0055109	3
AAEL000417 monocarboxylate transporter	-0.5895	0.0217701	12
AAEL006277 protein_coding	-0.5563	0.0620965	2
AAEL019696 protein_coding	-0.5510	0.0853716	4
AAEL002051 sodium/hydrogen exchanger 7, 9 (nhe7, nhe9)	-0.5509	0.0736327	10
AAEL003318 oligopeptide transporter	-0.5479	0.0118172	10
AAEL005539 protein_coding	-0.5458	0.0814036	4
AAEL003698 protein_coding	-0.5371	0.0570783	11
AAEL004657protein_coding	-0.5358	0.05170929	4
AAEL021771 protein_coding	-0.5258	0.0356762	3
AAEL001656 sodium-dependent phosphate transporter	-0.5243	0.0887935	11
AAEL008801 protein_coding	-0.5172	0.0938619	2
AAEL012041 sulphate transporter	-0.5139	0.0665416	11
AAEL005411 equilibrative nucleoside transporter	-0.4890	0.0774527	11

Table 5 continued

NAME	log2FC	FDR	# TM
AAEL006362 mitochondrial solute carrier	-0.4453	0.0942570	3
AAEL007792 protein_coding	0.4100	0.0993636	8
AAEL006855 UDP-galactose transporter	0.4690	0.0431129	10
AAEL005017 protein_coding	0.5117	0.0993636	2
AAEL012395 ATP-binding cassette transporter	0.5554	0.0277839	12
AAEL008693 Cation efflux protein/ zinc transporter	0.5872	0.0889097	6
AAEL000434 lipid a export ATP-binding/permease protein msba	0.5912	0.0640970	6
AAEL014896 protein_coding	0.5942	0.0665416	3
AAEL010347 protein_coding	0.6007	0.0569784	2
AAEL025631 protein_coding	0.6075	0.0901240	2
AAEL003438 protein_coding	0.6172	0.0640970	3
AAEL023104 protein_coding	0.6348	0.0217701	4
AAEL005026 ATP-dependent bile acid permease	0.6372	0.0942570	17
AAEL006800 sodium/chloride dependent transporter	0.6795	0.0726937	12
AAEL027424 protein_coding	0.7912	0.0075813	8
AAEL018150 protein_coding	0.8105	0.0327572	13
AAEL022465 protein_coding	0.8262	0.0219069	3
AAEL028119 protein_coding	0.8301	0.0123592	2
AAEL006071 protein_coding	0.9153	0.0785121	2
AAEL002129 protein_coding	1.0183	3.69E-05	2
AAEL005043 ATP-dependent bile acid permease	1.1916	8.42E-05	17
AAEL002599 protein_coding	1.2418	3.07E-05	2
AAEL021284 protein_coding	1.6055	1.95E-06	2
AAEL029008 protein_coding	1.7825	5.04E-12	2

Comparison of Midgut Heme Transporter Candidates to Those Found in Cultured Cells

In total 63 multipass transmembrane heme transporter candidates were identified in the differential expression analysis of the midgut samples, 40 downregulated in the presence of heme and 23 upregulated. Previously, many heme transporter candidates were identified in *Ae. aegypti* cultured cells across 2 different cell types and 4 different experiments, summarized in Table 6. These lists of genes were compared to identify whether any midgut heme transporter candidate genes were also identified in one or more

cultured cell experiments which would potentially indicate common mechanistic pathways of heme import between the cultured cells and midgut epithelial cells. In total, 16 of the 40 midgut heme importer candidates and 7 of the 23 midgut heme exporter candidates were found in 1 or more cultured cell datasets. Of the 16 shared heme importers, 12 were found in only 1 cultured cell dataset, 2 in 2 datasets and 2 in 3 datasets as shown in Table 7. In contrast, of the 7 total heme exporter candidates that were shared with the cultured cell experiments, only 1 was found in 2 cultured cell datasets with the remaining 6 only found in 1 dataset.

Table 6: Heme transporter candidates identified during cultured cell analyses

Cultured cell experiments	Potential Importers	Potential Exporters
Aag2 48hr heme treated	455	385
A20 72hr heme treated	448	143
Aag2 72hr L15 heme treated	229	197
Aag2 72hr Schn heme treated	238	240

Table 7: Midgut heme transporter candidates found also in one or more cultured cell dataset

Potential importers				Potential exporters			
Midgut+1	+2	+3	+4	Midgut+1	+2	+3	+4
AAEL012226	AAEL011918	AAEL012440		AAEL010347	AAEL003438		
AAEL005539	AAEL019696	AAEL001495		AAEL027424			
AAEL004657				AAEL028119			
AAEL021771				AAEL006855			
AAEL008801				AAEL012395			
AAEL005411				AAEL006800			
AAEL019869							
AAEL005013							
AAEL006480							
AAEL003619							
AAEL000461							
AAEL000417							

qPCR Validation of Sequencing Results

To validate the differential expression analysis of the RNA sequencing on heme rexposed *Aedes aegypti* midguts, quantitative real-time PCR was performed. The computationally derived fold change values obtained from the sequencing of 35 hour heme incubated dissected midguts *in vitro* were compared to the relative quantification (RQ) qPCR values. The expression of 5 genes out of the 63 TM (2+ domains) genes found highly differentially expressed in the presence of heme, see Figure 28, was examined; AAEL000434, AAEL002406, AAEL002557, AAEL009531 and AAEL012440. With the exception of AAEL000434, the RT-qPCR results did confirm the log2 fold change values determined computationally.

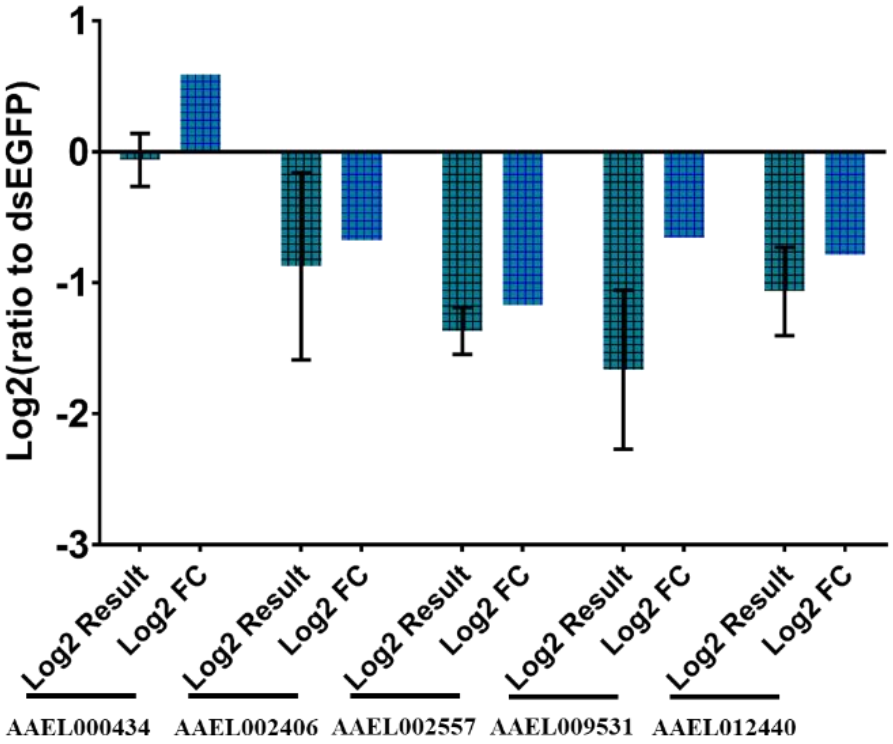

Figure 28: RT-qPCR of RNAseq-based differential expression midguts after 35-hour heme treatment

5 genes differentially expressed in midguts treated with 10µM heme when compared to 0µM heme control were selected to validate computational results, AAEL000434, AAEL002406, AAEL002557, AAEL009531 and AAEL012440. Teal bars indicate qPCR RQ values and blue bars indicate computational FC values.

Discussion

Irrespective of its role as a nutrient or signaling molecule in *Ae. aegypti*, the method of entry of heme into the midgut epithelial cells for degradation or incorporation into hemo-proteins is not currently known. Our study of heme overexposure and deficiency in the cultured cells Aag2 and A20 showed an increase in ZnMP fluorescence after heme deficiency treatment indicating gene expression changes resulting in an upregulation of heme import in these condtions (Chapter 2). As no clear candidate heme transport genes were identified from the differentially expressed genes, an analysis of *Ae. aegypti* midgut epithelial cells and their response to heme overload was performed. As the midgut epithelium is responsible for uptake of heme for degradation or incorporation into hemo-proteins during blood digestion, it is the ideal system to locate the membrane bound heme importers and exporters utilized during this time of massive heme overload.

The zinc mesoporphyrin fluorescent assays developed in the cultured cell analysis of heme import [Chapter2 & (Worthington et al., 2001)] were adapted to midguts harvested and treated with varying concentrations of heme in growth media. After treatment with heme, a reduction of ZnMP fluorscence was observed indicating that the midgut cells were adapting to changes of heme present in their environment. Unlike *C. elegans* and *R. microplus*, where previous experiments identified heme transportors, *Ae. aegypti* is able to synthesize heme (Perner et al., 2019). Biosythesized heme would be in addition to dietary heme obtained during blood digestion, and could alter the quantity of heme absorbed from the diet (Lara et al., 2015; Perner et al., 2019; Rajagopal et al., 2008; Rao et al., 2005). Inhibition of the last enzyme in heme biosynthesis pathway,

ferrochelatase, could cause an increase in uptake of dietary heme leading to a stronger ZnMP signal in *Ae. aegypti* midguts.

Examination of differential expression of mRNA transcripts at the gene level, found 65 significant DE genes at the adjusted p-value cut off of 0.0001, 38 of which are TM containing and only 2 genes showing high expression changes, AAEL019570 (-2.04 log2, ~0.243), unknown function, and AAEL000717 (3.91 log2, ~15.03), a protocadherin. When this p-value is altered to 0.1, 328 genes were found differentially expressed (152 TM genes), however no new highly expressed genes are identified. Not included in this analysis due to location in the mitochondria were 12 highly upregulated genes that had log2 fold changes ranging from 12 to 2.7 and all had logCPM values ~10. Comparison of DE genes identified in heme treated midguts to those in cultured cells showed 23 of 63 DE midgut genes (36.5%) present in at least 1 cultured cell experiment, 16 of 40 downregulated and 7 of 23 upregulated. Two genes of the 16 potential import genes were found in 2 of the cultured cell analyses, AAEL011918 (-0.62 log2), unknown function, and AAEL019696 (-0.55 log2), unknown function with another 2 of 16 in 3 cell datasets, AAEL012440 (-0.78 log2), sodium bile acid cotransporter, and AAEL001495 (-0.76 log2), unknown function. Of the seven potential export genes identified, only one was found in more than one cultured cell experiment, AAEL003438 (0.62 log2) which has an unknown function. A modest number of candidate heme transport genes were identified in this analysis with this list further reduced by examining those genes located additionally in one or more cultured cell datasets.

Overall, the transcriptional changes observed in the midgut heme exposure analysis are much smaller than those in the cultured cell heme exposure analyses and those

identified in whole body differential expression during blood digestion (Bonizzoni et al., 2011). However, Bonizzoni et al. (2011) examined differential expression across the whole body of bloodfed females vs sugar fed thus emphasizing those DE genes found across the carcass while potentially diluting those specific to the midgut epithelium. Of the ~53 TM genes found highly differentially expressed in bloodfed females (>2 log2 or <-2 log2; >100 reads in at least 1 sample) by Bonizonni et al (2011), 10 were also identified in our heme-treated midgut analysis. However none of those 10 genes contained fold change values above 2 log2 or below -2 log2, indicating their expression was less in the midgut than what was measured across the whole body. These ten genes include four with two or more transmembrane domains: an oligopeptide transporter (AAEL003318), sulphate transporter (AAEL012041) and two with unknown functions (AAEL000829 & AAEL006277), only one of which had a fold change below -1 log2 (AAEL000829; -1.32 log2, ~0.40) in our analysis. The high number of low transcriptional expression changes present in our differential expression analysis could also be due to the high expression variability observed between the heme replicates, Figure 26B. While the heme replicates were distinct from the 0µM heme samples, they did not cluster together indicating differential expression was occurring between them. These variable expression changes between replicates could have reduced the statistical power of the differential expression analysis yielding very few genes with above a 4 fold expression change. As Bonizonni et al. (2011) showed significant differential expression at 5 hours post blood meal, heme exposure may very well initiate transcriptional changes at an earlier timepoint than examined at this study. Therefore, we would suggest examining ZnMP uptake after *in vitro* heme incubation at 6 hours post dissection as this limits the time spent in the culture medium

before measurement yet still allowing heme induced expression or proteomic changes to occur.

This analysis sought to shed some light onto an area little explored previously, heme import into the midgut epithelium during blood digestion. Midguts taken from adult sugar fed females, were incubated *in vitro* with growth media containing various heme concentrations. Differential expression analysis comparing midguts incubated with 0µM and 10µM heme resulted in a little over 300 DE genes, 63 of which were identified as potential heme transporters based on number of TM domains present and preposed function. These results taken together with the heme exposure analysis performed in cultured cells (Chapter 2), indicate that if the heme transport mechanism is post-transcriptionally regulated it is done so with a redundant system of many different transport genes all contributing to heme uptake as neither set of analyses found highly differentially expressed candidate genes. Characterization of a small selection of those candidates found in both the midgut and cell culture analyses have yet to be performed. Much remains to be discovered about heme import in this mosquito species.

CHAPTER IV

REVERSE GENETIC ANALYSIS OF CANDIDATES FOUND IN MULTIPLE CELL CULTURE ANALYSES AND THE MIDGUT ANALYSIS

Introduction

A typical blood meal ingested by an *Aedes aegypti* mosquito releases ~10mM heme over the course of digestion as the blood protein hemoglobin is broken down (Pascoa et al., 2002). This large influx of heme is transported into the midgut epithelium where it is used in hemoproteins or digested by cytosolic heme oxygenase [see review of HO mechanisms (Yanatori et al., 2019)]. A study of heme overexposure and deficiency in *Ae. aegypti* cultured cells (Chapter 2) and midgut epithelial cells (Chapter 3) sought to identify the membrane bound transporter(s) responsible for heme uptake during blood digestion. A number of candidates were identified based on their differential expression in response to heme exposure, their number of predicted TM domains and their presence in more than one dataset. In midgut epithelial cells, 63 genes, 40 downregulated and 23 upregulated, with 2 or more TM domains were found differentially expressed in response to 10µM heme exposure of which 23 were also identified as candidates in cultured cells, 16 downregulated and 7 upregulated. To confirm the functions of a subset of these top heme transporter candidates, a reverse genetic analysis was performed based on RNA interference in adult mosquitoes.

RNA interference is a major innate immune response found in many organisms including the mosquito *Ae. aegypti*. The RNA-induced silencing complex (RISC) is a multi-protein complex which incorporates small single strand RNA processed by Dicer2 to

act as a guide targeting degradation of specific messenger RNAs [see the following reviews for further details (Bagasra and Prilliman, 2004; Blair, 2011; Samuel et al., 2018)]. The RNAi pathway in *Ae. aegypti* is the major innate immune response for many viruses including dengue, which upon infection releases double-stranded RNA into the cytoplasm resulting in the production of siRNAs (Sanchez-Vargas et al., 2009). Once produced and loaded onto the RISC complex, these siRNAs target the degradation of viral mRNA based on sequence similarity thus inhibiting viral replication. This same immune response can be harnessed to inhibit expression of endogenous genes, leading to a temporary reduction of their resulting proteins, which sometimes results in a measurable phenotypic response when compared to control samples. The RNAi knockdown of the *C. elegans* genes *hrg1* and *hrg4* confirmed their role as heme transporters due to the changes observed in the fluorescence of zinc mesoporphyrin. Thus, HRG-4 was shown to control heme import into the intestinal cells, as no ZnMP was shown upon knockdown in the whole worm, while HRG-1 controlled heme homeostasis by isolating excess heme into an intercellular compartment as shown when a larger quantity of ZnMP was isolated in the intestinal cells (Rajagopal et al., 2008). ABCB10 from *R. microplus* was also characterized through RNAi-based gene knockdown followed by heme analog fluorescence changes, as an accumulation of zinc protoporphyrin was observed in the digestive vacuoles following knockdown indicating this gene's role in transporting heme out of those vacuoles after hemoglobin digestion (Lara et al., 2015). Thus, RNAi knockdown is a viable approach to study heme transporters in many organisms especially in conjunction of a heme fluorescent analog and can be adapted to study heme import in *Ae. aegypti*.

In addition to RNAi, heterologous expression of a candidate gene in a model organism to induce a gain of function phenotype allows insight into the function of the encoded protein. The *Arabidopsis thaliana* iron transporter IRT1 was shown to be an iron transporter following cloning an *Arabidopsis* cDNA library into a yeast strain lacking its own mechanism of iron transport, then isolating and sequencing those yeast cultures that showed restored iron uptake (Eide et al., 1996). LIT1 in *L. amazonensis*, an ortholog of the *A. thaliana* IRT1, was also characterized as an iron transporter through the addition of an expression plasmid to yeast deficient in iron-transport (Jacques et al., 2010). The function of the mouse gene *Zip14* (Slc39a14) was determined to be an iron transporter by overexpression in HEK 293H cells and by a gain of function experiment in the insect cells Sf9 where *Zip14* cDNA was introduced via a baculovirus (Liuzzi et al., 2006). Preliminary observations indicated that *D. melanogaster* S2 cells were extremely tolerant of high exposure to heme, suggesting the possibility that this cell line was deficient in heme import. If true, S2 cells would be an ideal system to heterologously express potential heme import proteins as if treated with ZnMP only those cells that gained heme import would fluoresce red.

In this study, a reverse genetic analysis was performed on a select number of genes identified as potential membrane bound heme importer or exporters in *Ae. aegypti* midgut epithelial cells and cultured cells. The phenotypic effects when these genes' expression was depleted through RNAi knockdown and/or gained through heterologous expression in *Drosophila* S2 cells were analyzed to hypothesize their function. Depletion of a membrane bound import gene was hypothesized to lead to reduced cytosolic heme levels while targeting export genes will increase the cytosolic heme pool. In S2 cells, if the protein

introduced encodes a heme importer, treatment with a heme fluorescent analog will yield uptake and the cells will fluoresce, while if the protein's function is unrelated to heme transport then no uptake, and thus no fluorescence will be observed.

Methods

Cultured Cell Growth Conditions

A. aegypti Aag2 cells were maintained in Schneider's *Drosophila* Media (Thermo Fisher) with 10% FBS (Atlanta Biologicals) and 1% Pen-strep (Corning) at 28^{o}C. *A. aegypti* A20 cells were maintained in Leibovitz's L15 media with 10% FBS (Atlanta Biologicals) and 1% Pen-strep (Corning) at 28^{o}C. *D. melanogaster* S2 cells, stocks from ATCC and DGRC (ATCC, VA; DGRC, IN), and S2R+ (DRSC, MA) were grown in 10% heat inactivated FBS (Atlanta Biologicals) and 1% Pen-strep (Corning) at 25^{o}C. FBS used to maintain *Drosophila* lines was heat inactivated by incubating in a 56^{o}C water bath for 30 minutes.

Inducing Expression of Heme Importers in Drosophila melanogaster *Cultured Cells*

Cloning Expression Plasmids

Two multicistronic expression plasmids were selected to construct plasmids encoding heme importers, Ac5-STABLE1-neo and Ac5-STABLE2 gifts from Rosa Barrio & James Sutherland (Addgene plasmid #32425; http://n2t.net/addgene:32425, RRID:Addgene_32425 and Addgene plasmid #32426, http://n2t.net/addgene:32426, RRID:Addgene_32426 respectively)(Gonzalez et al., 2011). Once the plasmids were obtained in *E. coli* cultures, the cultures were streaked onto LB agar plates which was grown overnight at 37^{0}C. Culture tubes were prepared with 3mL of LB Broth mixed with

3µL 100mg/mL Ampicillin. A pipette tip was then used to collect E. coli from a single colony from each plate and dropped into culture tubes. Tubes were then incubated overnight at 37^0C and 215rpm in the Excella E24 Shaker incubator (New Brunswick Scientific/Eppendorf, Germany). Two large cultures were prepared for each plasmid using the small culture grown in the culture tube the next day; 200mL LB broth, 200µL 100mg/mL Ampicillin and 2mL small culture. These cultures were allowed to grow overnight at 37^0C and 215rpm in the shaking incubator. Each large culture was aliquoted into 4 50mL conical tubes and centrifuged at 4^0C 4000rpm for 20min in a Heraeus Megafuge 16R Centrifuge (Thermo Scientific, MA). After centrifugation, the pellets were frozen at -80^0C. Plasmid purification was performed using the NucleoBond® Xtra EF kit (MACHEREY-NAGEL GmbH & Co. KG, Germany). ·

Cloning Known Heme Importers into Expression Plasmids

The sequence of HRG1 from *C. elegans* and of ABCB10 from *R. microplus*, 2 known heme importers, were sequenced de novo by Epoch Life Sciences (Epoch Life Sciences, INC, TX). The resulting HRG1 and ABCB10 plasmids were transformed into 5-alpha *E. coli* following manufacturer's protocol (NEB, MA). Transformed aliquots were diluted 1:10 and 1:100 and 3 LB plates seeded for each plasmid, one of each dilution and one of the undiluted transformed *E. coli*. The plates were allowed to grow at 37^0C overnight before 3 colonies per plasmid were selected to grow small cultures in culture tubes. All small cultures were grown in the shaking incubator overnight at 37^0C and 215rpm. DNA was isolated from all cultures using the NucleoSpin® Plasmid miniprep kit (MACHEREY-NAGEL GmbH & Co. KG, Germany). A double digest at 37^0C for 15 minutes was set up

for each of the STABLE1 and HRG1 plasmids, 1µg each, with 10 units of the NheI-HF and BamHI-HF restriction enzymes in the CutSmart® Buffer (NEB, MA). A triple digest with 10 units of the NheI-HF, BamHI-HF and BsaI enzymes was performed with 1µg of the ABCB10 plasmid incubating for 1hr at 37^0C in the CutSmart® Buffer to digest the backbone to allow for easier identification of the ABCB10 gene fragment by size. The whole digestion volume was loaded and run on a 1% agarose gel for each digestion and the ~6000bp fragment from the STABLE1 digestion, the 617bp fragment from the HRG1 digestion and 2000bp fragment from the ABCB10 digestion were cut from the gel. DNA was extracted using the NucleoSpin® Gel and PCR Clean-up kit (MACHEREY-NAGEL GmbH & Co. KG, Germany). To add the heme importers onto the STABLE1 backbone, ligation reactions with T4 DNA Ligase were set up with 1:0, 1:3, 1:5 and 0:3 Vector:Insert ratios for each importer following the manufacturer's protocol and incubated for 10 minutes at room temperature (NEB, MA). The entire ligation mix from each reaction was then transformed into E. coli following the procedure described above before plating on a LB Amp plate and incubated overnight at 37^0C. A colony PCR was then performed using the primers listed in Table 8 below to identify which colonies contained the STABLE1-ABCB10 and STABLE-HRG1 plasmids. Each colony selected for PCR confirmation was also streaked onto a LB plate which was incubated at 37^0C overnight. *Taq* DNA polymerase in standard *Taq* reaction buffer, 10mM dNTPs, 10µM primers and 5µL E. coli from a colony mixed with H_2O, were prepared for each colony tested (NEB, MA). The thermocycler program used is given in Table 9 below.

Table 8: Colony PCR primers

Primer Name	Sequence
STABLE1_D_F	GAGGGCAGAGGAAGTCTTCTAAC
S1_ABCB10_D_R	CTCATCAATGTATCTTATCATGT
S1_HRG1_D_R	AACTCATCAATGTATCTTATCA

Table 9: Colony PCR thermocycler program

Temperature (^{0}C)	Time	
95	2 minutes	
95	15 seconds	30 cycles
46	1 minute	
72	1 min (HRG1) or 2:30 min (ABCB10)	
72	7 minutes	
4	∞	

An aliquot of each colony PCR reaction was loaded and run on a 1% agarose gel, only those colonies containing the correct insert amplified during the PCR reaction and thus contained one band on the agarose gel. Eight cultures were prepared from the grid LB plates prepared before the colony PCR from the plasmids that tested positive to having the correct insert, 4 per plasmid. Culture tubes were prepared with 3mL of LB Broth mixed with 3µL 100mg/mL Ampicillin and incubated overnight at 37^{0}C and 215rpm in the Excella E24 Shaker incubator (New Brunswick Scientific/Eppendorf, Germany). The next day plasmid DNA was isolated from all cultures using the NucleoSpin® Plasmid miniprep kit (MACHEREY-NAGEL GmbH & Co. KG, Germany). To confirm that the correct sequence was present in both the STABLE-1 HRG1 and STABLE-1 ABCB10 plasmids, aliquots of the 4 plasmids from each type were digested with BsaI or EcoRI-HF respectively (NEB). Both digestions occurred at 37^{o}C, BsaI for 1 hour, EcoRI-HF for 25

minutes, using 10 units of enzymes, 1µg of plasmid and the CutSmart® Buffer (NEB). Once complete, the entire reaction volume was loaded onto a 1% agarose gel to examine the size and number of bands present from each digested plasmid. Finally, three samples of each plasmid were sequenced using the forward and reverse primers given in Table 8 to confirm the presence of HRG-1/ABCB10 in the STABLE-1 plasmid backbone.

4mL cultures of 2 confirmed colonies per plasmid type were started using the grid LB plates grown using the colonies tested in the colony PCR and placed in the 37ºC shaking incubator overnight. Large cultures were started of all 4 small cultures grown the previous night by adding 2mL of *E. coli* from the small culture into 200mL LB broth and 200µL 100mg/mL Ampicillin. The large cultures were grown overnight into the shaking incubator at 37ºC and 215rpm. The next morning the cultures were aliquoted into 4 50mL conical tubes, which were then pelleted using a centrifuge, 20 min 4000rpm at 4ºC. LB broth was decanted into bleach and the pellets frozen at -80ºC. Plasmids were purified using the NucleoBond® Xtra EF plasmid purification kit (MACHEREY-NAGEL).

Exploring Expression Plasmid Transfection Ability and ZnMP Uptake in Cultured Cells

Transfection of Control Plasmids in Cultured Cell Lines

To examine whether the *D. melanogaster* cell lines were capable of uptaking the STABLE plasmids (STABLE1-NEO, STABLE1-HRG1, STABLE1-ABCB10, STABLE2) along with a control plasmid IE1-GFP, transfections were performed using Effectene (Qiagen Hilden, Germany) following the DRSC/TRiP standard transfection protocol with cells at 70-80% confluency. Specifically, 2µg of dsRNA, 16µL Enhancer, 182µL Buffer EC and 20µL Effectene was used for each well of a 12-well plate. At 24, 48 & 72 hours after

transfection, an aliquot of the transfected cells was wet mounted onto slides and imaged using the GFP filter of the Zeiss Axio Observer Microscope (Carl Zeiss Microscopy, Thornwood NY).

ZnMP Assay to Determine Ability of Cells to Uptake Heme

Zinc Mesoporphyrin (ZnMP) (Frontier Scientific, Logan, UT) stock solution was made at 0.3mM concentration by dissolving the ZnMP into a 1% Ethanol-amine (Sigma Aldrich) and 10mg/mL Bovine Serum Albumin (Sigma Aldrich) solution (Vreman et al., 1989). This was filter sterilized using a 0.22µm filter (EMD Millipore), split into 500µL aliquots and stored at -20^{o}C. Aag2 or A20 cells were seeded onto a 12 well plate and treated with 0, 5 & 10µM ZnMP for 30 minutes. *Drosophila* S2 and S2R+ cells were harvested from a T75 flask, counted using a hemocytometer. S2 cells were placed into microcentrifuge tubes at 1x10^{7} cells/mL and incubated with 0, 5, 10, 20 & 100µM ZnMP. The uptake buffer used during the incubation and wash procedures consisted of 50mM HEPES, pH 7.4, 130mM NaCl, 10mM KCl, 1mM $CaCl_2$ and 1mM $MgSO_4$ (Worthington et al., 2001). All subsequent steps were performed in as dark of conditions as were practical. ZnMP stock solution was freshly diluted in uptake buffer prior to use and added to cells after medium was removed. All media and buffers were removed from the *Drosophila* cells by centrifugation at 4^{o}C 500xg for 5 min followed by decantation. Following the ZnMP incubation, the cells were washed once with uptake buffer + 5% BSA, then 2x with uptake buffer. *Drosophila* cells were mounted onto a slide prior to cell imaging. Cells were imaged in 1x PBS at 100x magnification using the DsRED filter of the Zeiss Axio Observer Microscope (Carl Zeiss Microscopy, Thornwood NY).

RNAi Knockdown in **Aedes aegypti** *Cultured Cells and Adult Females*

dsRNA Production

PCR amplicons of each candidate heme importer were generated using Phusion polymerase following standard manufacturer's protocol for a 50µL reaction volume (New England Biolabs Ipswich, MA). The EGFP amplicon was based off a GFP containing plasmid, Ac5-STABLE1-neo a gift from Rosa Barrio & James Sutherland (Addgene plasmid #32425; http://n2t.net/addgene:32425 ; RRID:Addgene_32425)(Gonzalez et al., 2011). The PCR primers and annealing temperatures used for each gene are given in Table 10. Primers with T7 sequences were designed using SeqBuilder® (SeqBuilder® v14 DNASTAR Madison, WI) and made by IDT. Following the manufacturer's protocol, RNA from female *Aedes aegypti* was isolated using the TRIzol reagent (Thermo Fisher). The resulting RNA was DNase-treated (DNase I: New England Biolabs) and quantified using a Nanodrop (Thermo Fisher). cDNA was prepared using a random primer mix (SuperScript® IV Reverse Transcriptase: Thermo Fisher). The MEGASCRIPT RNAi kit (Thermo Fisher) was used to make the dsRNA with T7 polymerase enzyme making both strands during the same 5-hour incubation at 37^{o}C. The resulting dsRNA was nuclease treated at 37^{o}C for 1 hour to remove any ssRNA and dsDNA template remaining in the sample. Purification of the dsRNA was performed using the MEGACLEAR kit (Thermo Fisher).

Table 10: Primers for dsRNA Gene targets

Name	Forward sequence	Reverse sequence	Temp
AAEL000417	taatacgactcactagggTTAACGGCCGATCTACAGGACGAG	taatacgactcactagggAACGACGGCAGGCAGATAGATGAA	60
AAEL000434	taatacgactcactagggCCGGCCTATTTCGCAACAGTG	taatacgactcactagggCGAAGCCCGTCCGAAAGATT	60
AAEL000461	taatacgactcactagggGAAGCCGCGTACCGATTGATGT	taatacgactcactagggTCGGAGGGAAAGATTTGTTGTAGC	65
AAEL001495	taatacgactcactagggCGAAAACGGTGGCGGACTTG	taatacgactcactagggGTGGGGACGGAAATGAGACAGC	65
AAEL001938	taatacgactcactagggGGTGCGCATCCGAATCAAAT	taatacgactcactagggTGCATACCCCCAGACAGACTCG	60
AAEL002406	taatacgactcactagggGAAAAAGCCCATCGCAGAACC	taatacgactcactagggGAACCCGAACACGCAAAGAAT	60
AAEL002557	taatacgactcactagggTGTTGGCCCTGTTCATCATCATTG	taatacgactcactagggGCAGGCACCGGCGTAGAAAAG	65
AAEL003318	taatacgactcactagggCCTATCCATCCCGGTACGAAATCA	taatacgactcactagggAGTAGTACGCGAGCACGGCAAATA	65
AAEL003619	taatacgactcactagggTCGTTACCCGGGAGTGAAGAT	taatacgactcactagggTAGCGCATACAGCCCAAACGAC	65
AAEL003698	taatacgactcactagggACGGGGCGGATTGTCTCG	taatacgactcactagggAATGCCACTGCCAGCTATGAAACC	65
AAEL004513	taatacgactcactagggGGGCACGGCGGAAAAGGAC	taatacgactcactagggGCCGAAGCCAACGTGATGAAC	65
AAEL004657	taatacgactcactagggGTCGCATCATTCTTGTTCTTCTCC	taatacgactcactagggAAAATACCAGCCGCATACG	60
AAEL008664	taatacgactcactagggAAAATGGGCGCAAACTTCC	taatacgactcactagggCCAACGCCAGGTAATCTTC	60
AAEL009531	taatacgactcactagggGCTTCCCGGCCGTCAATAGAGG	taatacgactcactagggGCAGTCATCGGGGCGTAGCAGA	60
AAEL012226	taatacgactcactagggACACATTTCCGGCCGTTCCATAC	taatacgactcactagggCTCCGCCAGCTGTCCCATCAT	60
AAEL012440	taatacgactcactagggGACGGCTCGCATCCTGGTG	taatacgactcactagggGGAAAAAAAACGCGTGACGGCTTTGT	60
EGFP	taatacgactcactagggATGGTGAGCAAGGGCGAGGAGC	taatacgactcactagggATCTTGAAGTTCACCTTGATGCCGTT	60

Cell Growth Conditions

Ae. aegypti Aag2 cells were maintained in Schneider's *Drosophila* Media (Thermo Fisher) with 10% FBS (Atlanta Biologicals) and 1% Pen-strep (Corning) at 28^{o}C.

Transfection

To characterize candidate importers and exporters for a role in heme transport, dsRNA transfections were performed using Effectene (Qiagen Hilden, Germany) following the standard transfection protocol with cells at 70-80% confluency. Specifically, 2.5µg of dsRNA, 8µL Enhancer, 129.5µL Buffer EC and 25µL Effectene was used for each well of a 6-well plate. A control dsRNA targeting GFP was performed with each plate. At 24 hours after transfection, the media was replaced in each well of the 6-well plate with 2mL Schneider's *Drosophila* media + 1% Pen-strep (0µM heme). At 3 days post transfection, the cells were washed off each well, collected in microcentrifuge tubes and counted using a

hemocytometer. Cells were seeded at 2 x 10^6 cells/mL per well with a total volume in each well of 100µL into a 96-well black clear bottomed BRANDplate® Cell grade Premium (Brand Wertheim, Germany) 12 wells per dsRNA, with any remaining cells pelleted by centrifugation at 4^{o}C and frozen at -80^{o}C after discarding the supernatant.

Zinc Mesoporphyrin & Calcein AM Assay

Zinc Mesoporphyrin (ZnMP) (Frontier Scientific, Logan, UT) stock solution was made at 0.3mM concentration by dissolving the ZnMP into a 1% Ethanol-amine (Sigma Aldrich) and 10mg/mL Bovine Serum Albumin (Sigma Aldrich) solution (Vreman et al., 1989). This was filter sterilized using a 0.22µm filter (EMD Millipore), split into 500µL aliquots and stored at -20^{o}C. The uptake buffer used during the incubation and wash procedures consisted of 50mM HEPES, pH 7.4, 130mM NaCl, 10mM KCl, 1mM $CaCl_2$ and 1mM $MgSO_4$ (Worthington et al., 2001). All subsequent steps were performed in as dark of conditions as were practical. Transfected cells seeded in 96 well plates as described in the previous section were incubated with 5µM ZnMP for 30 minutes at 28^{o}C, 100µL solution per well, after the media was removed from each well. Following the incubation, the cells were washed once with uptake buffer + 5% BSA, then 2x with uptake buffer, 100µL solution per well for each wash step. Next, 100µL of 2.5µM Calcein AM (Thermo Fisher) diluted in 1xPBS was added to each well and allowed to incubate at 28^{o}C for 30 minutes protected from light exposure. A total of 21 fluorescence measurements were measured across each well at Ex. 540/Em. 580 using a Spectramax i3x with the average fluorescence per well determined from these values. The monochromator optical configuration, fluorescent read mode and well scan read type with pattern selected as ‘fill’ was selected

for each Spectramax run. The number of cells present in each well was determined by Calcein fluorescence using a Minimax 300 (Molecular Devices, San Jose CA). The MiniMax optical configuration, Imaging read mode and Endpoint read type were selected for each Minimax run. Only the green channel was imaged, Ex. 456/Em. 541, with 4 photos taken per well focusing on the middle portion of each well. Pictures were taken at 5ms exposure and 120µm focus adjustment and cells were counted by training the software to identify cells based on their green fluorescence.

Statistical Analysis

The ZnMP fluorescence per cell was calculated by dividing the mean fluorescence per well by the number of cells counted. These values were then normalized to the exogenous GFP control dsRNA values. The lme4 package in the R statistical software was used to run a linear mixed-effects model analysis on the data to determine which genes were significantly different from the control (Bates et al., 2015). GFP was set as the reference for the analysis using the relevel command and the p-values obtained were rounded to 5 digits. The hypothesized formula for the model is given below with the relationship between cell fluorescence and dsRNA gene knockdown accounting for the potential random effects due to the day each experiment was performed.

$$Fluorescence \sim Gene + (1|Day) + \varepsilon$$

Finally, all data for each replicate were pooled and graphed using GraphPad Prism v7.02 (San Diego, CA).

Knockdown Confirmation

Transfection, ZnMP & Calcein AM Fluorescence Assay of Candidates Found to change ZnMP Uptake in the Previous Knockdown Screen

The procedure above was followed to design and make new dsRNA targeting new regions of the genes found to change heme import in the previous screen (Table 11). These genes were AAEL001495, AAEL004657, AAEL008664, AAEL012226, AAEL012440 and EGFP control. Aag2 cells were then transfected with each dsRNA singly as well as 2 mixes containing AAEL008664 & AAEL012226 both showed increased heme import and AAEL001495, AAEL004657 & AAEL012440 all with decreased heme import. The transfection procedure above was followed to transfect the cells, change the media at 24 hours post transfection, and harvest the cells at 3 days post transfection. Cells were counted using a hemocytometer then seeded at 2 x 10^6 cells/mL per well with a total volume in each well of 100µL into a 96-well black clear bottomed BRANDplate® Cell grade Premium (Brand Wertheim, Germany) 12 wells per dsRNA, with any remaining cells pelleted by centrifugation at 4^{o}C and frozen at -80^{o}C after discarding the supernatant. The ZnMP & Calcein fluorescent assay above was followed to incubate the 96 well plate and measure the fluorescence using the SpectraMax/Minimax 300. The data was then analyzed according to statistical analysis procedure above.

Table 11: Primer sequences for new dsRNA candidates

Name	Forward sequence	Reverse sequence	Temp
AAEL001495_2	taatacgactcactagggGAAACAGGCCAACAACAAATCCAG	taatacgactcactagggACGCCCTCACCCAGACCCCACTT	60
AAEL004657_2	taatacgactcactagggAGAAACCCGATCCCCCTCAGT	taatacgactcactagggAAGCGAAGCCCAGCACGAA	60
AAEL008664_2	taatacgactcactagggAAGTTCGCGGCCCAAGTTC	taatacgactcactagggGCGCCCATTTTCCGTCTCG	65
AAEL012226_2	taatacgactcactagggCGCCGGTAAGATTGACGAGAC	taatacgactcactagggCCGGGGACTGCGAGGATG	60
AAEL012440_2	taatacgactcactagggACATTCCCACGCTCAAGGTCA	taatacgactcactagggAATAGCGGCCATGGGTTTCAGA	65

RT-qPCR Validation of Knockdown

Primers were designed for 10 genes that were used to confirm RNAi knockdown in Aag2 cells. Primer3 server (version 4.1.0) was used to design the primers aiming for amplified sequence with a length of 80-150bp with DNA hairpin folding accounted for using mfold with folding temperature set to 60°C and Mg^{++} set to 1.5mM (Untergasser et al., 2012; Zuker, 2003). A total of 2-5 pairs of primers were designed for each gene, however only 1 was selected to move forward with depending on the results of both the primer gradient PCR and primer efficiency calculations. Quantitative real-time PCR (qPCR) was performed on CFX69 Touch Real-Time PCR Detection System with SsoAdvanced Universal SYBR Green Supermix (Bio-Rad, CA). The range of annealing temperatures examined for each primer was 55-65°C. The program run on the thermocycler was 95°C for 30 seconds, followed by 39 cycles of 15 seconds at 95°C and 30 seconds 55-65°C annealing temperature gradient, finishing with a melt curve of 65-95 measuring every 0.5°C. Primers with a single peak in the melt curves at the 59 or 61.4°C annealing temperature reactions, were selected to move forward with the qPCR run containing a tenfold serial dilution of cDNA at the annealing temperature selected. Primer efficiencies for each primer were calculated using the slope of the average C_T values for each cDNA dilution: $E = -1 + 10^{(-1/Slope)}$. The final primer pairs that showed low C_T values at the

annealing temperatures selected and primer efficiency between 90-110% were selected for qPCR analysis are shown in Table 12. rpS7 was used as a reference gene for each qPCR plate. Results were normalized to EGFP knockdown control samples and graphed using GraphPad Prism v7.02 (San Diego, CA). Statistical significance between the control EGFP and each gene knockdown was determined using an unpaired two-tailed t-test to a cut off of p-value < 0.05.

Table 12: Primer sequences RNAi knockdown in cultured cells

Gene	Forward sequence	Reverse sequence	Temp	Efficiency %
AAEL000417	CAACTTTTGACCGTGTCCGT	GGAACCGCGTGACAGTTTTA	59	100.53
AAEL000461	AGCACTGTTTTCTTGTTTTCTCA	GCTTCTGTCCTGCATTTGTTTC	59	101.38
AAEL001495	AGCAGTCCCATTCGATCGAT	TCCGCTGACAGTTGGATCTT	59	109.74
AAEL004513	AGTCTACCTTCACGCCTGTC	TATCGTCGACTGTGCATCCA	61.4	100.42
AAEL002557	ATGGAAACCTTCGGACCCTT	TGACACTCGGGGAAGAATGG	59	100.35
AAEL003619	ACTGAAGTCTGGTACGAGGC	GGAGAAGCTGTTGAACGAGG	61.4	101.49
AAEL004657	AAGAGCTCGAACAAGGAAGC	TCAACCCAGTACGATTGTCTGA	59	96.73
AAEL008664	GACATTGGCCCGTGTGTTG	AAGCATTACGATCGGAACCC	61.4	98.64
AAEL012226	AGGATCATCAGTCAGCAGGG	CGAATCAAGGCCTTCTCCCT	59	100.23
AAEL012440	GGTGAGTTCAACGTATCGGG	CGTGAACACCTTGTCGATGA	59	98.36
rpS7	ACCGCCGTCTACGATGCCA	ATGGTGGTCTGCTGGTTCTT	59	104.9

Adult Female RNAi Knockdown Injections, Dissection and ZnMP Fluorescence Measurement

Mosquito Rearing

Aedes aegypti Liverpool strain was reared at 28^{o}C in growth chambers at 70% relative humidity and a day: night cycle of 14 hours:10 hours. All mosquitoes were fed a 10% sucrose solution prior to injection. Females 1-3 days old were selected for all experiments.

Females were starved of 10% sucrose 12hr prior to bloodfeeding. All bloodfeeding was performed with defibrinated sheep blood (Colorado Serum Company, Denver CO) using an artificial feeding system.

Injection

A total of 400ng dsRNA was injected into each adult female *Ae. aegypti* using a Nanoject III microinjector (Drummond) with a glass needle drawn from a capillary. For each dsRNA, 3 replicates were performed with ~30 females per replicate. A control group of females was injected for each experiment with dsRNA targeting EGFP. The survival of each group of injected mosquitoes was recorded daily for 3 days post injection.

Dissection, ZnMP Incubation and Fluorescence Measurement

At 3 days post injection, midguts were dissected from all surviving females in 1x PBS and placed into 1.5mL microcentrifuge tubes. The remaining steps were performed in as close to dark conditions as practical. A 30-minute incubation in 10µM ZnMP at room temperature was performed by adding 1mL of 0.3mM ZnMP diluted in uptake buffer to each tube of dissected midguts. Tubes were covered in aluminum foil to protect from light and placed on a tube rotator (VWR). After the incubation, the solution was removed and the midguts washed with uptake buffer + 5% BSA, followed by 2 washes with uptake buffer for each dsRNA group as adapted from the established procedure (Worthington et al., 2001). Treated midguts were placed on microscope slides in 1xPBS sectioned off with an ImmEdge^{TM} hydrophobic barrier pen (Vector Laboratories), with one midgut per section and 10 midguts per slide. After all midguts were placed on a slide, a coverslip was

sealed into place. Images were taken of each midgut at 16x magnification with the DsRED filter of the Leica M165 FC stereomicroscope equipped with a DFC3000C digital camera. The resulting images were analyzed by ImageJ (Schindelin et al., 2012) to determine mean pixel intensity per midgut.

Statistical Analysis

The mean pixel intensity values were normalized to the EGFP control dsRNA values. A linear mixed-effects model analysis on the normalized values was performed using the lme4 package in the R statistical software to determine which genes were significantly different from the control (Bates et al., 2015). GFP was set as the reference for the analysis using the relevel command and the p-values obtained were rounded to 5 digits. The hypothesized formula for the model is given below with the relationship between cell fluorescence and dsRNA gene knockdown accounting for the potential random effects due to the day each experiment was performed and area of a midgut.

$$Fluorescence \sim Gene + (1 + Day|Area) + \varepsilon$$

Finally, all data for each replicate were pooled and graphed using GraphPad Prism v7.02 (San Diego, CA).

Combination Knockdown of Candidate Genes Found to Reduce Heme Import in RNAi Screen

Injection

The dsRNA of candidate genes found to reduce heme import in the RNAi screen, AAEL000417, AAEL003318, AAEL004513 and AAEL012440, were pooled combining 400ng of each per mosquito. The injection procedure was followed as above to inject dsGFP and the mix dsRNA into ~90 female mosquitoes each. The survival of each group was recorded daily for 3 days post injection.

ZnMP Assay of a Subset of Midguts and Blood feed of Remaining Females

At 3 days post transfection, ~30 females were removed from each injected group and the remaining were blood fed following the procedure above for 1 hour at 9am. The 30 females from each group were then dissected, midguts harvested and ZnMP treatment performed following the protocol above.

12hr and 24hr Post Blood Feed Dissection and Ovary Photos

At 12 and 24 hours post bloodfeeding ~30 females were dissected harvesting the midguts and the ovaries. The meal was then removed from the midguts and all the midguts were pooled into a 1.5mL centrifuge tube in 50µL 1x PBS for each group. The tubes were then frozen in liquid N_2 and stored at -80^{o}C. Each pair of ovaries was photographed at 25x magnification with the MU300 AmScope microscope digital camera attached to a Leica M60 microscope (AmScope Irvine, CA; Leica, Germany) on a reticle stage micrometer microscope slide (Electron Microscopy Sciences, PA).

Ovary Size Calculation and Statistical Analysis

The resulting ovary images were analyzed by ImageJ (Schindelin et al., 2012) to length and size of each ovary. Each picture was normalized by scaling the photos by the 100µm ruler present on the slide. The length and size measurements were normalized to the EGFP control dsRNA values and a two-tailed unpaired t test performed. Finally, all data for each replicate were pooled and graphed using GraphPad Prism v7.02 (San Diego, CA).

qPCR Validation of Multiplex RNAi Knockdown in Adult Females

Primers were designed for AAEL000417, AAEL003318, AAEL004513 and AAEL012440 that were used to confirm RNAi knockdown in *Ae. aegypti* midguts. Primer sequences, annealing temperatures and primer efficiencies are given in Table 12, with the exception of AAEL003318 which had an annealing temperature of 59^0C and an efficiency of 98.11% (primer 1, F: TCTACGACTGTACATCCCGC, R: CCTGCATCTGATCGGGTTTG). Primer design followed the same protocol for the design of qPCR primers for RNAi knockdown confirmation in cell culture samples. Quantitative real-time PCR (qPCR) was performed on CFX69 Touch Real-Time PCR Detection System with SsoAdvanced Universal SYBR Green Supermix (Bio-Rad, CA). The range of annealing temperatures examined for each primer was 55-65ºC. The program run on the thermocycler was 95ºC for 30 seconds, followed by 39 cycles of 15 seconds at 95ºC and 30 seconds 55-65ºC annealing temperature gradient, finishing with a melt curve of 65-95 measuring every 0.5ºC. Primers with a single peak in the melt curves at the 59 or 61.4ºC annealing temperature reactions, were selected to move forward with the qPCR run containing a tenfold serial dilution of cDNA at the annealing temperature selected. Primer efficiencies

for each primer were calculated using the slope of the average C_T values for each cDNA dilution: $E = -1 + 10^{(-1/Slope)}$. The final primer pairs that showed low C_T values at the annealing temperatures selected and primer efficiency between 90-110% were selected for qPCR analysis are shown in Table 12. rpS7 was used as a reference gene for each qPCR plate. Results were normalized to EGFP knockdown control samples and graphed using GraphPad Prism v7.02 (San Diego, CA). Statistical significance between the control EGFP and each gene knockdown was determined using an unpaired two-tailed t-test to a cut off of p-value < 0.05.

Results

Utilizing STABLE1 and STABLE2 Expression Plasmids to Induce Expression of Known Heme Transporters in Drosophila *Cells*

Two known membrane bound heme transporters, HRG-1 from *C. elegans* and ABCB10 from *R. microplus*, were selected to clone into an expression plasmid with the goal to induce expression of heme transport in *Drosophila* cells. The expression plasmids selected were chosen due to their ability to co-express 2 or 3 genes from the same promotor, STABLE1 containing GFP and Neomycin and STABLE2 containing mCherry, Neomycin and GFP.

After successful creation of positive control expression plasmids containing the known heme transporter sequences HRG-1 and ABCB10, the expression of these plasmids was tested via transfection into S2 and S2R+ cell lines. A control plasmid IE1-GFP was transfected alongside the STABLE1 plasmids to act as a positive transfection control.

Transfection was not successful in the S2 cell line obtained from ATCC with any of the plasmids tested, as evidenced by the lack of EGFP fluorescence (Figure 29A). However, in both the DGRC S2 cell line and the S2R+ cell line, all plasmids produced visible GFP within 3 days after transfection (Figure29B-C).

To determine whether any of the *Drosophila* cell lines examined had the ability to uptake heme from their environment, all cells were treated with a dilution series of Zinc Mesoporphyrin. The S2 cell line obtained from the ATCC showed no ability at any of the ZnMP concentrations tested (0, 5, 10, 20 & 100µM ZnMP) to take in dietary heme (Figure 30A). On the other hand, the S2 cell line obtained from the DGRC did show the ability to uptake ZnMP at the 5µM and 10µM concentrations tested (Figure 30B). However, when the cells were treated with higher concentrations, 20µM and 100µM, cell pellets turned bright pink indicating large intake of ZnMP during incubation and did not resuspend into solution during the wash steps prior to imaging indicating mass cell death had occurred. Like the 2nd S2 line examined, the S2R+ cell line showed uptake after ZnMP incubation and mass cell death at higher concentrations examined, except cell death was observed at 10µM ZnMP and above (Figure 30C). Therefore, as no *Drosophila* cell line was identified with both the absence of a native heme import pathway and the ability to transfect expression plasmids, RNAi knockdown in Aag2 cells and adult female *Ae. aegypti* was performed to characterize a selection of TM containing genes, previously identified as potentially playing a role in heme transport.

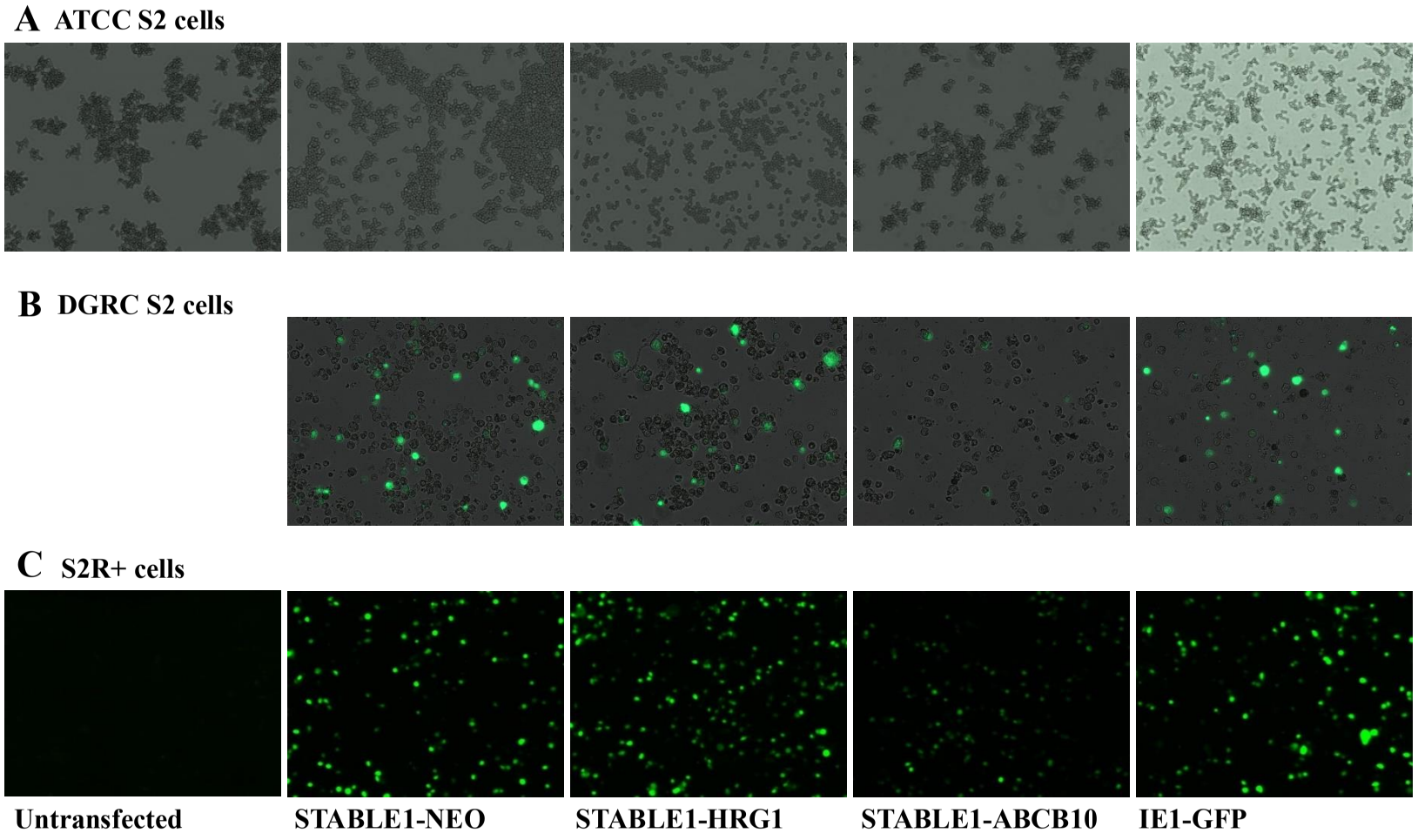

Figure 29: GFP fluorescence of STABLE1 plasmids transfected into *Drosophila* cell lines
STABLE1 plasmids containing neomycin, HRG-1 and ABCB10 were transfected with a control plasmid IE1-GFP into *Drosophila* S2 cells A) ATCC and B) DGRC in origin and C) S2R+ cells. All pictures were obtained 3 days post transfection

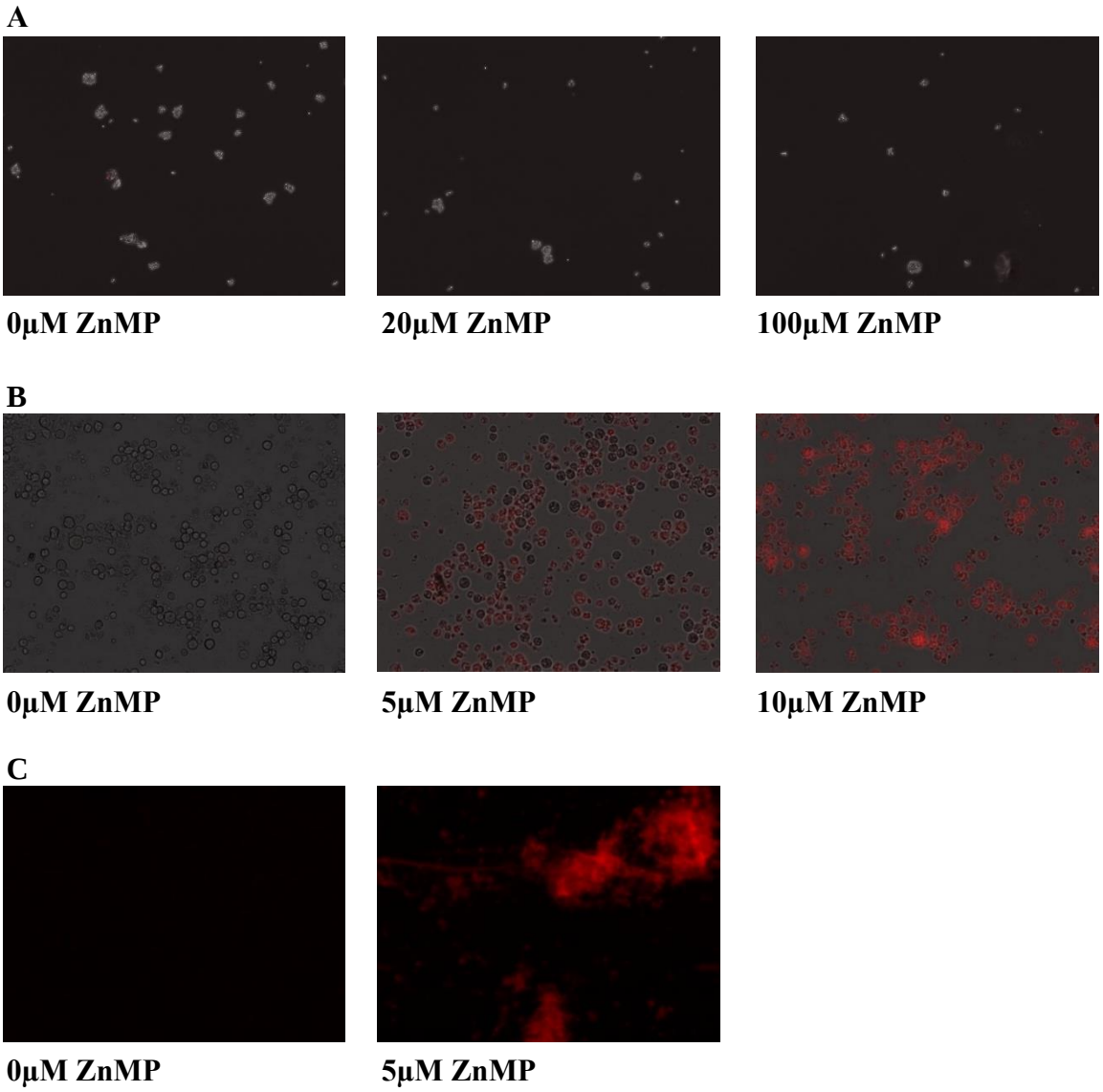

Figure 30: Fluorescence after ZnMP treatment of *Drosophila* cell lines to determine the presence of a native heme import system
A) S2 cells (ATCC) treated with 0µM, 20µM and 100µM Zinc Mesoporphyrin, cells shown at 200x magnification. B) S2 cells (DGRC) treated with 0µM, 5µM and 10µM ZnMP, images taken at 200x magnification. C) S2R+ cell treated with 0µM and 5µM ZnMP, cells imaged at 120x.

RNAi of Aedes aegypti *Cultured Cells*

An RNAi knockdown screen of a selection of candidate transporters previously identified in Chapter II was performed in Aag2 cells; see Table 13 for candidate list. After transfection of dsRNA, ZnMP and Calcein fluorescence was measured via the Spectramax i3x/Minimax 300 and ZnMP fluorescence per cell calculated. The fluorescent values observed for cells subject to each candidate gene knockdown, normalized to the EGFP control, are shown in Figure 31. Candidate genes potentially involved in heme transport were selected based on the p-values obtained from a linear mixed-effects model with a p-value cut off of 0.05. Knockdown of AAEL001495 (p-value=0.0004) or AAEL004657 (p-value<0.0001) resulted in a 19.9% and 38.3% decrease in ZnMP fluorescence as compared with EGFP respectively, indicating these genes may play a possible role in heme import. Inversely, knockdown of genes AAEL012226 (p-value=0.0363), AAEL008664 (p-value=0.0104), AAEL000417 (p-value=0.0036) & AAEL000461 (p-value=0.0356) resulted in a 23.8%, 28.4%, 13.8% and 13.8% increase in fluorescence compared to EGFP respectively, indicating these genes may play a possible role in heme export.

Table 13: Cultured cell candidates selected for RNAi knockdown in Aag2 cells

Gene	Annotation	# TM	Dataset Identified in	Type of transporter
AAEL000417	monocarboxylate transporter	12	A20 72hr	Import
AAEL000461	protein_coding	3	A20 72hr	Import
AAEL002557	cationic amino acid transporter	12	Aag2 48hr	Export
AAEL001495	protein_coding	6	Aag2 48hr/A20/Aag2 Schn	Import
AAEL003619	Na/Cl dependent amino acid transporter	12	Aag2 L15	Import
AAEL004513	neurotransmitter gated ion channel	3	Aag2 48hr	Export
AAEL004657	protein_coding	4	Aag2 48hr	Import
AAEL008664	protein_coding	2	Aag2 48hr/Aag2 Schn	Export
AAEL012226	protein_coding	4	Aag2 48hr/Aag2 Schn	Import/Export
AAEL012440	sodium-bile acid cotransporter	10	Aag2 48hr/A20/Aag2 L15	Import

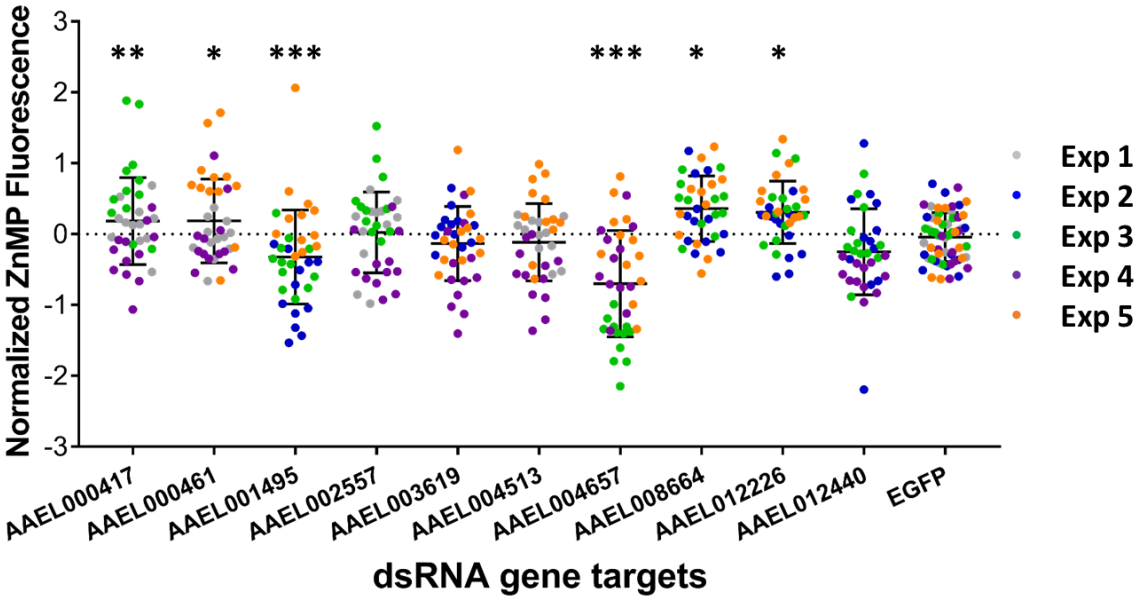

Figure 31: dsRNA knockdown of candidate heme importers in *Aedes aegypti* cultured cells
Double-stranded RNAs corresponding to *Ae. aegypti* genes AAEL000417, AAEL000461, AAEL002557, AAEL004513, AAEL012226, AAEL001495, AAEL008664, AAEL012440, AAEL003619 and AAEL004657. Calcein AM fluorescence was used to count live cells with Minimax 300 and ZnMP fluorescence measured with Spectramax i3x (Molecular Devices). The average ZnMP fluorescence per cell was normalized to the dsGFP control. * Indicates genes that exhibited significantly different fluorescence than control with p-values below 0.05, ** p-values <0.01 and *** p-values <0.001.

To further confirm the genes identified as playing a role in heme import or export in the previous screen, Figure 31, the top 4 genes found to have a significant change in ZnMP fluorescence when compared to the control, AAEL001495, AAEL004657, AAEL008664 and AAEL012226 were knocked down again in cultured cells with independent dsRNAs targeting different regions of each gene. The gene AAEL012440 which showed a non-significant (p-value=0.2813) downward trend in Figure 31 of a 15.8% decrease in fluorescence was also selected to knockdown again with a new dsRNA. Two dsRNA mixes were also prepared and used to knockdown all the potential heme importers (AAEL001495, AAEL004657 and AAEL012440) or the potential heme exporters (AAEL008664 & AAEL012226) simultaneously to hopefully see an increased change in fluorescence if the expression of multiple transporters are reduced at the same time. The results of this analysis, Figure 32, confirmed only AAEL008664 as a potential exporter, as it showed an increase in fluorescence just as with the previous screen with a p-value of 0.00059. The percent increase in fluorescence only dropped by 4% to 24.4 from 28.8% previously. AAEL004657 also was identified involved in heme export as it showed a 27.3% increase in fluorescence when compared to the GFP control (p-value=0.0002), however that was the opposite of the trend observed in the previous experiment where it showed a 38.3% decrease fluorescence.

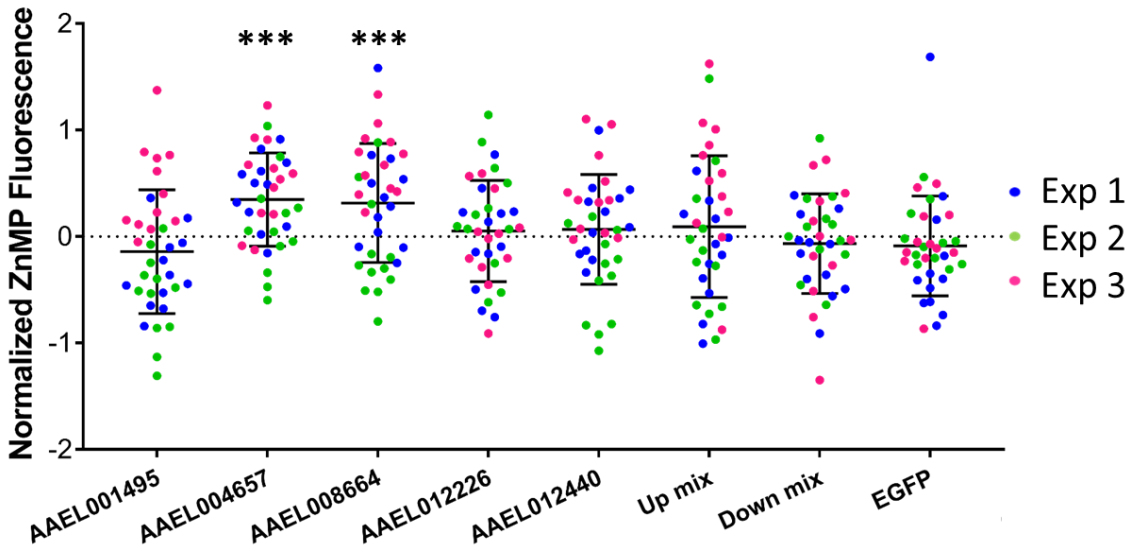

Figure 32: dsRNA knockdown of candidate genes found to effect ZnMP uptake previously in *Aedes aegypti* cultured cells
Double-stranded RNAs corresponding to *Ae. aegypti* genes AAEL012226, AAEL001495, AAEL008664, AAEL012240, and AAEL004657. Up mix was composed of genes that upon knockdown had an increase in ZnMP fluorescence: AAEL012226 and AAEL008664. Down mix was composed of AAEL001495, AAEL004657 and AAEL012440. Calcein AM fluorescence was used to count live cells with Minimax 300 and ZnMP fluorescence measured with Spectramax i3x (Molecular Devices). The average ZnMP fluorescence per cell was normalized to the dsGFP control. *** Indicates genes that exhibited significantly different fluorescence than control with p-values below 0.001.

RT-qPCR Validation of RNAi in Cultured Cells

To confirm RNAi knockdown of candidate genes performed in Aag2 cultured cells, cell pellets harvested 3 days post transfection were subject to RNA extraction, cDNA synthesis, and expression analysis using RT-qPCR. In the first experiment, of the 10 genes targeted by RNAi, 8 were confirmed to be knocked-down by RT-qPCR; AAEL000417 (-2.38 log2), AAEL000461 (-2.12 log2), AAEL001495 (-1.58 log2), AAEL002557 (-2.41 log2), AAEL004513 (-3.38 log2), AAEL004657 (-7.17 log2), AAEL008664 (-3.48 log2) and AAEL012440 (-2.51 log2) (Figure 33A). All 8 genes with knockdown confirmation showed above 3-fold decreased expression with, AAEL004657 showing reduced

expression above 140-fold decreased expression. Knockdown was not confirmed in AAEL003619 and AAEL012226, which showed no change in ZnMP fluorescence and an increase in fluorescence respectively.

Knockdown of the 5 genes selected from the previous screen was performed again with newly designed dsRNAs targeting different areas of their mRNA transcripts. Knockdown was confirmed on all but AAEL012440; AAEL001495 (Single: -1.14 log2), AAEL004657 (Single: -3.12 log2), AAEL008664 (single: -2.42 log2), AAEL012226 (single: -1.87 log2) (Figure 33B).

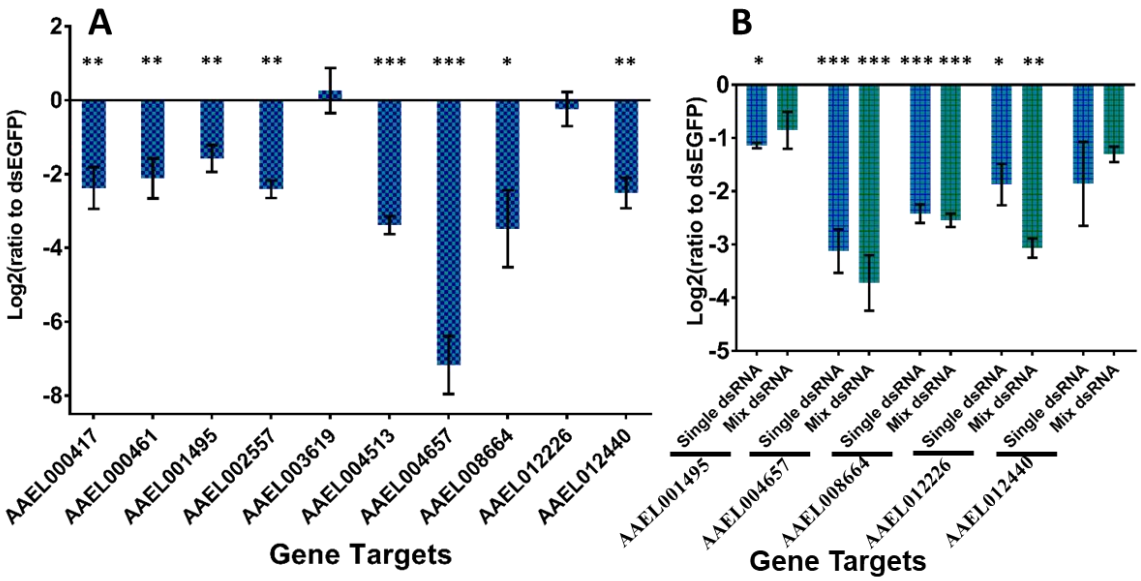

Figure 33: RT-qPCR confirmation of RNAi knockdown of candidate heme transporters in Aag2 cells
RT-qPCR confirmation of RNAi knockdown of DE genes found differentially expressed in cultured cells treated with heme overload or deficiency. A) AAEL000417, AAEL000461, AAEL001495, AAEL002557, AAEL003619, AAEL004513, AAEL004657, AAEL008664, AAEL012226 and AAEL012440. B) 5 DE genes knocked down with new dsRNA, AAEL001495, AAEL004657, AAEL008664, AAEL012226 and AAEL012440. Blue bars indicate single dsRNA knockdown and teal bars indicate a mix of dsRNAs transfected together. dsGFP was transfected in each experiment as a knockdown control.

RNAi of Aedes aegypti *Midguts*

In the differential expression analysis performed in Chapter III, 63 multi-pass transmembrane heme transporter candidates were identified in *Ae. aegypti* midgut epithelial tissue, 40 downregulated in the presence of heme and 23 upregulated. Of these candidates, 12 were selected for an RNAi knockdown screen that was performed in 3-5 day old *Ae. aegypti* sugar fed females; see Table 14 for candidate list. Adult females were injected at 1-2 days old with midguts harvested and ZnMP treated at 4-5 days old. The fluorescent values observed normalized to the EGFP control are shown in Figure 34. Candidate genes potentially involved in heme transport were selected based on the p-values obtained from a linear mixed-effects model with a p-value cut off of 0.05. Decreased fluorescence compared to EGFP was observed in AAEL000417 (34.9% reduction, p-value<0.0001), AAEL000434 (4.0%, p-value= 0.0047), AAEL003318 (20.4%, p-value=0.0036), AAEL004513 (21.5%, p-value=0.001) and AAEL012240 (19.0%, p-value<0.0001) indicating these genes may play a possible role in heme import. Inversely, increased fluorescence was observed in AAEL000461 (19.1% increase, p-value=0.0005), AAEL002557 (25.2%, p-value=0.0049) and AAEL003698 (56.1%, p-value=0.0036) indicating that these genes may play a possible role in heme export. All genes had 3 replicates performed, except AAEL003698 which only had 1 successful knockdown experiment performed.

Table 14: Midgut heme transporter candidates selected for RNAi knockdown in adult *Ae. aegypti*

Gene ID	log2FC	FDR	Annotation	# TM
AAEL000417	-0.58947	0.02177	monocarboxylate transporter	12
AAEL000434	0.59120	0.06410	lipid a export ATP-binding/permease protein msba	6
AAEL000461	-0.59269	0.00551	protein_coding	3
AAEL001938	-0.85206	0.00624	ATP-binding cassette sub-family A member 3, putative	17
AAEL002406	-0.67558	0.06981	protein_coding	6
AAEL002557	-1.17180	9.42E-07	cationic amino acid transporter	12
AAEL003318	-0.54787	0.01182	oligopeptide transporter	10
AAEL003698	-0.53707	0.05708	protein_coding	11
AAEL004513	-0.75116	0.00589	neurotransmitter gated ion channel	3
AAEL004657	-0.53580	0.05171	protein_coding	4
AAEL009531	-0.65507	0.00053	niemann-pick C1	14
AAEL012440	-0.78354	4.60E-05	sodium-bile acid cotransporter	10

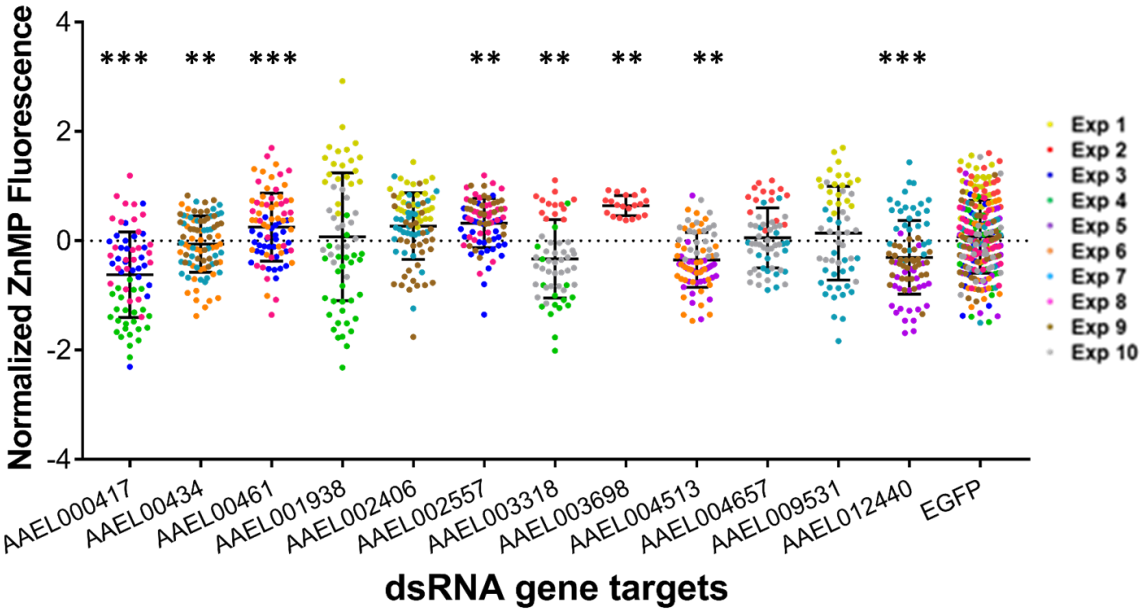

Figure 34: dsRNA knockdown in adult *Aedes aegypti* female midguts of candidate genes
Double-stranded RNAs corresponding to *Ae. aegypti* genes AAEL000417, AAEL000434, AAEL000461, AAEL001938, AAEL002406, AAEL002557, AAEL003318, AAEL003698, AAEL004513, AAEL004657, AAEL009531 and AAEL012440. The mean fluorescence per midgut was normalized to the GFP control across the replicates for each gene. ** Indicates genes that exhibited significantly different fluorescence than control with p-values below 0.01 and *** with p-values <0.001

While 5 genes were identified as potential heme importers based on the screen shown in Figure 34, they each only contributed less than 35% reduction in ZnMP fluorescence with one, AAEL000434 only showing a 4% reduction upon knockdown. If the role of heme transport into the midgut epithelium is due to many different membrane bound transporters, then the simultaneous knockdown of more than 1 transporter could lead to a higher reduction in fluorescence upon treatment with ZnMP as the competency of the cells to uptake heme has been reduced more than if only one transporter was removed. Therefore, the 4 genes with the highest percent reduction in ZnMP fluorescence, AAEL000417, AAEL003318, AAEL004513 and AAEL012440, were selected to make a dsRNA mix to inject simultaneously. Four replicates of injections of ~90 female mosquitoes 1-2 days old were performed of GFP control dsRNA and dsRNA mix of potential heme importers. All the data across the 4 experimental days were collected and normalized to the GFP control and a linear mixed-effects model utilized to determine that there was no significant difference between the groups (p-value= 0.3451), data shown in Figure 35. In addition to heme import measured by changes in ZnMP fluorescence, reproductive potential was measured by dissecting ~30 females and examining the ovaries at 12 hours post bloodfeeding with 4-5 day old injected females (Figure 36A) and again at 24 hours post feeding (Figure 36B). At 12 hours post bloodfeeding, the ovary size was determined to be smaller in the females injected with the dsRNA mix of potential heme importers than the GFP control using a two tailed unpaired t test with a p-value of 0.0191. This difference in ovary sizes did not continue at the 24-hour post bloodfeeding timepoint as the same statistical test yielded a p-value of 0.2723. While 4 replicates of ovary measurements were performed at the 12 hour post feeding timepoint, only 3 were

performed for the 24 hour timepoint as the first experimental group yielded more death due to the injection process than anticipated so there were not enough injected females left to perform both timepoints.

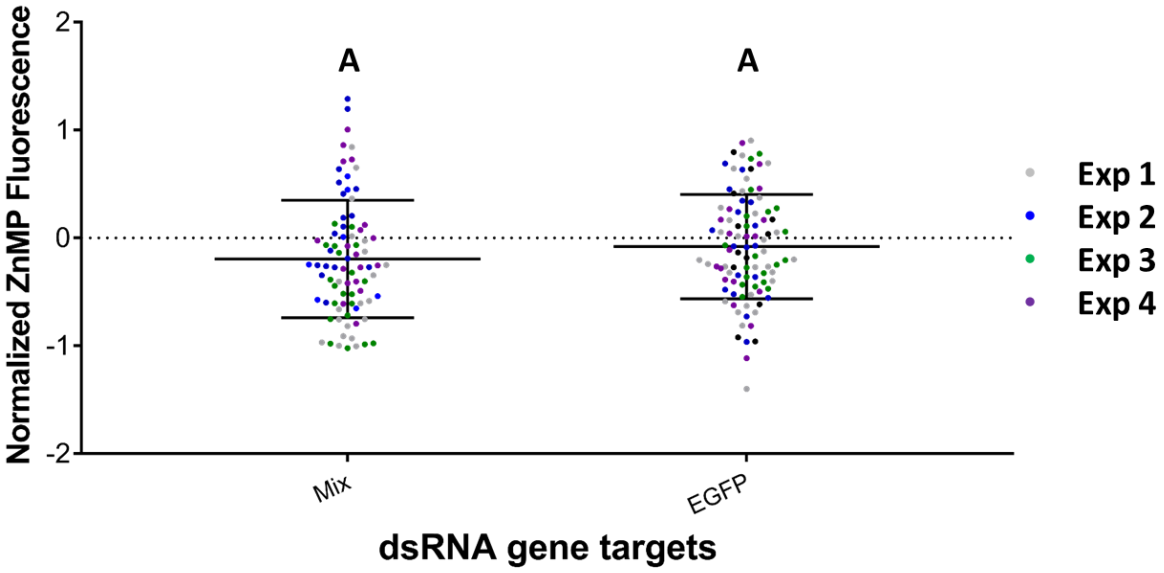

Figure 35: dsRNA knockdown in adult *Aedes aegypti* female midguts of candidate genes found significant in previous screen
Double-stranded RNAs corresponding to *Ae. aegypti* genes AAEL000417, AAEL003318, AAEL004513 and AAEL012240 were mixed and injected into adult females *Ae. aegypti* mosquitoes. The mean fluorescence per midgut was normalized to the GFP control across the mix replicates.

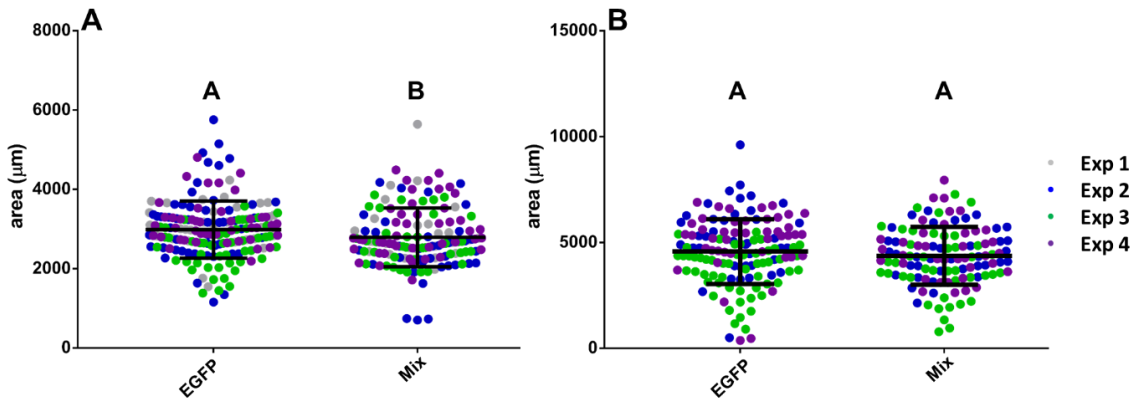

Figure 36: Reproductive potential after knockdown with GFP control and mix of dsRNAs targeting potential heme importers

Area in micrometers (µm) was measured for both ovaries of each dsRNA injected *Ae. aegypti* female harvested at A) 12 hours and B) 24 hours post blood feeding. Two tailed unpaired t tests were performed, yielding a significant difference between the GFP control and dsRNA mix with a p-value of 0.0191 for 12 hours post feeding and no significant difference in ovary size at 24 hours post feeding (p-value=0.2723) A) contains 4 replicates of ovary measurements. B) contains only 3 replicates of measurements, Exp 2-4

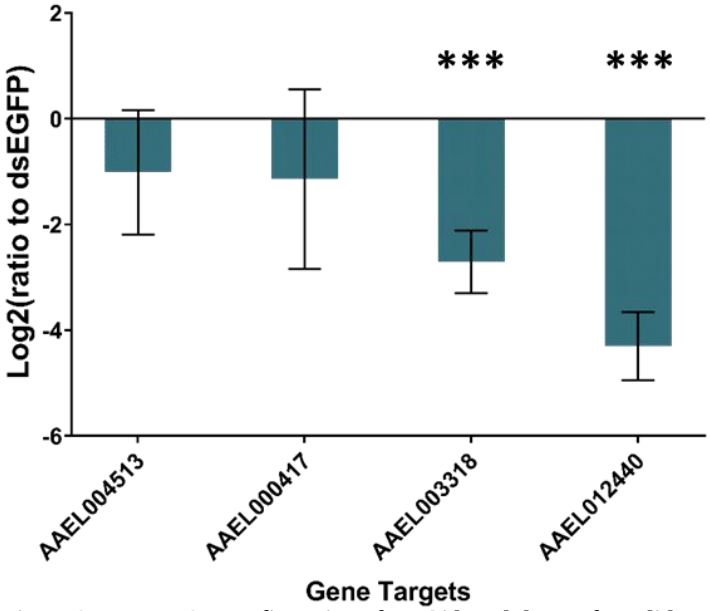

Figure 37: RT-qPCR confirmation of RNAi knockdown of candidate heme transporters in *Ae. aegypti* midguts

4 DE genes were found both differentially expressed in midguts treated with 10µM heme and showed reduce ZnMP fluorescence upon knockdown. RT-qPCR confirmation of RNAi knockdown of AAEL000417, AAEL004513, AAEL003318, and AAEL012440 injected together in a mix. Unpatterned bars indicate dsGFP injection (knockdown control) and patterned bars indicate a mix of dsRNAs injected together. AAEL003318 and AAEL012440 significantly different from EGFP to p-value =0.0003

RT-qPCR Confirmation of Knockdown of the 4 Genes Injected Together

To confirm RNAi knockdown of candidate genes performed in adult female *Ae. aegypti*, 12-hour post-blood fed midguts were harvested, RNA extracted, cDNA made, and expression of each gene measured using real time qPCR. Only 2 of the 4 genes injected, confirmed knockdown AAEL003318 (-2.70 log2) and AAEL012440 (-4.3 log2) (Figure 37). Knockdown was not confirmed in AAEL000417 and AAEL004513 both of which showed a significant reduction in ZnMP fluorescence 34.9% and 21.5% respectively during the individual RNAi knockdown screen (p-values=0.0003).

Discussion

After blood ingestion the female *Ae. aegypti* mosquito initiates the digestion of the contents of her midgut lumen releasing around 10mM heme from the blood protein hemoglobin as it is degraded (Pascoa et al., 2002). Despite heme's importance as a nutrient and a signaling molecule to initiate vitellogenesis (Cruz et al., 2012; Zhou et al., 2007), its method of entry into the midgut epithelial cells where it is degraded to release iron or incorporated into hemo-proteins is not yet known. A global expression analysis of cellular response to heme exposure in *Ae. aegypti* midguts (Chapter 3) and cultured cells (Chapter 2), revealed a number of potential heme membrane bound transport proteins, based on the number of predicted TM domains and the differential expression in response to heme exposure. A portion of these candidates were selected to characterize their potential role as heme transport proteins through use of gain of function in *Drosophila* cells and RNAi knockdown in both adult female mosquitoes and cultured cells.

Our previous observations indicated the possibility of the *D. melanogaster* S2 cell line lacking a native heme import system (Data not shown), therefore it could be a good candidate for a gain of function experiment through the heterologous expression of candidate heme importer genes. However, none of the *Drosophila* cell lines examined fit this criterion; in S2 cells obtained from ATCC, while no ZnMP fluorescence was observed indicating no native heme transport, none of the expression plasmids examined were able to be transfected. The other 2 cell lines examined, S2 (DGRC) and S2R+ cells, had ZnMP fluorescence indicating their ability to uptake dietary heme. Therefore, while STABLE1 expression plasmids containing 2 known heme import genes, *hrg-1* from *C. elegans* (Rajagopal et al., 2008) and *abcb10* from *R. microplus* (Lara et al., 2015), were prepared, no *Drosophila* lines were found that lacked native heme import systems and contained the ability to take in the expression plasmids. Despite this setback, the STABLE1 backbone, Ac5 promotor does also promote expression in *Ae. aegypti*, therefore this expression plasmid could be used in Aag2 cells to examine overexpression of heme transport like that of the mouse iron transporter gene, *Zip14*, characterized by overexpression in HEK 293H cells (Liuzzi et al., 2006).

Of the 63 heme transport candidate genes identified in the global expression analysis performed on heme exposed *Ae. aegypti* midguts (Chapter 3), 23 were also identified as candidates in cultured cells, 16 downregulated and 7 upregulated (Chapter 2). A selection of the of 63 candidates, 16 genes, were selected to analyze the phenotypic response of their RNAi knockdown in Aag2 cultured cells (10 of 16) and adult female midgut cells (12 of 16). The RNAi innate immune response pathway is a major immune pathway responsible for viral infection response in this mosquito species (Samuel et al.,

2018) and as a result this highly active pathway can be harnessed to inhibit expression of endogenous genes. The introduction of dsRNA with sequence similarity to a specific target gene's mRNA, once processed into siRNA acts as a guide locating the target mRNA and signaling its degradation which leads to a temporary reduction of the protein concentration in the cell. Like in the characterization of *hrg1* and *hrg4* in *C. elegans* as heme membrane bound transporters (Rajagopal et al., 2008), this study observed ZnMP fluorescence changes post knockdown to identify genes with potential heme transport functions. While 5 genes showed decreased or increased ZnMP fluorescence compared to the EGFP control in the cell culture study, one of which, AAEL012226, failed to confirm RNAi knockdown via RT-qPCR indicating that the 23.8% increase in fluorescence observed could have been due to off target effects. In the subsequent knockdown assay with new dsRNA targeting a different region of AAEL012226, no significant fluorescent changes were observed lending evidence towards no on target effect was shown in the previous assay. In addition, the knockdown of AAEL003619 was not confirmed in the first assay thus the nonsignificant ZnMP fluorescence change from the control observed could have been due to unsuccessful gene knockdown and further studies would be needed to determine this gene's role in heme response. Knockdown with new dsRNA's targeting different regions of each gene further confirmed AAEL008664 and AAEL004657 as potential heme transport candidates which had an increase in fluorescence in both experiments (28.8% & 24.4%) and had a decrease in the first experiment with an increase in the second (38.3% decreased, 27.3% increase) respectively.

When RNAi knockdown was performed on adult female mosquitoes, 4 genes were identified with punitive functions in heme import based on the ZnMP screen,

AAEL000417, AAEL003318, AAEL004513 and AAEL012440 all of which showed a reduction in fluorescence upon knockdown of >20%. To examine whether the possibility of heme transport into the midgut epithelium is due to multiple transport proteins working together to regulate heme uptake, all 4 genes were injected together to initiate a simultaneous knockdown. RT-qPCR showed that only 2 of the 4 genes were successfully knocked down, AAEL003318 and AAEL012440 and no changes in ZnMP fluorescence, a small decrease in ovary size at 12 hours post blood meal when compared to EGFP dsRNA injected females and no decrease in ovary size at 24hr post blood meal were observed across 4 replicate experiments. These results suggesting that these 2 genes may not play a role in heme uptake into the midgut epithelium. AAEL003318 was identified as highly upregulated 5 hours post blood-feeding in adult female *Ae. aegypti* (4.17 log2, ~18 fold increase) indicating importance potential role in blood digestion (Bonizzoni et al., 2011). As only -2.70 log2 decreased expression was observed upon knockdown at 12 hours post feeding, the knockdown may not have been strong enough to counteract the high upregulation that occurs during early blood digestion. Despite its success at locating some potential heme transporter candidate genes, the RNAi ZnMP screen had a large amount of variation among some of the genes including the EGFP control. During the screen, a correlation was noted for some replicates between the size of the midgut photographed and the amount of fluorescence observed. In general, the larger the midgut area, the dimmer the fluorescence. While the mixed effects model considered this variable when determining statistically significant differences in fluorescence from the control, the values shown in Figure 34 are uncorrected for this variable, which could have led to a loss of sensitivity in calculating percent fluorescent changes for each gene. As this high variation was present in

this screen and very few genes were identified with potential functions relating to heme transport, further characterization studies are needed to determine whether these genes functions are related to heme import such as CRISPR/Cas 9 knockout mosquitoes or heterologous expression in a model system lacking native heme import capabilities.

In the end, RNAi knockdown studies in *Ae. aegypti* cultured cells and midguts identified 2 potential membrane bound transport genes, AAEL008664 and AAEL004657 in Aag2 cultured cells, 2 proteins of unknown function, although further work is necessary to identify cellular location and specific function of each one. Both were also found differentially expressed in midguts, however the function of AAEL008664 has not yet been tested in adult females and AAEL004657 showed no changes in ZnMP fluorescence upon knockdown, although no knockdown confirmation was performed. No changes in ZnMP uptake were observed when the 2 genes AAEL003318 and AAEL012440 were knocked down in adult female midguts indicating either that the % knockdown was not sufficient to show a phenotypic effect, or these genes do not have a function related to heme transport. These results taken with the lack of strongly differentially expressed transporter candidates in both the cultured cell and midgut global expression analyses suggest that instead of one strong heme transport protein responsible for heme uptake in these cells, multiple may exist in *Ae. aegypti* creating a situation where they all contribute to heme import simultaneously. Other forms of regulation could also be responsible for heme transport regulation, instead of post-transcriptional regulation, as shown in the organisms *C. elegans* and *R. microplus* (Lara et al., 2015; Rajagopal et al., 2008), heme transport could be modified at the protein level post-translationally.

CHAPTER V

CONCLUSIONS AND DISCUSSION

Hematophagy is an essential physiological process in the mosquito species *Aedes aegypti*, as the meal provides the amino acids and other nutrients necessary for vitellogenesis (Marquardt and Kondratieff, 2005). In addition to the amino acids produced, the digestion of the blood proteins, hemoglobin and transferrin release heme-iron and free-iron into the midgut lumen (Zhou et al., 2007). While these pro-oxidant molecules are key nutrients in vitellogenesis (Cruz et al., 2012; Zhou et al., 2007), they also generate ROS when left unbound to proteins and allowed to roam freely in solution. One method of heme detoxification is its degradation by heme oxygenase in the midgut epithelial cells into biglutaminyl biliverdin IX, CO and iron (Pereira et al., 2007). However, in order for this degradation reaction to occur, heme must be transported across the plasma membrane into the cytoplasm of the midgut epithelial cells. This study sought to identify genes encoding major contributors to this activity, like those found in *C. elegans* and *R. microplus* (Lara et al., 2015; Rajagopal et al., 2008). Along the way we sought to explore whether or not *Ae. aegypti* cultured cells and midgut epithelial cells were able to adjust their gene expression in response to heme exposure, utilizing zinc mesoporphyrin, a heme fluorescent analog.

An examination of heme toxicity in *Ae. aegypti* cultured cells, showed the expression of AAEL008467, a cysteine synthase, never decreased over constant heme exposure across 9 days and across multiple concentrations of heme. As the cellular availability of cysteine is a limiting factor in the synthesis of glutathione, an antioxidant

and free radical scavenger, high upregulation of this gene consistently should be a strong marker for the cellular ROS stress response. Therefore, it would seem that both cell types examined were unable to limit the amount of heme entering their cells overtime. However, when exposed to heme deficiency conditions these same cell lines showed increased ZnMP fluorescence, suggesting an upregulation of heme import activity. These results taken together could explain why very few TM genes were identified in similarity as potential heme transporter candidates between the 24hr 50µM heme exposure experiment performed in Aag2 cells (Bottino-Rojas et al., 2015) and the heme deficiency analyses performed in this study. The heme fluorescent analog, zinc mesoporphyrin, has been characterized to enter mammalian cultured cells through active transport that is competitively inhibited by heme during heme ZnMP co-incubation suggesting that both molecules enter cells through the same active transport mechanism (Worthington et al., 2001). In fact, ZnMP incubated in *C. elegans* worms determined the type of heme transport occurring during dietary heme uptake and even along with the RNAi knockdown of candidate transporter genes, characterized their specific functions (Rajagopal et al., 2008; Rao et al., 2005). A similar examination of *Ae. aegypti* midguts *in vitro* (Chapter IV), showed a linear decrease in ZnMP uptake in response to increasing concentrations of heme, suggests that heme exposure does lead to expression changes of its transport gene in this tissue. This novel approach to studying heme uptake had not been used previously in this organism. However, a similar study of digest cells in *R. microplus* cultured in growth media, showed changes in metalloporphyrin accumulation during knockdown of the candidate transporter ABCB10, suggesting ZnMP's use in primary cultures to characterize heme import (Lara et al., 2015).

Despite, having identified candidate transporter genes in both cultured cells and midguts exposed to heme deficiency or overload respectively, very few candidates were highly differentially expressed across multiple datasets. We presumed that if candidate genes were found differentially expressed in more than one experiment, experiment-specific variables were less likely to influence the final candidate list. As few genes changed more than 4-fold either through upregulation or down, this could indicate the presence of a system of many genes working together to maintain the cytosolic heme pool in this species. RNAi of some of the candidates identified in midguts and cultured cells did show no more than 38% change in ZnMP fluorescence upon knockdown of a single gene with the majority of genes examined ranging from a 4% to 28% change in fluorescence. Only 2 genes were characterized as potential heme transporters due to ZnMP changes, AAEL008664 and AAEL004657 in cultured cells, although more work is needed to determine localization and specific functions of these proteins. As no strong change in fluorescence was observed upon knockdown, a multiplex knockdown analysis of potential import genes was performed in adult *Ae. aegypti* mosquitoes. By multiplexing 4 genes with about a 20% reduction in fluorescence singly, we hoped to see a larger percent reduction indicating multiple of these genes were affecting heme transport simultaneously. This was not the case unfortunately, leaving this hypothesis unsolved, as in the end only 2 of the 4 genes were successfully knocked down and no change in fluorescence and very little change in ovary development was observed between the multiplex knockdown and the EGFP control. One candidate successfully knocked down, AAEL003318, was also found upregulated in the blood fed female mosquito, 5hrs post bloodmeal (Bonizzoni et al., 2011)

indicating its potential importance in blood digestion. However further work is needed to characterize its function, as the multiplex knockdown performed in this experiment showed no changes in ZnMP fluorescence.

Future work should focus on isolating the mechanism behind heme transport in this organism through continued examination of the hypothesis that multiple genes contribute to heme import in this mosquito through multiplex RNAi experiments. In addition, an analysis of the midgut transcriptome exposed to heme at different timepoints would be useful in following heme induced expression changes over time. Additionally, the possibility does exist of the regulation of heme transport proteins occurring post-translationally instead of post-transcriptionally. This hypothesis could be tested by performing a proteomic analysis following the same heme exposure conditions as for the NGS-RNA sequencing approach examined in this study. However, we note that this will still be limited to detected overall changes in abundance and could not distinguish all potential protein regulatory changes. Modifications such as phosphorylation that alter active site structure, for example, would still leave unusable protein present in the cell allowing its detection in this analysis. A proteomic analysis was recently performed in *Aedes aegypti* examining the peritrophic matrix and its heme-binding proteins (Whiten et al., 2018b), the protocol of which could be adapted here to examine midgut epithelial cells instead. Additionally, future candidates could be identified by cDNA library transformation in a model organism such as yeast (Eide et al., 1996) or *C. elegans* that has been modified to remove heme import functionality at least transiently through the use of tetracycline (Wurmthaler et al., 2019). Yeast preferentially take in iron to produce their own heme rather than scavenging heme from their environment (Protchenko et al., 2008).

This inducible heme uptake system, is not activated until heme biosynthesis is compromised, therefore a mutant strain deficient in *FET3*, the ferroxidase component of the ferrous transport complex, would be ideal to induce gain of function of heme transport genes as both the native iron and heme transport systems are inactivated. However, rescue of heme import in these organisms would be dependent on proper exogenous protein folding and the transport protein's ability to function as a homo-oligomer. In conclusion, while this work has provided evidence against strong transcriptional regulation in heme import in the *Ae. aegypti* mosquito, much work still remains to determine what type of regulation is influencing heme transport and which genes are responsible for heme transport during blood digestion.

REFERENCES

Aicart-Ramos, C., Valhondo Falcón, M., Ortiz de Montellano, P.R., Rodriguez-Crespo, I., 2012. Covalent Attachment of Heme to the Protein Moiety in an Insect E75 Nitric Oxide Sensor. Biochemistry 51, 7403-7416.

Al-Owais, M.M., Dallas, M.L., Boyle, J.P., Scragg, J.L., Peers, C., 2015. Heme Oxygenase-1 Influences Apoptosis via CO-mediated Inhibition of K+ Channels, in: Peers, C., Kumar, P., Wyatt, C., Gauda, E., Nurse, C.A., Prabhakar, N. (Eds.), Arterial Chemoreceptors in Physiology and Pathophysiology. Springer International Publishing, Cham, Switzerland, pp. 343-351.

Andrews, S.C., 2010. The Ferritin-like superfamily: Evolution of the biological iron storeman from a rubrerythrin-like ancestor. Biochimica et Biophysica Acta 1800, 691-705.

Arredondo, M., Kloosterman, J., Nunez, S., Segovia, F., Candia, V., Flores, S., Le Blanc, S., Olivares, M., Pizarro, F., 2008. Heme iron uptake by Caco-2 cells is a saturable, temperature sensitive and modulated by extracellular pH and potassium. Biological Trace Element Research 125, 109-119.

Bagasra, O., Prilliman, K.R., 2004. RNA interference: the molecular immune system. Journal of Molecular Histology 35, 545-553.

Barillas-Mury, C., Wells, M.A., 1993. Cloning and sequencing of the blood meal-induced late trypsin gene from the mosquito *Aedes aegypti* and characterization of the upstream regulatory region. Insect Molecular Biology 2, 7-12.

Barletta, A.B., Silva, M.C., Sorgine, M.H., 2012. Validation of *Aedes aegypti* Aag-2 cells as a model for insect immune studies. Parasites and Vectors 5:148.

Bates, D., Mächler, M., Bolker, B., Walker, S., 2015. Fitting Linear Mixed-Effects Models Using lme4. Journal of Statistical Software 67, 1-48.

Blair, C.D., 2011. Mosquito RNAi is the major innate immune pathway controlling arbovirus infection and transmission. Future Microbiology 6, 265-277.

Bonizzoni, M., Dunn, W.A., Campbell, C.L., Olson, K.E., Dimon, M.T., Marinotti, O., James, A.A., 2011. RNA-seq analyses of blood-induced changes in gene expression in the mosquito vector species, *Aedes aegypti*. BMC Genomics 12:82.

Bottino-Rojas, V., Talyuli, O.A.C., Jupatanakul, N., Sim, S., Dimopoulos, G., Venancio, T.M., Bahia, A.C., Sorgine, M.H., Oliveira, P.L., Paiva-Silva, G.O., 2015. Heme Signaling Impacts Global Gene Expression, Immunity and Dengue Virus Infectivity in *Aedes aegypti*. PLOS ONE 10:e0135985

Brackney, D.E., Isoe, J., W.C. Iv, B., Zamora, J., Foy, B.D., Miesfeld, R.L., Olson, K.E., 2010. Expression profiling and comparative analyses of seven midgut serine proteases from the yellow fever mosquito, *Aedes aegypti*. Journal of Insect Physiology 56, 736-744.

Braz, G.R.C., Coelho, H.S.L., Masuda, H., Oliveira, P.L., 1999. A missing metabolic pathway in the cattle tick *Boophilus microplus*. Current Biology 9, 703-706.

Brouard, S., Berberat, P.O., Tobiasch, E., Seldon, M.P., Bach, F.H., Soares, M.P., 2002. Heme oxygenase-1-derived carbon monoxide requires the activation of transcription factor NF-kappa B to protect endothelial cells from tumor necrosis factor-alpha-mediated apoptosis. Journal of Biological Chemistry 277, 17950-17961.

Byon, J.C., Chen, J., Doty, R.T., Abkowitz, J.L., 2013. FLVCR is necessary for erythroid maturation, may contribute to platelet maturation, but is dispensable for normal hematopoietic stem cell function. Blood 122, 2903-2910.

Chu, Y., Corey, D.R., 2012. RNA sequencing: platform selection, experimental design, and data interpretation. Nucleic Acid Therapeutics 22, 271-274.

Cruz, J., Mane-Padros, D., Zou, Z., Raikhel, A.S., 2012. Distinct roles of isoforms of the heme-liganded nuclear receptor E75, an insect ortholog of the vertebrate Rev-erb, in mosquito reproduction. Molecular and Cellular Endocrinology 349, 262-271.

Cui, L., Yoshioka, Y., Suyari, O., Kohno, Y., Zhang, X., Adachi, Y., Ikehara, S., Yoshida, T., Yamaguchi, M., Taketani, S., 2008. Relevant expression of *Drosophila* heme oxygenase is necessary for the normal development of insect tissues. Biochemical Biophysical Research Communications 377, 1156-1161.

Damulewicz, M., Loboda, A., Jozkowicz, A., Dulak, J., Pyza, E., 2017a. Haeme oxygenase protects against UV light DNA damages in the retina in clock-dependent manner. Scientific Reports 7:5197.

Damulewicz, M., Loboda, A., Jozkowicz, A., Dulak, J., Pyza, E., 2017b. Interactions Between the Circadian Clock and Heme Oxygenase in the Retina of *Drosophila melanogaster*. Molecular Neurobiology 54, 4953-4962.

Dashti, Z.J.S., Gamieldien, J., Christoffels, A., 2016. Computational characterization of Iron metabolism in the Tsetse disease vector, *Glossina morsitans*: IRE stem-loops. BMC Genomics 17:561.

Devenport, M., Alvarenga, P.H., Shao, L., Fujioka, H., Bianconi, M.L., Oliveira, P.L., Jacobs-Lorena, M., 2006. Identification of the *Aedes aegypti* Peritrophic Matrix Protein AeIMUCI as a Heme-Binding Protein†. Biochemistry 45, 9540-9549.

Devenport, M., Fujioka, H., Donnelly-Doman, M., Shen, Z., Jacobs-Lorena, M., 2005. Storage and secretion of Ag-Aper14, a novel peritrophic matrix protein, and Ag-Muc1 from the mosquito *Anopheles gambiae*. Cell and Tissue Research 320, 175-185.

Dimopoulos, G., Seeley, D., Wolf, A., Kafatos, F.C., 1998. Malaria infection of the mosquito *Anopheles gambiae* activates immune-responsive genes during critical transition stages of the parasite life cycle. The EMBO Journal 17, 6115-6123.

Dinglasan, R.R., Devenport, M., Florens, L., Johnson, J.R., McHugh, C.A., Donnelly-Doman, M., Carucci, D.J., Yates Iii, J.R., Jacobs-Lorena, M., 2009. The *Anopheles gambiae* adult midgut peritrophic matrix proteome. Insect Biochemistry and Molecular Biology 39, 125-134.

Donohue, K.V., Khalil, S.M., Sonenshine, D.E., Roe, R.M., 2009. Heme-binding storage proteins in the Chelicerata. Journal of Insect Physiology 55, 287-296.

Dore, S., Snyder, S.H., 1999. Neuroprotective action of bilirubin against oxidative stress in primary hippocampal cultures. Annals of the New York Academy of Sciences 890, 167-172.

Dunkov, B., Georgieva, T., 2006. Insect iron binding proteins: insights from the genomes. Insect Biochemistry and Molecular Biology 36, 300-309.

Dunkov, B.C., Georgieva, T., Yoshiga, T., Hall, M., Law, J.H., 2002. *Aedes aegypti* ferritin heavy chain homologue: feeding of iron or blood influences message levels, lengths and subunit abundance. Journal of Insect Science 2:7.

Edwards, M.J., Moskalyk, L.A., Donelly-Doman, M., Vlaskova, M., Noriega, F.G., Walker, V.K., Jacobs-Lorena, M., 2000. Characterization of a carboxypeptidase A gene from the mosquito, *Aedes aegypti*. Insect Molecular Biology 9, 33-38.

Eide, D., Broderius, M., Fett, J., Guerinot, M.L., 1996. A novel iron-regulated metal transporter from plants identified by functional expression in yeast. Proceedings of the National Academy of Sciences of the United States of America 93, 5624-5628.

Evans, A.M., Aimanova, K.G., Gill, S.S., 2009. Characterization of a blood-meal-responsive proton-dependent amino acid transporter in the disease vector, *Aedes aegypti*. The Journal of Experimental Biology 212, 3263-3271.

Farrugia, G., Szurszewski, J.H., 2014. Carbon monoxide, hydrogen sulfide, and nitric oxide as signaling molecules in the gastrointestinal tract. Gastroenterology 147, 303-313.

Folwell, J.L., Barton, C.H., Shepherd, D., 2006. Immunolocalisation of the *D. melanogaster Nramp* homologue *Malvolio* to gut and Malpighian tubules provides evidence that *Malvolio* and *Nramp2* are orthologous. Journal of Experimental Biology 209, 1988-1995.

Freyvogel, T.A., Jaquet, C., 1965. The prerequisites for the formation of a peritrophic membrane in *Culicidae* females. Acta Tropica 22, 148-154.

Futschik, M.E., Carlisle, B., 2005. Noise-robust soft clustering of gene expression time-course data. Journal of Bioinformatics and Computational Biology 3, 965-988.

Galay, R.L., Aung, K.M., Umemiya-Shirafuji, R., Maeda, H., Matsuo, T., Kawaguchi, H., Miyoshi, N., Suzuki, H., Xuan, X., Mochizuki, M., Fujisaki, K., Tanaka, T., 2013. Multiple ferritins are vital to successful blood feeding and reproduction of the hard tick *Haemaphysalis longicornis*. Journal of Experimental Biology 216, 1905-1915.

Galay, R.L., Umemiya-Shirafuji, R., Bacolod, E.T., Maeda, H., Kusakisako, K., Koyama, J., Tsuji, N., Mochizuki, M., Fujisaki, K., Tanaka, T., 2014. Two Kinds of Ferritin Protect *Ixodid* Ticks from Iron Overload and Consequent Oxidative Stress. PLOS ONE 9:e90661.

Galay, R.L., Umemiya-Shirafuji, R., Mochizuki, M., Fujisaki, K., Tanaka, T., 2015. Iron metabolism in hard ticks (*Acari: Ixodidae*): the antidote to their toxic diet. Parasitology International 64, 182-189.

Geiser, D.L., Chavez, C.A., Flores-Munguia, R., Winzerling, J.J., Pham, D.Q., 2003. *Aedes aegypti* ferritin. European Journal of Biochemistry 270, 3667-3674.

Geiser, D.L., Shen, M.C., Mayo, J.J., Winzerling, J.J., 2009. Iron loaded ferritin secretion and inhibition by CI-976 in *Aedes aegypti* larval cells. Comparative Biochemistry and Physiology Part B: Biochemistry and Molecular Biology 152, 352-363.

Geiser, D.L., Zhou, G., Mayo, J.J., Winzerling, J.J., 2013. The effect of bacterial challenge on ferritin regulation in the yellow fever mosquito, *Aedes aegypti*. Insect Science 20, 601-619.

Girvan, H.M., Munro, A.W., 2013. Heme sensor proteins. Journal of Biological Chemistry 288, 13194-13203.

González-Morales, N., Mendoza-Ortíz, M.Á., Blowes, L.M., Missirlis, F., Riesgo-Escovar, J.R., 2015. Ferritin Is Required in Multiple Tissues during *Drosophila melanogaster* Development. PLOS ONE 10:e0133499.

Gonzalez, M., Martin-Ruiz, I., Jimenez, S., Pirone, L., Barrio, R., Sutherland, J.D., 2011. Generation of stable *Drosophila* cell lines using multicistronic vectors. Scientific Reports 1:75.

Gorman, M.J., Dittmer, N.T., Marshall, J.L., Kanost, M.R., 2008. Characterization of the multicopper oxidase gene family in *Anopheles gambiae*. Insect Biochemistry and Molecular Biology 38, 817-824.

Graça-Souza, A.V., Maya-Monteiro, C., Paiva-Silva, G.O., Braz, G.R.C., Paes, M.C., Sorgine, M.H.F., Oliveira, M.F., Oliveira, P.L., 2006. Adaptations against heme toxicity in blood-feeding arthropods. Insect Biochemistry and Molecular Biology 36, 322-335.

Grace, T.D., 1962. Establishment of four strains of cells from insect tissues grown in vitro. Nature 195, 788-789.

Guengerich, F.P., 2007. Mechanisms of cytochrome P450 substrate oxidation: MiniReview. Journal of Biochemical and Molecular Toxicology 21, 163-168.

Gullotta, F., di Masi, A., Coletta, M., Ascenzi, P., 2012. CO metabolism, sensing, and signaling. BioFactors 38, 1-13.

Gutierrez, L., Zubow, K., Nield, J., Gambis, A., Mollereau, B., Lazaro, F.J., Missirlis, F., 2013. Biophysical and genetic analysis of iron partitioning and ferritin function in *Drosophila melanogaster*. Metallomics 5, 997-1005.

Hajdusek, O., Sojka, D., Kopacek, P., Buresova, V., Franta, Z., Sauman, I., Winzerling, J., Grubhoffer, L., 2009. Knockdown of proteins involved in iron metabolism limits tick reproduction and development. Proceedings of the National Academy of Sciences of the United States of America 106, 1033-1038.

Hao, Z., Aksoy, S., 2002. Proventriculus-specific cDNAs characterized from the tsetse, *Glossina morsitans morsitans*. Insect Biochemistry and Molecular Biology 32, 1663-1671.

Harizanova, N., Georgieva, T., Dunkov, B.C., Yoshiga, T., Law, J.H., 2005. *Aedes aegypti* transferrin. Gene structure, expression pattern, and regulation. Insect Molecular Biology 14, 79-88.

Hooda, J., Shah, A., Zhang, L., 2014. Heme, an essential nutrient from dietary proteins, critically impacts diverse physiological and pathological processes. Nutrients 6, 1080-1102.

Huynh, C., Yuan, X., Miguel, D.C., Renberg, R.L., Protchenko, O., Philpott, C.C., Hamza, I., Andrews, N.W., 2012. Heme Uptake by *Leishmania amazonensis* Is Mediated by the Transmembrane Protein LHR1. PLOS Pathogens 8:e1002795.

Ida, H., Suyari, O., Shimamura, M., Tien Tai, T., Yamaguchi, M., Taketani, S., 2013. Genetic link between heme oxygenase and the signaling pathway of DNA damage in *Drosophila melanogaster*. Tohoku Journal of Experimental Medicine 231, 117-125.

Jacques, I., Andrews, N.W., Huynh, C., 2010. Functional characterization of LIT1, the *Leishmania amazonensis* ferrous iron transporter. Molecular and Biochemical Parasitology 170, 28-36.

Jeffrey Man, H.S., Tsui, A.K., Marsden, P.A., 2014. Nitric oxide and hypoxia signaling. Vitamins and Hormones 96, 161-192.

Jiang, Q., Hall, M., Noriega, F.G., Wells, M., 1997. cDNA cloning and pattern of expression of an adult, female-specific chymotrypsin from *Aedes aegypti* midgut. Insect Biochemistry and Molecular Biology 27, 283-289.

Jochim, R.C., Teixeira, C.R., Laughinghouse, A., Mu, J., Oliveira, F., Gomes, R.B., Elnaiem, D.-E., Valenzuela, J.G., 2008. The midgut transcriptome of *Lutzomyia longipalpis*: comparative analysis of cDNA libraries from sugar-fed, blood-fed, post-digested and *Leishmania infantum* chagasi-infected sand flies. BMC Genomics 9:15.

Kim, D., Langmead, B., Salzberg, S.L., 2015. HISAT: a fast spliced aligner with low memory requirements. Nature Methods 12, 357-360.

Klowden, M.J., Lea, A.O., 1979. Abdominal distention terminates subsequent host-seeking behaviour of *Aedes aegypti* following a blood meal. Journal of Insect Physiology 25, 583-585.

Koh-Tan, H.H., Strachan, E., Cooper, K., Bell-Sakyi, L., Jonsson, N.N., 2016. Identification of a novel beta-adrenergic octopamine receptor-like gene (betaAOR-like) and increased ATP-binding cassette B10 (ABCB10) expression in a *Rhipicephalus microplus* cell line derived from acaricide-resistant ticks. Parasites and Vectors 9:425.

Kokoza, V.A., Martin, D., Mienaltowski, M.J., Ahmed, A., Morton, C.M., Raikhel, A.S., 2001. Transcriptional regulation of the mosquito vitellogenin gene via a blood meal-triggered cascade. Gene 274, 47-65.

Korolnek, T., Zhang, J., Beardsley, S., Scheffer, G.L., Hamza, I., 2014. Control of metazoan heme homeostasis by a conserved multidrug resistance protein. Cell Metabolism 19, 1008-1019.

Kumar, L., M, E.F., 2007. Mfuzz: a software package for soft clustering of microarray data. Bioinformation 2, 5-7.

Lang, M., Braun, C.L., Kanost, M.R., Gorman, M.J., 2012. Multicopper oxidase-1 is a ferroxidase essential for iron homeostasis in *Drosophila melanogaster*. Proceedings of the National Academy of Sciences of the United States of America 109, 13337-13342.

Lara, F.A., Lins, U., Paiva-Silva, G., Almeida, I.C., Braga, C.M., Miguens, F.C., Oliveira, P.L., Dansa-Petretski, M., 2003. A new intracellular pathway of haem detoxification in the midgut of the cattle tick *Boophilus microplus*: aggregation inside a specialized organelle, the hemosome. Journal of Experimental Biology 206, 1707-1715.

Lara, F.A., Pohl, P.C., Gandara, A.C., Ferreira Jda, S., Nascimento-Silva, M.C., Bechara, G.H., Sorgine, M.H., Almeida, I.C., Vaz Ida, S., Jr., Oliveira, P.L., 2015. ATP Binding

Cassette Transporter Mediates Both Heme and Pesticide Detoxification in Tick Midgut Cells. PLOS One 10:e0134779.

Leger, P., Lara, E., Jagla, B., Sismeiro, O., Mansuroglu, Z., Coppee, J.Y., Bonnefoy, E., Bouloy, M., 2013. Dicer-2- and Piwi-mediated RNA interference in Rift Valley fever virus-infected mosquito cells. Journal of Virology 87, 1631-1648.

Leidgens, S., Bullough, K.Z., Shi, H.F., Li, F.M., Shakoury-Elizeh, M., Yabe, T., Subramanian, P., Hsu, E., Natarajan, N., Nandal, A., Stemmler, T.L., Philpott, C.C., 2013. Each Member of the Poly-r(C)-binding Protein 1 (PCBP) Family Exhibits Iron Chaperone Activity toward Ferritin. Journal of Biological Chemistry 288, 17791-17802.

Li, H., 2011. A statistical framework for SNP calling, mutation discovery, association mapping and population genetical parameter estimation from sequencing data. Bioinformatics 27, 2987-2993.

Li, H., Handsaker, B., Wysoker, A., Fennell, T., Ruan, J., Homer, N., Marth, G., Abecasis, G., Durbin, R., Genome Project Data Processing, S., 2009. The Sequence Alignment/Map format and SAMtools. Bioinformatics 25, 2078-2079.

Li, S., 2010. Identification of iron-loaded ferritin as an essential mitogen for cell proliferation and postembryonic development in *Drosophila*. Cell Research 20, 1148-1157.

Lima, V.L., Dias, F., Nunes, R.D., Pereira, L.O., Santos, T.S., Chiarini, L.B., Ramos, T.D., Silva-Mendes, B.J., Perales, J., Valente, R.H., Oliveira, P.L., 2012. The antioxidant role of xanthurenic acid in the *Aedes aegypti* midgut during digestion of a blood meal. PLOS One 7:e38349.

Liu, X., Sun, C., Liu, X., Yin, X., Wang, B., Du, M., An, S., 2015. Multicopper oxidase-1 is required for iron homeostasis in Malpighian tubules of *Helicoverpa armigera*. Scientific Reports 5:14784.

Liuzzi, J.P., Aydemir, F., Nam, H., Knutson, M.D., Cousins, R.J., 2006. Zip14 (Slc39a14) mediates non-transferrin-bound iron uptake into cells. Proceedings of the National Academy of Sciences of the United States of America 103, 13612-13617.

Magalhaes, T., Oliveira, I.F., Melo-Santos, M.A., Oliveira, C.M., Lima, C.A., Ayres, C.F., 2008. Expression of defensin, cecropin, and transferrin in *Aedes aegypti* (Diptera: Culicidae) infected with *Wuchereria bancrofti* (Spirurida: Onchocercidae), and the

abnormal development of nematodes in the mosquito. Experimental Parasitology 120, 364-371.

Mandilaras, K., Pathmanathan, T., Missirlis, F., 2013. Iron Absorption in *Drosophila melanogaster*. Nutrients 5, 1622-1647.

Mangia, C., Vismarra, A., Kramer, L., Bell-Sakyi, L., Porretta, D., Otranto, D., Epis, S., Grandi, G., 2016. Evaluation of the in vitro expression of ATP binding-cassette (ABC) proteins in an *Ixodes ricinus* cell line exposed to ivermectin. Parasites and Vectors 9:215.

Marquardt, W.C., 2005. Biology of Disease Vectors. Elsevier Academic Press, Burlington, MA, pp. 297-310.

Marquardt, W.C., Kondratieff, B.C., 2005. Biology of disease vectors, 2nd ed. Elsevier Academic Press, Burlington, MA.

Martin, D., Wang, S.F., Raikhel, A.S., 2001. The vitellogenin gene of the mosquito *Aedes aegypti* is a direct target of ecdysteroid receptor. Molecular and Cellular Endocrinology 173, 75-86.

Martínez-Barnetche, J., García Solache, M., Neri Lecona, A., Tello López, A.T., Carmen, R.M., Gamba, G., Vázquez, N., Rodríguez, M.H., Lanz-Mendoza, H., 2007. Cloning and functional characterization of the *Anopheles albimanus* DMT1/NRAMP homolog: implications in iron metabolism in mosquitoes. Insect Biochemistry and Molecular Biology 37, 532-539.

McCarthy, D.J., Chen, Y., Smyth, G.K., 2012. Differential expression analysis of multifactor RNA-Seq experiments with respect to biological variation. Nucleic Acids Research 40, 4288-4297.

Mercurio, S., Petrillo, S., Chiabrando, D., Bassi, Z.I., Gays, D., Camporeale, A., Vacaru, A., Miniscalco, B., Valperga, G., Silengo, L., Altruda, F., Baron, M.H., Santoro, M.M., Tolosano, E., 2015. The heme exporter *Flvcr1* regulates expansion and differentiation of committed erythroid progenitors by controlling intracellular heme accumulation. Haematologica 100, 720-729.

Morlais, I., Severson, D.W., 2001. Identification of a polymorphic mucin-like gene expressed in the midgut of the mosquito, *Aedes aegypti*, using an integrated bulked segregant and differential display analysis. Genetics 158, 1125-1136.

Moskalyk, L.A., Oo, M.M., Jacobs-Lorena, M., 1996. Peritrophic matrix proteins of *Anopheles gambiae* and *Aedes aegypti*. Insect Molecular Biology 5, 261-268.

Narasimhan, S., Rajeevan, N., Liu, L., Zhao, Y.O., Heisig, J., Pan, J., Eppler-Epstein, R., DePonte, K., Fish, D., Fikrig, E., 2014. Gut Microbiota of the Tick Vector *Ixodes scapularis* Modulate Colonization of the Lyme Disease Spirochete. Cell Host & Microbe 15, 58-71.

Nichol, H., Law, J.H., Winzerling, J.J., 2002. Iron metabolism in insects. Annual Review of Entomology 47.

Oliveira, J.H.M., Talyuli, O.A.C., Goncalves, R.L.S., Paiva-Silva, G.O., Sorgine, M.H.F., Alvarenga, P.H., Oliveira, P.L., 2017. Catalase protects *Aedes aegypti* from oxidative stress and increases midgut infection prevalence of Dengue but not Zika. PLOS Neglected Tropical Diseases 11:e0005525.

Oliveros, J.C., 2007-2015. VENNY. An interactive tool for comparing lists with Venn Diagrams. Available: http://bioinfogp.cnb.csic.es/tools/venny/index.html. Version 2.1. Accessed 2019

Otho, S.A., Chen, K., Zhang, Y., Wang, P., Lu, Z., 2016. Silkworm ferritin 1 heavy chain homolog is involved in defense against bacterial infection through regulation of haemolymph iron homeostasis. Developmental and Comparative Immunology 55, 152-158.

Otterbein, L.E., Bach, F.H., Alam, J., Soares, M., Tao Lu, H., Wysk, M., Davis, R.J., Flavell, R.A., Choi, A.M., 2000. Carbon monoxide has anti-inflammatory effects involving the mitogen-activated protein kinase pathway. Nature Medicine 6, 422-428.

Paily, K.P., Kumar, B.A., Balaraman, K., 2007. Transferrin in the mosquito, *Culex quinquefasciatus* Say (Diptera: Culicidae), up-regulated upon infection and development of the filarial parasite, *Wuchereria bancrofti* (Cobbold) (Spirurida: Onchocercidae). Parasitology Research 101, 325-330.

Paiva-Silva, G.O., Cruz-Oliveira, C., Nakayasu, E.S., Maya-Monteiro, C.M., Dunkov, B.C., Masuda, H., Almeida, I.C., Oliveira, P.L., 2006. A heme-degradation pathway in a blood-sucking insect. Proceedings of the National Academy of Sciences of the United States of America 103, 8030-8035.

Pascoa, V., Oliveira, P.L., Dansa-Petretski, M.l., Silva, J.R., Alvarenga, P.H., Jacobs-Lorena, M., Lemos, F.J.A., 2002. *Aedes aegypti* peritrophic matrix and its interaction with heme during blood digestion. Insect Biochemistry and Molecular Biology 32, 517-523.

Peleg, J., 1968. Growth of arboviruses in primary tissue culture of *Aedes aegypti* embryos. American Journal of Tropical Medicine and Hygiene 17, 219-223.

Peng, Z., Dittmer, N.T., Lang, M., Brummett, L.M., Braun, C.L., Davis, L.C., Kanost, M.R., Gorman, M.J., 2015. Multicopper oxidase-1 orthologs from diverse insect species have ascorbate oxidase activity. Insect Biochemistry and Molecular Biology 59, 58-71.

Pereira, L.O., Oliveira, P.L., Almeida, I.C., Paiva-Silva, G.O., 2007. Biglutaminyl-biliverdin IX alpha as a heme degradation product in the dengue fever insect-vector *Aedes aegypti*. Biochemistry 46, 6822-6829.

Perner, J., Gasser, R.B., Oliveira, P.L., Kopacek, P., 2019. Haem Biology in Metazoan Parasites - 'The Bright Side of Haem'. Trends in Parasitology 35, 213-225.

Perner, J., Sobotka, R., Sima, R., Konvickova, J., Sojka, D., de Oliveira, P.L., Hajdusek, O., Kopacek, P., 2016. Acquisition of exogenous haem is essential for tick reproduction. eLife 5:e12318.

Peters, W., 1992. Peritrophic Membranes. Springer-Verlag, Berlin, Germany.

Pham, D.Q., Winzerling, J.J., 2010. Insect ferritins: Typical or atypical? Biochimica et Biophysica Acta 1800, 824-833.

Philip, M., Funkhouser, S.A., Chiu, E.Y., Phelps, S.R., Delrow, J.J., Cox, J., Fink, P.J., Abkowitz, J.L., 2015. Heme exporter FLVCR is required for T cell development and peripheral survival. Journal of Immunology 194, 1677-1685.

Philpott, C.C., Ryu, M.S., Frey, A., Patel, S., 2017. Cytosolic iron chaperones: Proteins delivering iron cofactors in the cytosol of mammalian cells. Journal of Biological Chemistry 292, 12764-12771.

Pierceall, W.E., Li, C., Biran, A., Miura, K., Raikhel, A.S., Segraves, W.A., 1999. E75 expression in mosquito ovary and fat body suggests reiterative use of ecdysone-regulated

hierarchies in development and reproduction. Molecular and Cellular Endocrinology 150, 73-89.

Pohl, P.C., Carvalho, D.D., Daffre, S., Vaz Ida, S., Jr., Masuda, A., 2014. *In vitro* establishment of ivermectin-resistant *Rhipicephalus microplus* cell line and the contribution of ABC transporters on the resistance mechanism. Veterinary Parasitology 204, 316-322.

Pohl, P.C., Klafke, G.M., Carvalho, D.D., Martins, J.R., Daffre, S., da Silva Vaz, I., Jr., Masuda, A., 2011. ABC transporter efflux pumps: a defense mechanism against ivermectin in *Rhipicephalus (Boophilus) microplus*. International Journal of Parasitology 41, 1323-1333.

Pohl, P.C., Klafke, G.M., Junior, J.R., Martins, J.R., da Silva Vaz, I., Jr., Masuda, A., 2012. ABC transporters as a multidrug detoxification mechanism in *Rhipicephalus (Boophilus) microplus*. Parasitology Research 111, 2345-2351.

Protchenko, O., Shakoury-Elizeh, M., Keane, P., Storey, J., Androphy, R., Philpott, C.C., 2008. Role of PUG1 in inducible porphyrin and heme transport in *Saccharomyces cerevisiae*. Eukaryotic Cell 7, 859-871.

Quigley, J.G., Yang, Z., Worthington, M.T., Phillips, J.D., Sabo, K.M., Sabath, D.E., Berg, C.L., Sassa, S., Wood, B.L., Abkowitz, J.L., 2004. Identification of a human heme exporter that is essential for erythropoiesis. Cell 118, 757-766.

Quinlan, A.R., Hall, I.M., 2010. BEDTools: a flexible suite of utilities for comparing genomic features. Bioinformatics 26, 841-842.

Rajagopal, A., Rao, A.U., Amigo, J., Tian, M., Upadhyay, S.K., Hall, C., Uhm, S., Mathew, M.K., Fleming, M.D., Paw, B.H., Krause, M., Hamza, I., 2008. Haem homeostasis is regulated by the conserved and concerted functions of HRG-1 proteins. Nature 453, 1127-1131.

Ramalho-Ortigão, M., Jochim, R.C., Anderson, J.M., Lawyer, P.G., Pham, V.-M., Kamhawi, S., Valenzuela, J.G., 2007. Exploring the midgut transcriptome of *Phlebotomus papatasi*: comparative analysis of expression profiles of sugar-fed, blood-fed and *Leishmania* major-infected sandflies. BMC Genomics 8:300.

Rao, A.U., Carta, L.K., Lesuisse, E., Hamza, I., 2005. Lack of heme synthesis in a free-living eukaryote. Proceedings of the National Academy of Sciences of the United States of America 102, 4270-4275.

Rayms-Keller, A., McGaw, M., Oray, C., Carlson, J.O., Beaty, B.J., 2000. Molecular cloning and characterization of a metal responsive *Aedes aegypti* intestinal mucin cDNA. Insect Molecular Biology 9, 419-426.

Reinking, J., Lam, M.M.S., Pardee, K., Sampson, H.M., Liu, S., Yang, P., Williams, S., White, W., Lajoie, G., Edwards, A., Krause, H.M., 2005. The *Drosophila* Nuclear Receptor E75 Contains Heme and Is Gas Responsive. Cell 122, 195-207.

Richards, A.G., Richards, P.A., 1977. The Peritrophic Membranes of Insects. Annual Review of Entomology 22, 219-240.

Robinson, M.D., McCarthy, D.J., Smyth, G.K., 2010. edgeR: a Bioconductor package for differential expression analysis of digital gene expression data. Bioinformatics 26, 139-140.

Rodrigues, V., Cheah, P.Y., Ray, K., Chia, W., 1995. malvolio, the *Drosophila* homologue of mouse NRAMP-1 (Bcg), is expressed in macrophages and in the nervous system and is required for normal taste behaviour. The EMBO Journal 14, 3007-3020.

Rose, C., Belmonte, R., Armstrong, S.D., Molyneux, G., Haines, L.R., Lehane, M.J., Wastling, J., Acosta-Serrano, A., 2014. An Investigation into the Protein Composition of the Teneral *Glossina morsitans morsitans* Peritrophic Matrix. PLOS Neglected Tropical Diseases 8:e2691.

Rosenzweig, A.C., 2002. Metallochaperones: bind and deliver. Chemistry and Biology 9, 673-677.

Sakurai, T., Kataoka, K., 2007. Basic and applied features of multicopper oxidases, CueO, bilirubin oxidase, and laccase. Chemical Record 7, 220-229.

Samuel, G.H., Adelman, Z.N., Myles, K.M., 2018. Antiviral Immunity and Virus-Mediated Antagonism in Disease Vector Mosquitoes. Trends in Microbiology 26, 447-461.

Sanchez-Vargas, I., Scott, J.C., Poole-Smith, B.K., Franz, A.W., Barbosa-Solomieu, V., Wilusz, J., Olson, K.E., Blair, C.D., 2009. Dengue virus type 2 infections of *Aedes aegypti* are modulated by the mosquito's RNA interference pathway. PLOS Pathogens 5:e1000299.

Schindelin, J., Arganda-Carreras, I., Frise, E., Kaynig, V., Longair, M., Pietzsch, T., Preibisch, S., Rueden, C., Saalfeld, S., Schmid, B., Tinevez, J.Y., White, D.J., Hartenstein, V., Eliceiri, K., Tomancak, P., Cardona, A., 2012. Fiji: an open-source platform for biological-image analysis. Nature Methods 9, 676-682.

Schorderet, S., Pearson, R.D., Vuocolo, T., Eisemann, C., Riding, G.A., Tellam, R.L., 1998. cDNA and deduced amino acid sequences of a peritrophic membrane glycoprotein, `Peritrophin-48', from the larvae of *Lucilia cuprina*. Insect Biochemistry and Molecular Biology 28, 99-111.

Sedlak, T.W., Snyder, S.H., 2004. Bilirubin benefits: cellular protection by a biliverdin reductase antioxidant cycle. Pediatrics 113, 1776-1782.

Segraves, W.A., 1994. Steroid receptors and orphan receptors in *Drosophila* development. Seminars in Cell and Developmental Biology 5, 105-113.

Segraves, W.A., Woldin, C., 1993. The E75 gene of *Manduca sexta* and comparison with its *Drosophila* homolog. Insect Biochemistry and Molecular Biology 23, 91-97.

Shao, L., Devenport, M., Fujioka, H., Ghosh, A., Jacobs-Lorena, M., 2005. Identification and characterization of a novel peritrophic matrix protein, Ae-Aper50, and the microvillar membrane protein, AEG12, from the mosquito, *Aedes aegypti*. Insect Biochemistry and Molecular Biology 35, 947-959.

Shao, L., Devenport, M., Jacobs-Lorena, M., 2001. The peritrophic matrix of hematophagous insects. Archives of Insect Biochemistry and Physiology 47, 119-125.

Shen, Z., Jacobs-Lorena, M., 1998. A Type I Peritrophic Matrix Protein from the Malaria Vector *Anopheles gambiae* Binds to Chitin: Cloning, Expression, and Characterization. Journal of Biological Chemistry 273, 17665-17670.

Shi, H., Bencze, K.Z., Stemmler, T.L., Philpott, C.C., 2008. A cytosolic iron chaperone that delivers iron to ferritin. Science 320, 1207-1210.

Shoji, O., Watanabe, Y., 2014. Peroxygenase reactions catalyzed by cytochromes P450. JBIC Journal of Biological Inorganic Chemistry 19, 529-539.

Stocker, R., 2004. Antioxidant activities of bile pigments. Antioxidants and Redox Signaling 6, 841-849.

Stocker, R., Yamamoto, Y., McDonagh, A.F., Glazer, A.N., Ames, B.N., 1987. Bilirubin is an antioxidant of possible physiological importance. Science 235, 1043-1046.

Stohler, H., 1961. The peritrophic membrane of blood-sucking *Diptera* in relation to their role as vectors of blood parasites. Acta Tropica 18, 263-266.

Tahara, T., Sun, J., Igarashi, K., Taketani, S., 2004a. Heme-dependent up-regulation of the alpha-globin gene expression by transcriptional repressor Bach1 in erythroid cells. Biochemical and Biophysical Research Communications 324, 77-85.

Tahara, T., Sun, J., Nakanishi, K., Yamamoto, M., Mori, H., Saito, T., Fujita, H., Igarashi, K., Taketani, S., 2004b. Heme positively regulates the expression of beta-globin at the locus control region via the transcriptional factor Bach1 in erythroid cells. Journal of Biological Chemistry 279, 5480-5487.

Tang, X., Zhou, B., 2013a. Ferritin is the key to dietary iron absorption and tissue iron detoxification in *Drosophila melanogaster*. The FASEB Journal 27, 288-298.

Tang, X., Zhou, B., 2013b. Iron homeostasis in insects: Insights from *Drosophila* studies. IUBMB Life 65, 863-872.

Taub, F.E., DeLeo, J.M., Thompson, E.B., 1983. Sequential comparative hybridizations analyzed by computerized image processing can identify and quantitate regulated RNAs. DNA 2, 309-327.

Tellam, R.L., Wijffels, G., Willadsen, P., 1999. Peritrophic matrix proteins. Insect Biochemistry and Molecular Biology 29, 87-101.

Thummel, C.S., 1996. Flies on steroids--*Drosophila* metamorphosis and the mechanisms of steroid hormone action. Trends in Genetics 12, 306-310.

Toh, S.Q., Gobert, G.N., Malagón Martínez, D., Jones, M.K., 2015. Haem uptake is essential for egg production in the haematophagous blood fluke of humans, *Schistosoma mansoni*. FEBS Journal 282, 3632-3646.

Toprak, U., Erlandson, M., Hegedus, D., 2010. Peritrophic matrix proteins. Trends in Entomology 6, 23-51.

Tsirigos, K.D., Peters, C., Shu, N., Kall, L., Elofsson, A., 2015. The TOPCONS web server for consensus prediction of membrane protein topology and signal peptides. Nucleic Acids Research 43, W401-407.

Tsujimoto, H., Anderson, M.A.E., Myles, K.M., Adelman, Z.N., 2018. Identification of Candidate Iron Transporters From the ZIP/ZnT Gene Families in the Mosquito *Aedes aegypti*. Frontiers in Physiology 9:380.

Untergasser, A., Cutcutache, I., Koressaar, T., Ye, J., Faircloth, B.C., Remm, M., Rozen, S.G., 2012. Primer3—new capabilities and interfaces. Nucleic Acids Research 40:e115.

Varma, M.G., Pudney, M., 1969. The growth and serial passage of cell lines from *Aedes aegypti* (L.) larvae in different media. Journal of Medical Entomology 6, 432-439.

Vinchi, F., Ingoglia, G., Chiabrando, D., Mercurio, S., Turco, E., Silengo, L., Altruda, F., Tolosano, E., 2014. Heme exporter FLVCR1a regulates heme synthesis and degradation and controls activity of cytochromes P450. Gastroenterology 146, 1325-1338.

Vreman, H.J., Gillman, M.J., Stevenson, D.K., 1989. *In vitro* inhibition of adult rat intestinal heme oxygenase by metalloporphyrins. Pediatric Research 26, 362-365.

Wegiel, B., Nemeth, Z., Correa-Costa, M., Bulmer, A.C., Otterbein, L.E., 2014. Heme oxygenase-1: a metabolic nike. Antioxidants and Redox Signaling 20, 1709-1722.

White, C., Yuan, X., Schmidt, P.J., Bresciani, E., Samuel, T.K., Campagna, D., Hall, C., Bishop, K., Calicchio, M.L., Lapierre, A., Ward, D.M., Liu, P., Fleming, M.D., Hamza, I., 2013. HRG1 is essential for heme transport from the phagolysosome of macrophages during erythrophagocytosis. Cell Metabolism 17, 261-270.

Whiten, S.R., Eggleston, H., Adelman, Z.N., 2018a. Ironing out the Details: Exploring the Role of Iron and Heme in Blood-Sucking Arthropods. Frontiers in Physiology 8:1134.

Whiten, S.R., Ray, W.K., Helm, R.F., Adelman, Z.N., 2018b. Characterization of the adult *Aedes aegypti* early midgut peritrophic matrix proteome using LC-MS. PLOS One 13:e0194734.

Wilks, A., Heinzl, G., 2014. Heme oxygenation and the widening paradigm of heme degradation. Archives of Biochemistry and Biophysics 544, 87-95.

Worthington, M.T., Cohn, S.M., Miller, S.K., Luo, R.Q., Berg, C.L., 2001. Characterization of a human plasma membrane heme transporter in intestinal and hepatocyte cell lines. American Journal of Physiology - Gastrointestinal and Liver Physiology 280, G1172-G1177.

Wurmthaler, L.A., Sack, M., Gense, K., Hartig, J.S., Gamerdinger, M., 2019. A tetracycline-dependent ribozyme switch allows conditional induction of gene expression in *Caenorhabditis elegans*. Nature Communications 10:491.

Xiao, G., Wan, Z., Fan, Q., Tang, X., Zhou, B., 2014. The metal transporter ZIP13 supplies iron into the secretory pathway in *Drosophila melanogaster*. Elife 3:e03191.

Yanatori, I., Richardson, D.R., Toyokuni, S., Kishi, F., 2017. The iron chaperone poly(rC)-binding protein 2 forms a metabolon with the heme oxygenase 1/cytochrome P450 reductase complex for heme catabolism and iron transfer. Journal of Biological Chemistry 292, 13205-13229.

Yanatori, I., Richardson, D.R., Toyokuni, S., Kishi, F., 2019. How iron is handled in the course of heme catabolism: Integration of heme oxygenase with intracellular iron transport mechanisms mediated by poly (rC)-binding protein-2. Archives of Biochemistry and Biophysics 672:108071.

Yanatori, I., Yasui, Y., Tabuchi, M., Kishi, F., 2014. Chaperone protein involved in transmembrane transport of iron. Biochemical Journal 462, 25-37.

Ye, Y.X., Pan, P.L., Kang, D., Lu, J.B., Zhang, C.X., 2015. The multicopper oxidase gene family in the brown planthopper, *Nilaparvata lugens*. Insect Biochemistry and Molecular Biology 63, 124-132.

Yoshiga, T., Georgieva, T., Dunkov, B.C., Harizanova, N., Ralchev, K., Law, J.H., 1999. *Drosophila melanogaster* transferrin. European Journal of Biochemistry 260, 414-420.

Zhang, A.S., Enns, C.A., 2009. Molecular mechanisms of normal iron homeostasis. Hematology. American Society of Hematology. Education Program, 207-214.

Zhou, G., Kohlhepp, P., Geiser, D., Frasquillo, M.d.C., Vazquez-Moreno, L., Winzerling, J.J., 2007. Fate of blood meal iron in mosquitoes. Journal of Insect Physiology 53, 1169-1178.

Zhou, G., Velasquez, L.S., Geiser, D.L., Mayo, J.J., Winzerling, J.J., 2009. Differential regulation of transferrin 1 and 2 in *Aedes aegypti*. Insect Biochemistry and Molecular Biology 39, 234-244.

Zhu, Y., Silverman, R.B., 2008. Revisiting heme mechanisms. A perspective on the mechanisms of nitric oxide synthase (NOS), Heme oxygenase (HO), and cytochrome P450s (CYP450s). Biochemistry 47, 2231-2243.

Zuker, M., 2003. Mfold web server for nucleic acid folding and hybridization prediction. Nucleic Acids Research 31, 3406-3415.

APPENDIX

List of supplementary material

The raw data from the differential expression and soft cluster analyses from all NGS-RNAseq datasets are included in separate Microsoft Excel files.

- Aag2_48hr_heme_treated_cells_SupplementFile
- A20_72hr_heme_treated_cells_SupplementFile
- Aag2_72hr_L15_heme_treated_cells_SupplementFile
- Aag2_72hr_Schneider_heme_treated_cells_SupplementFile
- 35hr_heme_treated_midguts_SupplementFile